Master Thesis

cand. mach. Olma Vilarrasa Pujol

Matrikelnr.: 2140658

Analytical description of the fiber orientation in the joining area of composite structures

wbk

Institute of Production Science

Karlsruhe Institute of Technology (KIT)

Kaiserstraße 12

76131 Karlsruhe

Prof. Dr.-Ing. Jürgen Fleischer

Prof. Dr.-Ing. Gisela Lanza

Prof. Dr.-Ing. habil. Volker Schulze

Statement of Originality

I sincerely affirm to have composed this thesis work autonomously, to have indicated completely and accurately all aids and sources used and to have marked anything taken from other works, with or without changes. Furthermore, I affirm to have observed the constitution of the KIT for the safeguarding of good scientific practice, as amended.

Karlsruhe, August 31st 2018

_____

Olma Vilarrasa Pujol

Acknowledgement

First of all, I would like to extend my sincere gratitude to my supervisor, Sven Roth, for his guidance and encouragement throughout this project.

I also want to extend my thanks to the “wbk Institute of Production Science” and “KIT Karlsruher Institüt für Technologie” for providing me the opportunity to join them in my exchange semester.

Finally, I wish to express a special gratitude to my family, who tried their best to support me in the distance and made possible my stage in Germany.

Abstract

The application of fiber reinforced composites in multi material assemblies increases because of the potential to create products with low weight and high load capacity. The joining methods used in the industry, often require of drilling holes, which produce damage and weaken in the composite. This thesis is focused on describe a model to predict the orientation of the fibers in the union area, concretely when an embedded insert is located. This joining methodology allows the optimization of the fiber orientation, thus the fibers are relocated around the hole instead of cut them.

The present work consists in different sequential stages. First, a study of the influencing factors might produce the curvilinear behavior is carried out. Then, using images from tested samples the real trajectories are described. And finally by statistical and geometrical analysis an analytical model to predict the orientation in the joining area is developed.

Table of Contents

Table of Abbreviations

Symbol	Measurement	unity
$\boldsymbol{p(\theta,\phi)}$	Fiber orientation vector	
$\psi(\boldsymbol{p})$	Probability density distribution function	
p_i, p_j	Components of vector $\boldsymbol{p}$ related to angles θ and ϕ	
$\mathbf{A}$	Orientation tensor	
σ_1	Principal stress	[N/mm²]
α	Direction angle of the principal stress	[°]
σ_x, σ_y	Normal stress plane perpendicular to the x-axis or y-axis	[N/mm²]
τ_{xy}	Tangential (shear) stress	[N/mm²]
d_{PA}	Diameter of the plasticized joining area	[mm]
d_{JP}	Diameter of the joining point	[mm]
l_0	Length of the unloaded fiber	[mm]
l_R	Length of the realigned fiber	[mm]
l_β	Arc length	[mm]
α_R	Realignment arc	[°]
β	Wrap angle	[°]
ε_B	Elongation of the fiber	
$\boldsymbol{V}$	Vector of design variables	
R	Angle residual vector	[°]
C_1, C_2, C_3 and C_4	Coefficients of the material	
r	Radius of the hole	[mm]
ψ	Shorter expression of $r + C_1 \cdot r + C_2$	
t	Distance between x-axis and the straight path	[mm]
a_i	Polynomial coefficient with i the degree of the term	
gap	Difference between y(0) and the radius	[mm]
x_P	x coordinate of the inflection point	[mm]
DFE	Degree of Freedom in the Error	
FRP	Fiber Reinforced Polymer	
HYPER	HYbrid PEnetrative Reinforcement	
LCM	Liquid Composite Molding	

PMC	Polymer-Matrix Composites	
RMSE	Root Mean Squared Error	
RTM	Resin Transfer Molding	
SSE	Sum of Squares due to the Error	
TRRA	Trust-Region-Reflective Algorithm	

1 Introduction

1.1 Motivation

Nowadays, fiber reinforced composites are increasingly used for different kinds of application. These composites play a very important role in the aerospace, the automotive and the sport equipment industry. The main driving force for this trend is the growing effort to obtain lightweight constructions and to increase the performance and the efficiency of the products. Simultaneously, composite materials have to be relatively cheap, comparatively easy to process and, also, they have to provide advantageous specific mechanical properties.

Fiber reinforced composites have been extensively employed in engineering fields, which possess considerable advantages over traditional metallic and nonmetallic materials in both weight and strength (Zhu et al. 2016). Especially carbon-fiber-reinforced plastics with a thermoset matrix, which lead to multi-material-assemblies with benefits such as high stiffness and low weight. According to the industrial requirements, mechanical interlocking joining methods, such as bolts and rivets, are the most common process to transferred higher loads. Therefore, it is often inevitable to join the composites to other traditional or lightweight materials, such as steel, aluminum or plastic by drilling a hole. Opening a hole in composite structures causes serious stress concentration problems and damage from the regions near the hole. Drilling holes also cuts off the continuous fibers and consequently weakens the strength of fiber reinforced composites, causing a significant drop in the mechanical performance. (Gebhardt & Fleischer 2014)

This decrease of performance could be alleviated by using embedded inserts with bolt shape. Inserts consist of a thin metal sheet which is embedded between the textile plies before the lamination process, achieving the integration with the composite layers itself. Hence, it allows the optimization of fiber orientation in the union zone. (Gebhardt & Fleischer 2014)

Some investigations with embedded inserts have shown that the tensile strength of drilled inserts decreases by 29% compared to the variant with deflected and continuous fibers. (Gebhardt 2018). Although, shifting the fibers around the joining area, allowing the fibers to relocate instead of breaking apart, results clearly in better mechanical properties. There is still no algorithms or models to predict the fiber trajectories of thermoset carbon fibers.

Figure 1.1. Relocation of the fibers around the insert.
(Gebhardt 2018)

1.2 Objective

The first purpose of the present work is to generate knowledge about the prediction of the fiber trajectories located near the joining areas. This will be done by studying the possible influence factors of the fiber course when an insert is located. The main goal is to develop an analytical model, describing the fiber orientation in the joining area in relation the obtained influencing factors. In order to achieve it, some tests will be carried out to figure out the behavior of the real fiberpaths and make predictions of an ideal situation. Images from the manufactured parts will provide the information to statistically describe the tendencies and validate the model.

1.3 Structure of the Thesis

Initially in Chapter 2, the basics of fiber plastic composites are described. Moreover, the production methods used in thermosetting carbon fibers are explained. Focusing on the process of Resin Transfer Moulding (RTM). The chapter ends with a classification of the joining methods between composites and metals.

Then, in Chapter 3, the state of the art in the field of fiber trajectories description are presented.

Chapter 4, “Own approach”, is focused on describe the methodology used throughout the different steps of this work. It is divided in two main subchapters, the first one which explains the procedure of the experimental design and data acquisition, and the second one which aims to describe the model creation stages.

In the “Results” chapter a detailed explanation and description of the measurements and plots obtained from the tested parts are presented. In that point, the real trajectories of the samples and the main influence factors are described. The next chapter, “Assessment”, uses the knowledge and information of the results to create the mathematical equations of the model’s coefficients. In the last part of this chapter, when the model is already defined, the final model expression is used to plot the predicted fiberpaths and they are validated using the real images.

Finally, a summary of this work and the future perspectives in this field of research are given.

2 Basics

The present chapter focuses on describe the basic knowledge of the composite material studied in this project. Moreover, the different joining methods between metal and composites will be introduced.

Composite materials have emerged as a major class of structural elements. These materials are light weight, flexible, and also have high corrosion resistance, impact strength, fatigue strength, etc. Because of these properties, composite materials are being considered as a replacement of traditional materials used in the aerospace, automotive, and other industries. The specialty of composites is that the engineering properties, which are required in the end product, can be achieved by a careful selection of matrix and reinforcement. The outstanding features of fiber-reinforced polymer composites (FRPs) are their high specific stiffness, high specific strength, and controlled anisotropy, which make them very attractive structural materials. (Kar 2017)

One simple scheme for the classification of composite materials is shown in Figure 2.1 , which consists of three main divisions: particle-reinforced, fiber-reinforced and structural composites.

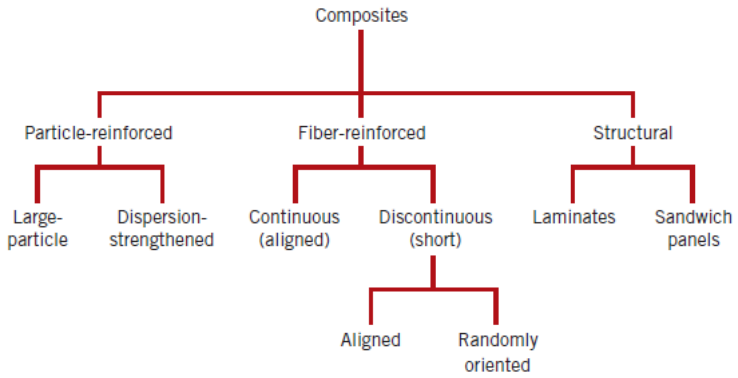

Figure 2.1. Classification of various composites types (Callister 2007)

2.1 Fiber reinforced polymer

Polymer-matrix composites (PMCs) consist of a polymer resin as the matrix, with fibers as the reinforcement medium.

Carbon is a high-performance fiber material that is the most commonly used reinforcement in advanced polymer-matrix composites (Callister 2007). The reasons for this are as follows:

1. Carbon fibers have the highest specific modulus and specific strength of all reinforcing fiber materials (Callister 2007).
2. They retain their high tensile modulus and high strength at elevated temperatures (Callister 2007).
3. At room temperature, carbon fibers are not affected by moisture or a wide variety of solvents, acids, and bases (Callister 2007).

4. These fibers exhibit a diversity of physical and mechanical characteristics, allowing composites incorporating these fibers to have specific engineered properties (Callister 2007).
5. Fiber and composite manufacturing processes have been developed that are relatively cost effective (Callister 2007).

The mechanical characteristics of a fiber-reinforced composite depend not only of the properties of the fiber, but also on the degree to which an applied load is transmitted to the fibers by the matrix phase (Callister 2007).

The arrangement or orientation of the fibers relative to one another, the fiber concentration, and the distribution all have a significant influence on the strength and other properties of fiber-reinforced composites. With respect to orientation, two extremes are possible: a parallel alignment of the longitudinal axis of the fibers in a single direction, and a totally random alignment. Continuous fibers are normally aligned (Figure 2.2 a), whereas discontinuous fibers may be aligned (Figure 2.2 b), randomly oriented (Figure 2.2 b), or partially oriented. Better overall composite properties are realized when the fiber distribution is uniform. (Callister 2007)

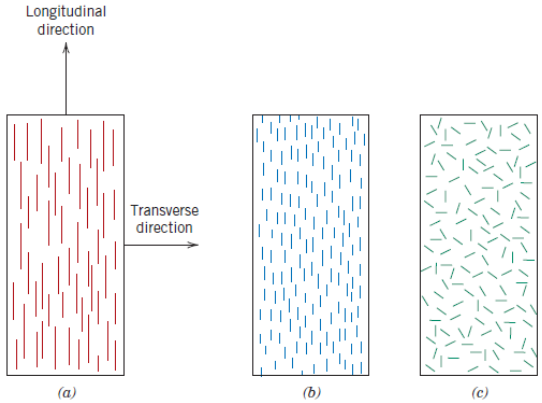

Figure 2.2. Schematic of a) continuous and aligned, b) discontinuous and aligned, and c) discontinuous and randomly oriented fiber reinforced composites (Callister 2007).

PMCs consists also of a polymer matrix, it binds the fibers together so as to transfer the load to and between them and protects them from environments and handling at work. Thermosets and thermoplastics are the two basic types of resin used in the manufacturing.

- Thermoset resins

Nowadays, in the advanced composite industry, thermoset resins dominate over the thermoplastic resins. In order to produce a product using thermoset resins, addition of a curing agent or hardener and impregnation onto a reinforcing material followed by curing are key steps. Thermoset composites are commonly based on fibers, glass or carbon, which are commonly incorporated in resins such as polyesters or epoxies. (Kar 2017)

- Thermoplastic resins

Currently, thermoplastic resins represent a relatively small part of the PMC industry. These resins are nonreactive materials; no chemical reaction occurs during processing. The final product can be made by application of heat and pressure. Unlike thermoset resins, the thermoplastic resins can usually be reheated and reformed into another shape, if desired. Common examples of thermoplastic resins are polyethylene, polystyrene, nylon, polycarbonate, polysulfone, polyphenylene sulfide and acrylonitrilebutadiene-styrene. (Kar 2017)

2.2 Manufacturing processes

There are several methods to manufacture FRPs, such as vacuum bagging, autoclave, filament winding, pultrusion, matching die set compression molding, resin transfer molding (RTM), resin infusion, and other liquid composite molding (LCM). Among these methods, autoclave is the best method for manufacturing of some aeronautic parts. But a major cost issue for manufacturing of FRPs and parts using autoclave is the requirement of expensive tooling and disposable bagging materials. Other disadvantages are long cure times, high energy consumption, volatile toxic byproducts, creation of residual stress and voids in the materials, and the use of expensive tooling that are capable of withstanding high autoclave temperature. Because of these negative points recently, LCM such as RTM is becoming more and more popular in the aeronautic and automotive industry. (A. C. Long 2005)

Liquid moulding describes a family of closed mould processes whereby a dry reinforcement is impregnated with a liquid thermosetting resin. Table summarises the most widely used processes and terminology.

RTM	Resin transfer moulding – positive pressure, matched mould variant with polymer resins.
VARI	Vacuum assisted resin injection – adaptation of RTM using vacuum sink to enhance pressure gradient.
SRIM	Structural reaction injection moulding – adaptation of RTM using reactive processing equipment and techniques, usually for urethanes.
VI, VARTM, RIFT, SCRIMP	Vacuum impregnation processes using one hard tool plus vacuum membrane. Usually involves flow-enhancing medium. Some variants are patent protected.
RFI	Resin film infusion – (usually) through thickness impregnation by stacking films and fabrics, increasing materials available in kit form.

Table 2.1. Glossary of terminology related to liquid moulding. (A. C. Long 2005)

The common liquid moulding applications are RTM products in the automotive industry. The principal resins are unsaturated polyester for automotive body structures and epoxies or bismaleimides for aerostructures. (Kar 2017; A. C. Long 2005)

2.2.1 Resin Transfer Molding (RTM)

The purpose of this section is to summarize the fundamentals of RTM. In the Figure 2.3 are shown the basics steps which take part in this specific manufacturing process and it follows by a short description of each one.

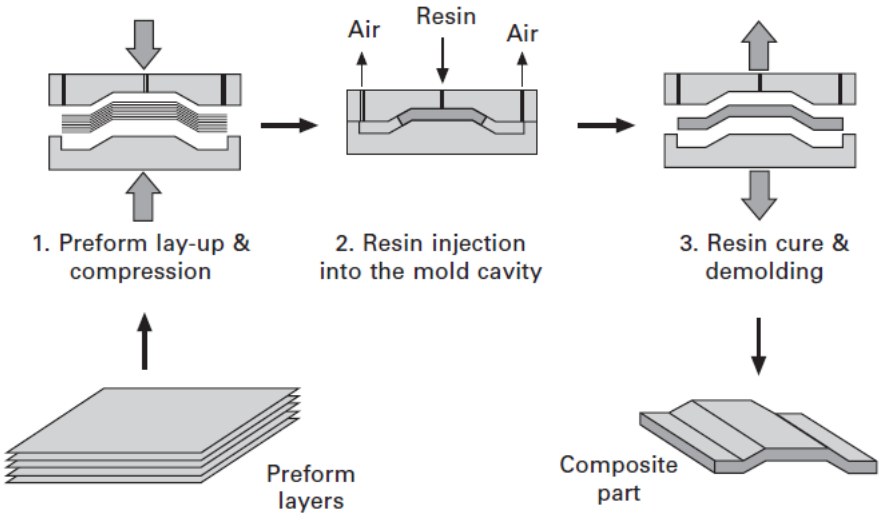

Figure 2.3. Basic steps of resin transfer molding. (A. C. Long 2005, p.242)

1. The textiles, which constitute the reinforcing component of the composite part, are cut from large rolls to the dimensions of the composite part to be manufactured. The textile sheets are placed into the mold. This process involves matching dies, the mold is closed and the mold cavity is sealed by fastening the mold with nuts and bolts, or by applying pressure with a press.
2. The resin is injected into the mold cavity through the gates at superatmospheric pressures (typically 2–20 bar). Resin advances through the fibrous preform owing to the injection pressure, pushing air out of the mold through the vents.

   Darcy's law is usually assumed to apply and the time taken to impregnate the preform therefore depends on the pressure gradient, the resin viscosity and the hydraulic conductivity or permeability of the fibre bed. Impregnation times range from a few minutes to several hours and the resin needs to be formulated taking this quantity into account.
3. After the injection step is complete, the resin in the mold cavity cures through a series of chemical reactions to form a solid part.

2.3 Joining of metal and composite materials

The application of mixed materials structures involves high lightweight potential. Especially composite-metal structures, are widely applied in industry. However, joining composite components is challenging for manufacturers, since they have to ensure a fiber-fair load transmission. (Jahn et al. 2016)

For the joining of thermosetting composite components with metallic components different concepts are used: Adhesive bonding, mechanical fastening or a combination of these mechanisms. (Jahn et al. 2016)

In this work the main joining methods metal-thermosetting composite are classified in three families: adhesive bonding, joints with drilling operations and before laminate joints.

2.3.1 Adhesive bonding

Adhesive bonding is a usually applied concept for the joining of composites components. It is widely used due to the suitability for joining of any combination of similar or dissimilar materials. A distinction is made between traditional bonding of cured components, co-bonding, and co-curing. (Jahn et al. 2016)

- **Co-bonding**

  The curing together of two or more elements, of which at least one is fully cured and at least one is uncured. This process requires a careful surface preparation of the previously cured substrate.

- **Co-curing**

  The act of curing a composite laminate and simultaneously bonding it to some other uncured composite laminate or to a core material such as honeycomb or foam.

Adhesively bonded joints have excellent fatigue properties. Adhesives are used extensively for secondary aircraft and automotive parts, and in some cases primary parts of aircraft. This method of joining is particularly attractive for joining relatively thin skinned or walled structures, particularly where fatigue is a problem. The success of adhesive bonding depends strongly on the surface treatment of the adherends, which needs to be optimised to ensure that structural integrity is maintained under service conditions for the required life of the component. (W R Broughton, L E Crocker and M R L Gower 2002)

2.3.2 Joints with drilling operations

Higher loads can be transferred by the joint due to mechanical interlocking, therefore this method is often used in automotive or aircraft industry. The union can be defined as the introduction of joint elements after consolidation in the cured laminate. Some methods need the drilling of a hole, which causes a weakening of the fusion zone, fiber damage and an interruption of load transmission.

- **Bolt and rivet joints**

  These traditional joining technology is used when structural components with a flat surface need to be joined. In the majority of cases an overlapping of the components is required. In the Figure 2.4 is shown an example of rivet method applied in automotive industry.

Figure 2.4. Rivet join in BMW 7 Series body

An advantage of the bolt joining technology is the separating of the connected components by the removal of the joint elements, whereby a subsequent recycling is possible. However, the strength and fatigue joint life are influenced by the fiber damage, the yielding polymer matrix in bolted joints and the loss of bolt clamp-up load. (Jahn et al. 2016; W R Broughton, L E Crocker and M R L Gower 2002)

- **Hole-clinching**

Hole-clinching is a suitable process for joining brittle materials such as composites with ductile metallic materials. This technology provides a geometrical interlocking with no additional joining elements. In Figure 2.5 the joining method is described. (Lee et al. 2014)

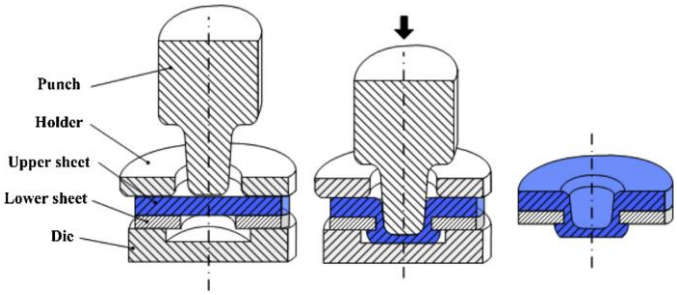

Figure 2.5. Schematic of hole-clinching process. (Lee et al. 2014)

Thus the production time and costs are reduced in comparison to other mechanical methods. Hence the clinching technology, especially for less stressed structures and mass production is easy to implement. Disadvantages are the high introduced loads, so fiber damage of the composite substrate and residual stress in the metal component cannot be avoided. (Lee et al. 2014; Jahn et al. 2016)

2.3.3 Before laminate joints

- **Hybrid penetrative reinforcement (HYPER)**

In opposite to previously described bolted, riveted and clinched composite-metal joints, HYPER joints use integrated joint elements. Hence it contains small pins, upsetted on the surface of

the metallic component which are integrated in the uncured composite substrate, see Figure 2.6. This provides a mechanical interlocking and additional epoxy adhesion around the pins and the level surface of the metal component. The HYPER technology is time and cost-intensive, due to the requirement of special tools and know-how. (Jahn et al. 2016; Parkes et al. 2014)

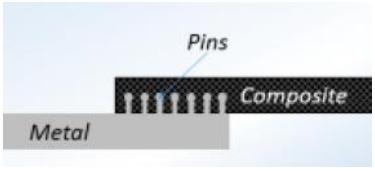

Figure 2.6. HYPER joint. (Jahn et al. 2016)

To integrate the metallic pins in composite substrate different processes are used. One option is the Resin Transfer Moulding (RTM), in which is laying dry ply onto metallic substrate following by the resin injection. Another possibility is the use of a pre-impregnated substrate and pressing the pins into the uncured laminate with an ultrasonic horn and following consolidation in an autoclave. (Jahn et al. 2016; Parkes et al. 2014)

- **Embedded inserts**

For thin-walled composite components usually metallic inserts are used consisting of a thin metal sheet which is embedded between the laminate plies in RTM-process or with the hand lay-up technique. As is shown in Figure 2.7, a threaded bolt introduces the load through the thin metal sheet into the composite laminate. (Gebhardt & Fleischer 2014)

Figure 2.7. Insert join. (Gebhardt & Fleischer 2014)

To increase the joint strength, bead patterns or surface treatments on the metal sheet are used. Advantages of using embedded inserts are the fiber load transmission and the possible optimization of fiber orientation in the union zone. Further benefit is the easy separation of the metal component regarding recycling aspects. Disadvantageous is the time and cost fabrication. (Gebhardt & Fleischer 2014)

3 State of the art

The analysis, both analytically and experimentally, of fiber orientation has been a research topic throughout the last decades. Due to the widely use of the injection molding, several studies has been done to accurately represent the orientation state of the fibers during the part molding process and from the orientation state predict, statistically, the resulting material characteristics.

This chapter sets an overview of fiber orientation models and aims to create a basis for the development of a specific model, which deals with endless fibers focused on the joining area.

3.1 Numerical predictions of fiber orientation

Development starts for the representation of a single fiber. A single fiber is regarded as a rigid cylindrical rod. The fiber's unit vector **p** along its axis direction can describe the fiber orientation. Orientation vector **p** is expressed in a surface spherical coordinate with the polar angle θ and the angle ϕ, Figure 3.1. (Advani & Tucker 1987)(David Abram Jack 2006)

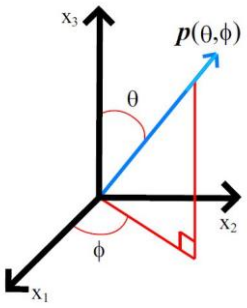

Figure 3.1: Coordinate system defining **p**(θ,ϕ) (David Abram Jack 2006).

For a concise representation of the orientation of a large population of fibers, Advani and Tucker defined the second order orientation tensor as:

$$\boldsymbol{A} = \oint \psi(\boldsymbol{p}) p_i p_j \, d\boldsymbol{p} = \begin{bmatrix} A_{11} & A_{12} & A_{13} \\ A_{12} & A_{22} & A_{23} \\ A_{13} & A_{23} & A_{33} \end{bmatrix} \qquad \text{Formula 3.1}$$

Where:

$\psi(\boldsymbol{p})$ *is the probability density distribution function over the orientation space*

$\boldsymbol{p}$ *is a unit vector parallel to the fiber*

p_i, p_j *are the components of vector* $\boldsymbol{p}$ *related to angles* θ and ϕ

The second-rank orientation tensor $\boldsymbol{A}$ is the symmetric matrix and its trace is $A_{11} + A_{22} + A_{33} = 1$. Physically, $\boldsymbol{A} = \boldsymbol{I}/3$ represents the isotropic orientation state, wherein $\boldsymbol{I}$ is the identity matrix. The diagonal components of the second order orientation tensor,A_{11}, A_{22}, and A_{33}, describe the degree of orientation in flow direction (x1-direction), cross-flow direction (x2-direction), and thickness direction (x3-direction), respectively. (Advani & Tucker 1987)(David Abram Jack 2006)

The orientation tensor is given as:

$$\boldsymbol{A} = \begin{bmatrix} 1/3 & 0 & 0 \\ 0 & 1/3 & 0 \\ 0 & 0 & 1/3 \end{bmatrix} \text{ for the isotropic distribution} \qquad \text{Formula 3.2}$$

$$\text{and } \boldsymbol{A} = \begin{bmatrix} 0 & 0 & 0 \\ 0 & 0 & 0 \\ 0 & 0 & 1 \end{bmatrix} \text{ for the perfect alignment.} \qquad \text{Formula 3.3}$$

The principal directions of the orientation tensor ***A*** are numbered in the order of the respective principal values, from the largest to the smallest. The first principal direction represents the direction along which the most fibers are aligned, and the third principal direction represents the one along which the fewest fibers are aligned. The larger principal value indicates a stronger alignment in the corresponding principal direction. (David Abram Jack 2006; Advani & Tucker 1987)

A physical interpretation of the orientation tensor is very similar to that of the stress tensor. The diagonal components of a fiber orientation tensor represent the strength of alignment in the respective directions. The values of the diagonal components range between 0 and 1, and the sum of all three diagonal components is 1. The off-diagonal components of a fiber orientation tensor represent the amount that alignments vary from the coordinate axes; they are zero when the coordinate axes coincide with the principal directions of the orientation tensor. Therefore, non-zero off-diagonal components indicate that x1, x2, and x3 axes are not the principal axes. (David Abram Jack 2006; Advani & Tucker 1987)

A time-evolution equation of the second-order orientation tensor is fixed on the derivative, denoted as $\dot{\boldsymbol{A}}$. Over the last three decades, theoretical researchers in the fiber suspension rheological field have made an effort to determine the dynamic fiber orientation states involving short and long fibers. (David Abram Jack 2006; Advani & Tucker 1987)

The modern models, based on the classic fiber orientation models, the pioneering Jeffery hydrodynamic model and the famous Folgar-Tucker IRD (Isotropic Rotary Diffusion) model, include the Phelps-Tucker ARD (Anisotropic Rotary Diffusion) model the Wang-Tucker RSC (Reduced Strain Closure) model and the ARD-RSC model. These modern models are available in commercial injection molding simulation software, such as the Autodesk Simulation Moldflow Insight (ASMI), providing the fiber orientation predictions practiced in most of injection molded fiber-reinforced thermoplastic products. (Jeffery & G 1922) (Fransisco Folgar and Charles L. Tucker & III 1983) (Phelps & Tucker 2009) (Wang, O'Gara & Tucker 2008)

3.2 Fiber paths optimization

Optimization of fiber paths in composite laminates so as to improve the mechanical performance has been studied since last decades. Lin prepared a composite plate with curvilinear fiber paths around the hole by embedding metal pins into the fiber before curing. Their work showed that the tensile strength and the compressive strength were improved dramatically compared with the traditional laminates with drilled holes, but straight fibers. (H. J. Lin & C. S. Tang 1994)

Currently, to optimize the fiber paths in composite laminates with open-holes, keeping the fiber paths consistent with the principal stress trajectories is one of the first priority aims in many studies. Once the fibers are oriented in the principal stress direction, the strength and the stiffness of composite laminates can be significantly improved.

3.2.1 Examples in nature

Analyzing the structural regulation principles in nature and adapting to defect zones provides a draft for the shape optimization of a joining point. For instance, maintenance of an uniform stress distribution in the affected zone is observed in trees. If a tree sustains damage by cracks, rottenness, or broken branches, a local structural weakness occurs. The resultant increased stress can be declined by building up material in the defect area. (Hubert Temmen, Richard Degenhardt, Tilmann Raible 2006) (Brebbia & A 2006)

Figure 3.2 shows how wood fibers are redirected radial at defects, caused by knotholes, as a way to neutralize the notch effects. This principle can be used on drilled holes as a design model for increasing the load capability and the strength of reinforcing fibers in technical applications. Based on this principle, optimization algorithms have been developed. (Ghiasi et al. 2010) (D. Reuschel 1999)

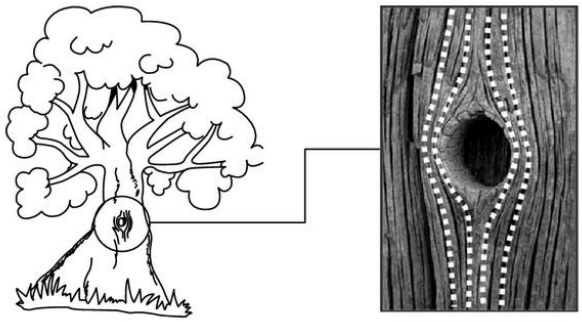

Figure 3.2: Load adjusted fiber orientation at the defect zone of trees. (Seidlitz, Ulke-Winter & Kroll 2014)

3.2.2 Alignment of the principal axes

3.2.2.1 Principal stress trajectories

In general, the stress distributions can be obtained by the finite element analysis in the pre-design stage, and the principal stress components and their angles with respect to the global coordinate can be calculated based on these stress distributions. Some commercial package, such as Ansys software, can be used to obtain the principal stress vectors. (Zhu et al. 2016) (Dr.Abdul & Mirzana 2016)

Since the first principal stress is the dominant stress component for the uniaxial loading case, the first principal stress trajectory is chosen as the desired fiber path. The first principal stress σ_1 and the direction angle α can be calculated by the following equation under the plane stress state using the stress components obtained by the finite element method. (Zhu et al. 2016) (Xavier Oliver Olivella i Carlos Agelet de Saracíbar Bosch 2003)

$$\sigma_1 = \frac{\sigma_x+\sigma_y}{2} + \sqrt{\left(\frac{\sigma_x-\sigma_y}{2}\right)^2 + \tau_{xy}^2} \qquad \text{Formula 3.4}$$

$$tan\,2\alpha = -\frac{2\cdot\tau_{xy}}{\sigma_x-\sigma_y} \qquad \text{Formula 3.5}$$

Where:

σ_1 is the principal stress value

α is the direction angle of the principal stress

σ_x is the normal stress acting on plane perpendicular to the x-axis

σ_y is the normal stress acting on plane perpendicular to the y-axis

τ_{xy} is the tangential (shear) stress acting on the plane perpendicular to x-axis in the direction of y-axis.

After the first principal stress and its direction angle are obtained, the first principal stress vectors can be illustrated, as shown in Figure 3.3. The trajectory of the principal stress is approximated by connecting the adjacent vectors, see the black solid line on the figure. (Zhu et al. 2016)

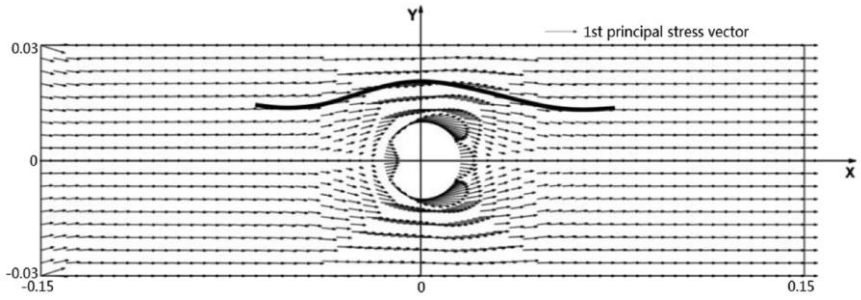

Figure 3.3. Vectors of the 1st principal stress for an isotropic laminate under uniaxial tensile load. (Zhu et al. 2016)

3.2.2.2 Geometrical description

In a research center of lightweight structures, located in Chemnitz, have been developed a new joining methodology for metal-thermoplastic matrix composite based on the knothole principle. Part of the study focused on define the plasticized area to ensure the radial displacement of the fibers within the polymer matrix. The realignment and the length variation of the fibers were described geometrically. In Figure 3.4. is shown the geometrical model description of an unidirectional ply with the most deflected fiber. (Seidlitz, Ulke-Winter & Kroll 2014)

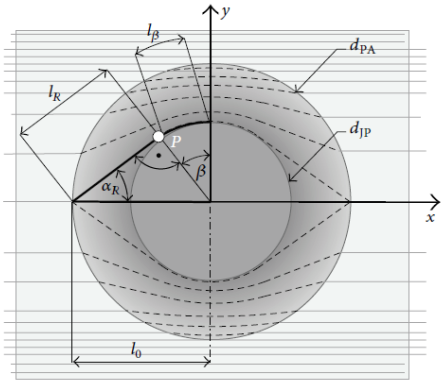

Figure 3.4: Geometrical description of the most deflected fiber. (Seidlitz, Ulke-Winter & Kroll 2014)

Where:

d_{PA} is the diameter of the plasticized joining area

d_{JP} is the diameter of the joining point

l_0 is the length of the unloaded fiber

P is the intersection of the tangent

l_R is the length of the realigned fiber until P

l_β is the arc length

α_R is the realignment arc

β is the wrap angle at the edge of the joining point

The diameter of the joining point d_{JP} is given and the realigned fiber with length l_R fits tangential at the edge of the joining point. Because of that the realignment angle α and the wrap angle β are equal and the following expressions can be derived:

$$l_\beta = \alpha_R \cdot \frac{d_{JP}}{2}$$ Formula 3.6

$$l_0 = \frac{d_{JP}}{2 \cdot \sin \alpha_R}$$ Formula 3.7

$$l_R = \frac{d_{JP}}{2 \cdot \tan \alpha_R}$$ Formula 3.8

The maximum elongation of the fiber can be described as:

$$\varepsilon_B = \frac{\Delta l}{l} = \frac{(l_R + l_\beta) - l_0}{l_0} = \frac{l_R + l_\beta}{l_0} - 1$$ *Formula 3.9*

Insert Formula 3.6, Formula 3.7 and Formula 3.8 in Formula 3.9 gives the expression of the maximum elongation in the most deflected fiber. (Seidlitz, Ulke-Winter & Kroll 2014)

$$\varepsilon_B = \frac{\frac{d_{JP}}{2}\cdot tan\,\alpha_R + \frac{d_{JP}}{2}\cdot\alpha_R}{\frac{d_{JP}}{2}\cdot sin\,\alpha_R} - 1 = cos\,\alpha_R + \alpha_R \cdot sin\,\alpha_R - 1 \qquad \text{Formula 3.10}$$

All realigned fibers have specific lengths as well as realignment arcs, which depend from the distance to the joining point center, $l_0 = f(y)$ and $\alpha_R = f(y)$. If the boundaries of the plasticized area are described by the circle equation $x^2 + y^2 = (d_{PA}/2)^2$ every length l_0 of an unloaded fiber within the plasticized joining area can be determined as $x = l_0(y)$:

$$l_0(y) = \sqrt{\frac{1}{4}\cdot {d_{PA}}^2 - y^2} \qquad \text{Formula 3.11}$$

The realignment of fibers occurs at the joint in the interval between $0 \le y \le d_{JP}/2$. (see Figure 3.4). The realignment arc α_R can be described as follows:

$$tan\,\alpha_R = \frac{\frac{d_{JP}}{2} - y}{l_0(y)} \qquad \text{Formula 3.12}$$

Inserting Formula 3.11 gives the realignment arc α_R as a function of y, for every realigned fiber on the plasticized area:

$$\alpha_R(y) = tan^{-1}\left(\frac{d_{PA} - y}{\sqrt{(1/4)\cdot {d_{PA}}^2 - y^2}}\right) \qquad \text{Formula 3.13}$$

The strain of every fiber can be determined considering the expression of elongation, Formula 3.10, with $\alpha_R(y)$. (Seidlitz, Ulke-Winter & Kroll 2014)

$$\varepsilon_\beta(y) = \cos\left(\tan^{-1}\left(\frac{d_{PA} - y}{\sqrt{(1/4)\cdot {d_{PA}}^2 - y^2}}\right)\right) + \tan^{-1}\left(\frac{d_{PA} - y}{\sqrt{(1/4)\cdot {d_{PA}}^2 - y^2}}\right)\cdot \sin\left(\tan^{-1}\left(\frac{d_{PA} - y}{\sqrt{(1/4)\cdot {d_{PA}}^2 - y^2}}\right)\right) - 1$$

Formula 3.14

The resulting expression allows to describe the dimensioning joining area.

3.2.2.3 Curvilinear family description

Recently, more papers and technical articles were focused on optimize the fiber path in composites laminates with centered holes. The following approach assumes a family of curves as the fiber paths, which can approximate the principal stress trajectories.

The optimization is started from the introduction of the fiber trajectory function. Is assumed that in the Cartesian coordinate system, the trajectory function y with N discrete points (x_i, y_i) is given by $y = f(x, t, \boldsymbol{V})$ where the vector $\boldsymbol{V}$ contains M design variables (M<N), which are to be optimized by the weighted least squares method. The coefficient t is the factor of the family of curves. It should be noted that the shapes of the family of curves are controlled by the design variable $\boldsymbol{V}$ and the factor t. The number of design variables also influences the shapes of curves and the optimization accuracy. (Zhu et al. 2016)

For any point in the trajectory function, the tangent function of the fiber angle θ is defined by the first derivative of the assumed trajectory function. (Zhu et al. 2016)

$$tan\,\theta = \frac{dy}{dx} = \frac{df(x,t,\boldsymbol{V})}{dx} \qquad \text{Formula 3.15}$$

The difference between the angle of assumed function and the angle of principal stress trajectory composes the angle residual vector **R**, which is defined as:

$$R_i(x_i, y_i) = \theta_i(x_i, y_i, V) - \alpha_i(x_i, y_i) \qquad \text{Formula 3.16}$$

Where $\theta_i(x_i, y_i, V)$ and $\alpha_i(x_i, y_i)$ represent the angles of the assumed function and the principal stress trajectory at the position (x_i, y_i) respectively. The residual vector **R** consists of N residual components. (Zhu et al. 2016)

The objective function is defined to minimize the sum constructed by the product of the weights and the squares of the residuals R_i.When the laminate is highly stressed by an axial tensile load, it is better to arrange the fiber paths along with the first principal stress trajectories. Otherwise, the mechanical performance of the fibers cannot be fully utilized. This consideration is the reason to take the principal stress as the weight. So the larger weight values imply the higher requirement of the consistency between the fiber angles and the stress trajectories, while the smaller weight values imply the tolerance of the angle difference. (Zhu et al. 2016)

$$Objective\ function = MIN\left(\sum_{i=1}^{N} |\sigma_{1i}| \cdot R_i^2\right) \qquad \text{Formula 3.17}$$

The aim of the optimization is to realize a set of optimal design variables that minimizes the objective function using the nonlinear weighted least squares method. Once the optimal design variables are obtained, the optimal family of curves is determined and the fiber paths are described. (Zhu et al. 2016)

To guarantee good accuracy, the family of curves should closely follow the trajectories of the first principal stress to improve the consistency between the fiber angle and the first principal stress angle. Moreover, the trajectories are symmetric to the y axis and have very close shape with the cosine function in a period. Thirdly, the trajectory becomes straight line in the stress non-concentrated areas, which implies the $\tan\theta$ is zero in these regions. Finally, the family of curves also has to guarantee the smooth transition from the stress concentrated area to non-concentrated area to avoid the stress concentration. (Zhu et al. 2016)

Following the mentioned design rules, the family of curves for the upper and lower half plane is assumed by piecewise functions using three design variables. However, to simplify the family of curves and reduce the design variables, the design variable v_3 is set to one and the family of curves are described as the following equations. The first one represents the upper half plane and the second one the lower half plane. (Zhu et al. 2016)

$$y = f(x,t,\boldsymbol{V}) = \begin{cases} \left(\frac{r+v_1\cdot t}{2}\right)\cdot\cos\left(\frac{2\pi}{v_2\cdot r}\cdot x\right)+\left(\frac{r+t}{2}\right), x\,\epsilon\left[-\left|\frac{v_2\cdot r}{2}\right|,\left|\frac{v_2\cdot r}{2}\right|\right]\cap y\,\epsilon\left[0,-\frac{r}{2}\left(1-\frac{1}{v_1}\right)\right] \\ y_i, x\notin\left[-\left|\frac{v_2\cdot r}{2}\right|,\left|\frac{v_2\cdot r}{2}\right|\right]\cup y\notin\left[0,-\frac{r}{2}\left(1-\frac{1}{v_1}\right)\right] \end{cases}$$

Formula 3.18

$$y = f(x,t,\boldsymbol{V}) = \begin{cases} -\left(\frac{r+v_1\cdot t}{2}\right)\cdot\cos\left(\frac{2\pi}{v_2\cdot r}\cdot x\right)-\left(\frac{r+t}{2}\right), x\,\epsilon\left[-\left|\frac{v_2\cdot r}{2}\right|,\left|\frac{v_2\cdot r}{2}\right|\right]\cap y\,\epsilon\left[0,-\frac{r}{2}\left(1-\frac{1}{v_1}\right)\right] \\ y_i, x\notin\left[-\left|\frac{v_2\cdot r}{2}\right|,\left|\frac{v_2\cdot r}{2}\right|\right]\cup y\notin\left[\frac{r}{2}\left(1-\frac{1}{v_1}\right),0\right] \end{cases}$$

Formula 3.19

To optimize the design variables in the nonlinear weighted least squares methods, there are many algorithms, such as the Trust-Region-Reflective algorithm (TRRA), which can be performed in the commercial package MATLAB. In the current application using six pairs of design variables are prepared for the initiation, where the variable v1 is initiated by a negative value and v2 is initiated by a positive value. After the iterations using the different initial design values, the optimal design variables $\boldsymbol{V}^*$ is obtained. Finally, these vector $\boldsymbol{V}^*$ is used to illustrate the family of curves, shown in Figure 3.5, which is very close to the original trajectories of the first principal stress. (Zhu et al. 2016)

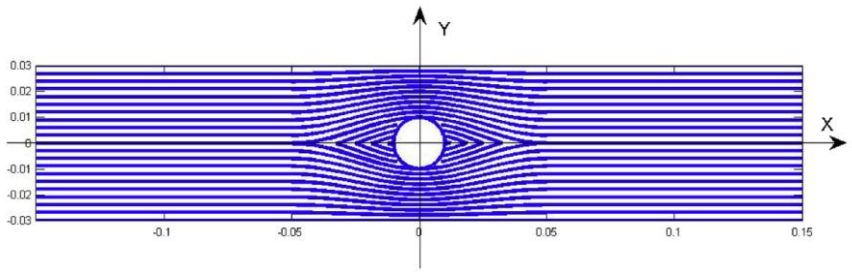

Figure 3.5. Optimized family of curves with two design variables (Zhu et al. 2016)

4 Own approach

4.1 Influencing factors candidates

To develop the analytical model a previous study of the influencing factors is required. The following chapter describe the design of the experiments and the methodology used to plot the real trajectories of the tested samples.

In the industry the forming of the holes is realized before the injection of the fibers, by piercing through the textile. Then the textile is placed into the mold and resin is injected, see chapter 2.2.1 for more details. However, in the tests and analysis carried out in this work the textile part without resin is used. Therefore, the fiberpaths of the textile will be analyzed just after the hole manufacturing.

4.1.1 Design of experiments

In an experiment, one or more process variables or factors are deliberately changed in order to observe the effect the changes have on one or more response variables. The statistical design of experiments is an efficient procedure for planning experiments so that the data obtained can be analyzed to yield valid and objective conclusions.

The design begins with determining the objectives of an experiment and selecting the process factors for the study.

4.1.1.1 Objectives, response variables

In the present design the data will be obtained of images of the tested samples. In one hand, measurements of real points of different fiber paths will be made; this information will be used later to define the analytical model. In the other hand, the area that suffers deformation due to the punch hole will be measured in order to do the statistical analysis and select the most influential factors.

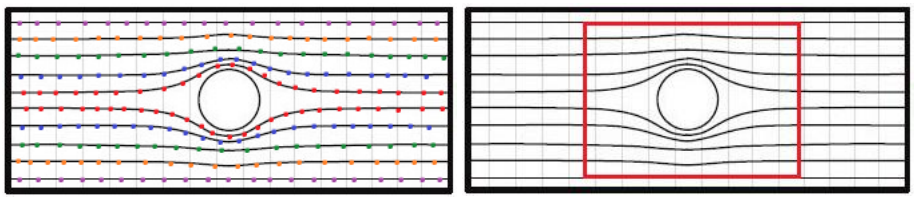

Figure 4.1. Objective measurements, fiber path points and deformed area.

4.1.1.2 Levels and factors selection

Drawings such as cause and effect diagram, Figure 4.2, are useful to illustrate the possible factors.

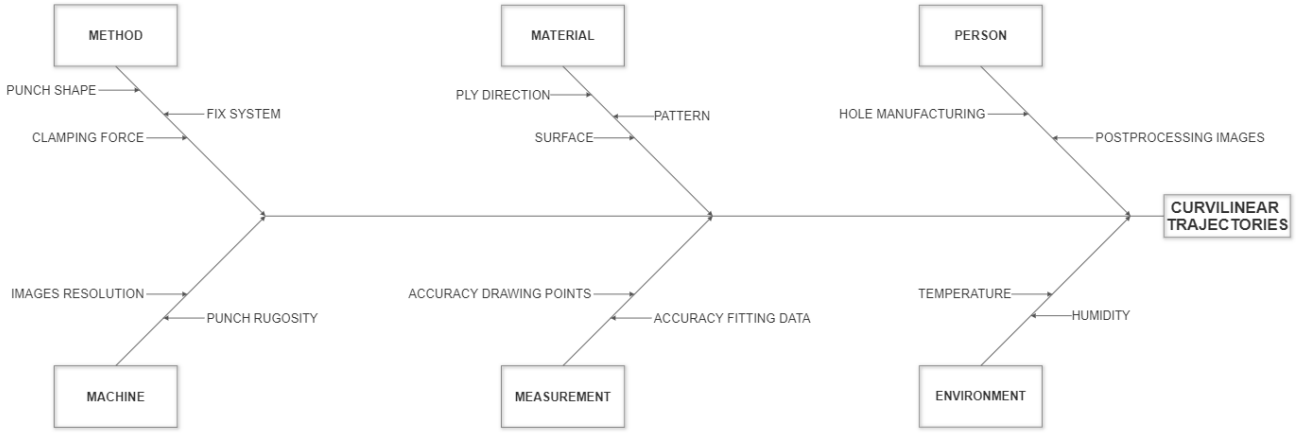

Figure 4.2. Cause and effect diagram

Once the possible factors that can be included in our design have been proposed, is necessary evaluate which are reasonable and transcendent to put on the design. After this valuation the surface and the fix system variables have been fixed, the measurements will be made in the same size samples and the fix system described in the previous subchapter. Noise factors, such as the operator and environmental conditions are not considerate as a potential factors and they will be minimized. The same operator will pierce the textile parts and the experiments will take place in the same place and at more or less the same hour. Five factors are chosen to be part of the design: hole diameter, material, shape of the pin, angle of the pin and clamping force.

The most popular experimental designs are two-level designs. There are a number of good reasons why two is the most common choice amongst engineers: some reasons are that it is ideal for screening designs, simple and spent less resources (Prat Bartés et al. 2000). A sequential strategy is adopted because of the limited time and amount of fiber available. A first experiment will be done in order to achieve information and then decide the conditions for possible further experiments.

In the following lines the factors and their respective levels are defined:

- **Material**

  The chosen materials are the ones used in previous studies and available in the Institut WBK. Both materials are carbon fiber with similar density. However, they differ in the pattern and ply composition The low level is defined by a -45/45 ply and the high level by 0/90. In the Figure 4.3 there are detail images of the both textiles and the different stitching patterns are clearly shown.

Figure 4.3. Textiles pattern used in the testing. Ply (-45, /45) in the left and ply (0/90) in the right.

.

- **Diameter of the hole**

In previous studies made in wbk a punch of 18mm had been used to pierce the textile, taking that as a reference of maximum diameter, some pre-testing was performed. From the observation, the ideal specimen size is 75 mm x 75 mm and 9 mm is taken as a low level. (Jordy Luberizky Permadi 2018)

- **Shape and angle of the pin**

To determine the shape of the pin an overlook in the textile industry is made. Needles are usually common to punch textile materials without produce damage. The end of the needle is called point and exist a widely variety depends on the material. A needle point is classified broadly into two types: round points or cutting points. The sharp shapes are more suitable for cutting operations. On the other hand, round shapes are used to pass through materials.

The pins ends will be described with two features: the shape and the sharpness. The considered shapes are conical end and ellipse end. Regarding the angle, some pre-tests were and the values of 10º and 20º were chosen. The geometrical description of the two possible pin's configurations are shown in Figure 4.4 and Figure 4.5.

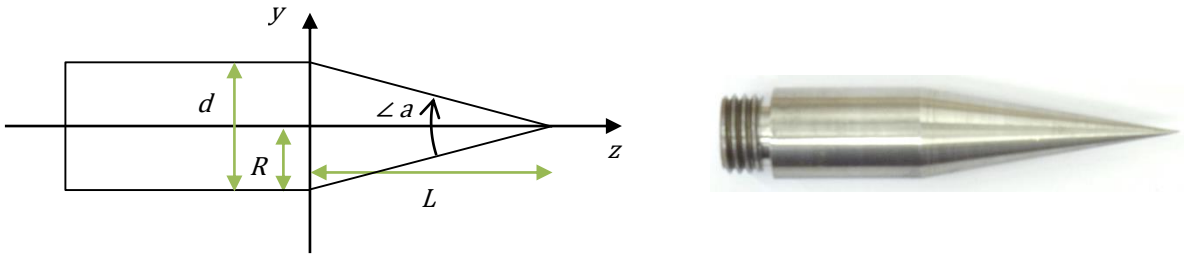

Figure 4.4. Geometry of conic pins. (Jordy Luberizky Permadi 2018)

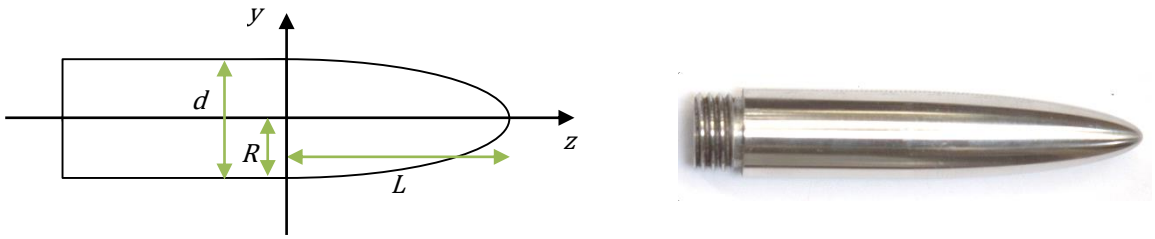

Figure 4.5. Geometry of ellipse pins. (Jordy Luberizky Permadi 2018)

Moreover, the body of the pin will be as the same size as the studied diameter. That means that the pin's geometry is defined by three variables: diameter, shape and angle. It results in a total of 8 different pins.

- **Clamping force**

Clamping force is essential to fix the textile during the perforation. It could cause fibers to behave differently when clamped with various forces. The amount of clamping force required might also be influenced by punch forms, certain punches generate and exert more drag force on specimen. The selection of the appropriate clamp forces was done after made some pre-test with different weights and the pins' shapes previously defined. (Jordy Luberizky Permadi 2018)

The studied weights varied from 5 to 30 kg, achieving the lowest fiber deflections when the mass is higher. Due to this fact, the considered clamping masses to introduce in the design are 15kg and 30kg. (Jordy Luberizky Permadi 2018)

To sum up, the influencing factors studied in the experiment are the following:

Factor	Hole Ø	Material	Shape pin	Angle pin	Clamping mass
Low level (-)	9mm	Ply (-45 /45)	Ellipse	10º	15 Kg
High level (+)	18mm	Ply (0 /90)	Cone	20º	30 Kg

Table 4.1. Possible influencing factors and their levels.

4.1.1.3 Factorial design

Even if the number of factors, k, in a design is small, the 2^K runs specified for a full factorial can quickly become very large. Moreover, replication trials are needed to reduce the variability of the noise factors. For that reason, a fractional factorial design is chosen. For the fractional designs the notation 2^{k-p} is used, where 2 is still the number of levels, k the number of factors that will be experienced and the letter p indicates the degree of fractionation. Therefore, with the factors that have been decided to use and the corresponding levels, the resulting design is a 2^{5-1} resolution V. The resolution is a term which describes the degree to which estimated main effects are aliased with estimated 2-level interactions, 3-level interactions, etc. In the resolution V designs no main effect or two-factor interaction is aliased with any other main effect or two-factor interaction, but

two-factor interactions are aliased with three-factor interactions. (Prat Bartés et al. 2000; Minitab Inc 2017)

The design matrix of the fractional factorial design looks as follows:

	Hole Ø	Material	Shape pin	Angle pin	Clamping force
1	-	-	-	-	+
2	+	-	-	-	-
3	-	+	-	-	-
4	+	+	-	-	+
5	-	-	+	-	-
6	+	-	+	-	+
7	-	+	+	-	+
8	+	+	+	-	-
9	-	-	-	+	-
10	+	-	-	+	+
11	-	+	-	+	+
12	+	+	-	+	-
13	-	-	+	+	+
14	+	-	+	+	-
15	-	+	+	+	-
16	+	+	+	+	+

Table 4.2. Basic design matrix for 2_V^{5-1}experiment.

The completely randomization of the trials order is suitable to protect the factors against not considerate or unknown effects. Moreover replications are needed to reduce the variability of the system, it means performing the same treatment combination more than once. In this experiment five replications will be done, thus it gives a total of eighty runs. See appendix for details about the randomly order used.

4.1.2 Real trajectories description

After the punch testing, images of each trial are obtained, Figure 4.6. The pictures were taken with a camera Nikon D5300 using a len Nikkor 85mm Macro. (Jordy Luberizky Permadi 2018)

The original pictures had a size of 6000x4000px, with a resolution of 300ppp.They will be postprocessed in order to have an approximation of the real trajectories of the carbon fiber samples.

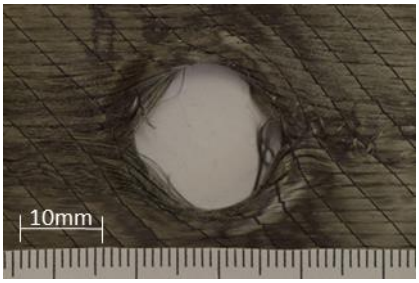

Figure 4.6. Result image after the punching testing of one sample.

By the software GIMP v.2.8 the images are filtered to maximize the color contrast and see clearer the paths of the fibers. Then with the help of a grid, points are plotting manually following the trajectories.

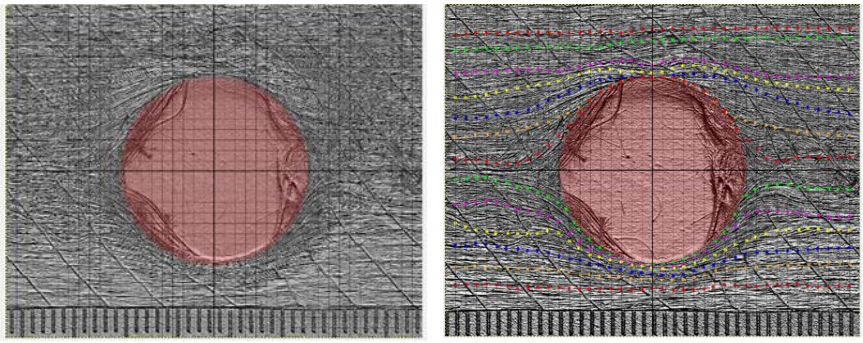

Figure 4.7. Plotting of the real fiber paths

In red the hole diameter is drawn. However, the images were taken with the pin removed thus some fibers in the borderline of the hole are moved. In this situation an overlapping between fibers and the red zone is done, for the plotting process the criteria of following the border of the red circle is taken.

Another scene that can occurs is that the fibers do not always lie on the same plane along the material, sometimes the fibers found on the surface may dip into under layers and resurface again. The method used is approximate the direction that might as well include jumping to the nearest fiber.

A color code is used and the paths which are overlapped are plotted in different layers. These are saved as an image file. Using a specific software, WebPlotDigitizer, which can digitalize the images with a color restriction, the coordinate points are read and exported in an excel file.

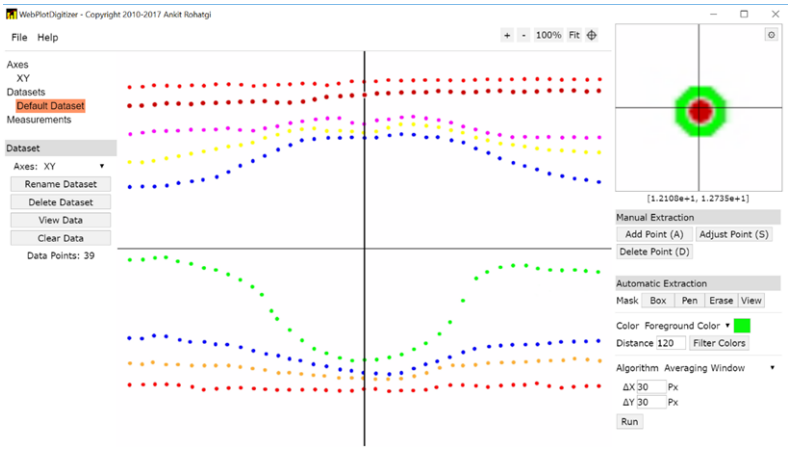

Figure 4.8. Digitalization of the dots

The coordinate system has the origin in the center of the pin's hole. To export the data, this reference and the known length of the axes are used. In this step the color code is useful to recognize each path easily and make this process faster and the different images of every layer have been done to avoid the overlapping effect, hence color recognition problems.

4.1.3 Statistical analysis

The second aim of the tests is the selection of the main factors which effect in the material behavior during the punch process, see beginning of chapter 4.1.4.

Two different responses have been done. Regarding the deformed area, the height and width are define measuring the pixels of the image, Figure 4.9. The area is calculated from the ratio between pixels and mm, this relationship is known through a reference distance in the images, rule.

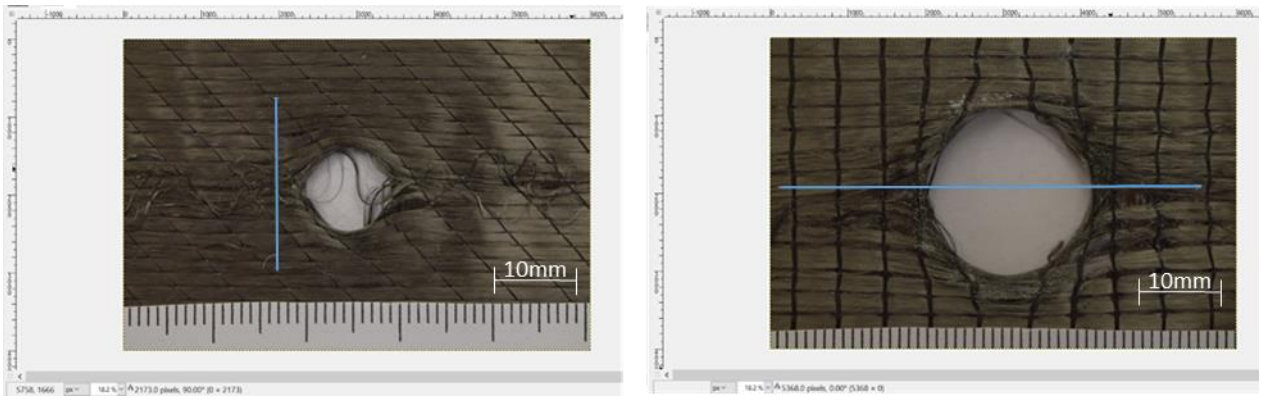

Figure 4.9. Measuring process of the deformed area.

Due to the textile production process, the fibers are grouped into different beams. To determine the height, the measure has been done between the center lines of the beams and in the case of the width, between the points where there is no curvature anymore over the x axis. The measurement process was carried out with the software Gimp V2.8. The measurement process is in almost all images very subjective, therefore the same person did all the measurements and five

repeat trials for each factors combination were tested. In the scene that horizontal fibers are not visible or do not exist, because of the entire sample presents a slight undulation, the measurement has been made in the beam where this phenomenon begins.

For all the images a second output is measured, the grade of waviness. It is defined in a qualitative way by the use of a color scale. In the Figure 4.10 the three situations are shown, in the left image the presence of waviness is high, in the middle image the presence is defined as medium and in the right one the waviness is very low, the color scale used is red, yellow and green respectively.

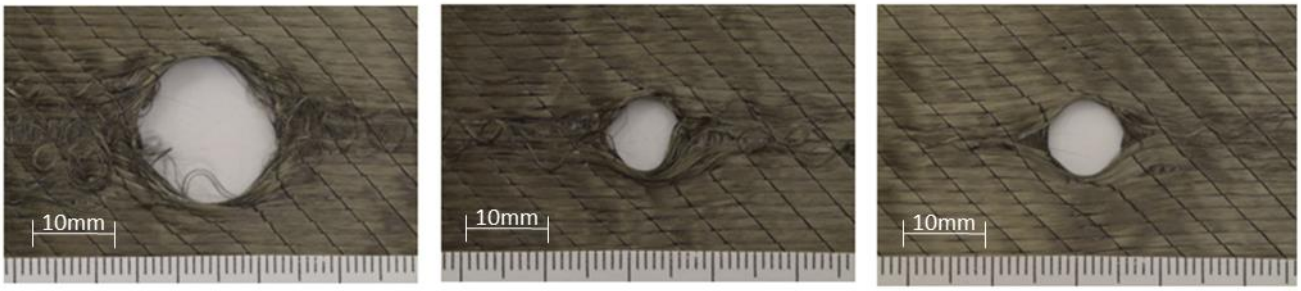

Figure 4.10. Waviness levels. From left to right: Run45, Run20 and Run39.

Moreover, a less subjective method is used to quantify the waviness region. Taking the original images of the samples the waviness is measured in pixels units using the software gimp 2.8. The interested regions are selected using the *Free Select* tool and the number of pixels inside the selection is read in the *Histogram* dialogue box.

The amount of waviness, express in pixels, is the result of the sum of all the selected regions

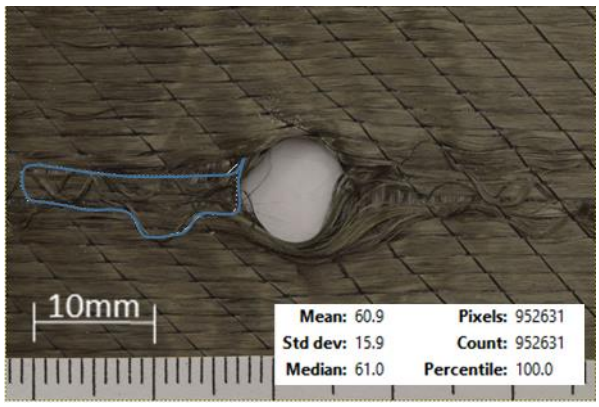

Figure 4.11. Selection of a wave region and histogram dialogue box

In that point the statistical analysis starts. To do it the statistics software Minitab 18.1 is used. First of all, the data is introduced in the worksheet of the program. Five repeat trials were done; it means that the test were done five times in the same conditions it is important remark that it does not mean repeat the measure process of the same tested part. The first step is the calculation of the mean and the standard deviation of the repeat trials, the mean helps to reduce the variability of

the response and the standard deviation allows study the significant effects of the factors over the variability.

With the data of the eighty trials already introduced, an analysis is carried out to see and evaluate the effects of the factors on the response, using the Minitab Analyze Factorial Design option.

Then another analysis, to study the effect of the factors on the variability of the response, will be done. In this step, the logarithms of standard deviations have been used.

Analyzing the resulting plots and the values of the effects coefficients will provide some criteria to select the main factors to introduce in the self-developed model.

4.2 Analytical model

An analytical model is a mathematical equation that describes relationships among variables in a historical data set. The equation either estimates or classifies data values. In essence, a model draws a "line" through a set of data points that can be used to predict outcomes. Algorithms that create analytical models, or equations, come in all shapes and sizes.

Development of the analytical model needs to adhere to a methodology to work productively and generate the most as possible accurate model. The modeling process used in this project consists of distinct steps.

4.2.1 Project definition

Although defining an analytical project does not take as long as some of the other steps, it is the most critical task in the process.

Building the set of candidate models is partially a subjective art; that is why the published literature and other experiences in similar topics can be used to help formulate a set of hypothesis or initial models. In the chapter 3 an overview in some previous works were done. Although any of them where focused on thermoset reinforced polymers, they provide the following ideas or tools to describe the fiber trajectories:

- Representation of a single or group of fibers using a tensor.
- Stress trajectories using a finite element method.
- Geometrical description of the elongation of the fiber.
- Fit minimizing the difference between the angle of assumed function and the angle of principal stress trajectory.

Of the list above, the two last are particularly interesting. The use of geometrical description contributes to figure out trends of the data. Moreover, usually are more friendly methods than tensor and vectors descriptions, which requires a high computational sources.

In addition, the error minimization of a fitting compared to a known data seems a good way to achieve accuracy expressions. Therefore, both methodologies or descriptions will be keep on mind throughout this project.

In the following lines a set of hypothesis are formulated in order to simplify the final expression of the model. Hence the analytical model described an ideal situation:

- Piecewise function

The model is described as a piecewise function, one part to characterize the curvilinear trajectories and another for the straight fibers.

- Symmetry by x and y axis

In an ideal punch process exists symmetry between both axis, thus the description of one quadrant is enough to extrapolate the others.

- Mainly concave shape

Concave shapes are preferred over the convex ones to describe the fiberpaths around the hole. In situations where the convex shapes are also possible the concaves ones will be chosen.

- Defects are not considered

The waviness or another not predictable behaviors of the trajectories are not included in the model. As it was said before the model represents an ideal situation.

4.2.2 Data analysis and regression type selection

Generally, alternative models will involve differing numbers of parameters; the number of parameters will often differ by at least an order of magnitude across the set of candidate models. The more parameters used, the better the fit of the model to the data that is achieved. Large and extensive data sets are likely to support more complexity, and this should be considered in the development of the candidate models.

While this process one must worry about errors due to both underfitting and overfitting. The aim of this chapter is define a procedure to decide the magnitude order and the main shape of the candidate model. In order to achieve it, an analysis of different regression types is done.

Because of the large amount of data, have no sense made the regression analysis of all the trajectories and all the images. In the last subchapter the hypothesis of symmetry to y axis was formulated, thus the regression analysis will be applied only in the half part of five images. The images will be chosen regarding minimize the waviness, consequently clearer paths. The criteria to select the images is a waviness area (px) lower than 40.000px, the both levels of each factor need to be present and repeated combinations are avoided. With these constraints the chosen samples are the ones showed in and Figure 4.12. Their respectively data files will be evaluated, which correspond of the coordinate points of real paths, details in 4.1.2 and 5.1.

Run	Hole Ø	Material	Shape pin	Angle pin	Clamping force	Waviness(px)
42	-	+	+	-	+	117131
76	-	+	-	+	-	133757
63	-	+	-	+	+	187682
3	+	+	+	+	+	364699
39	-	-	+	+	+	397196

Table 4.3. Selected runs for the regression analysis

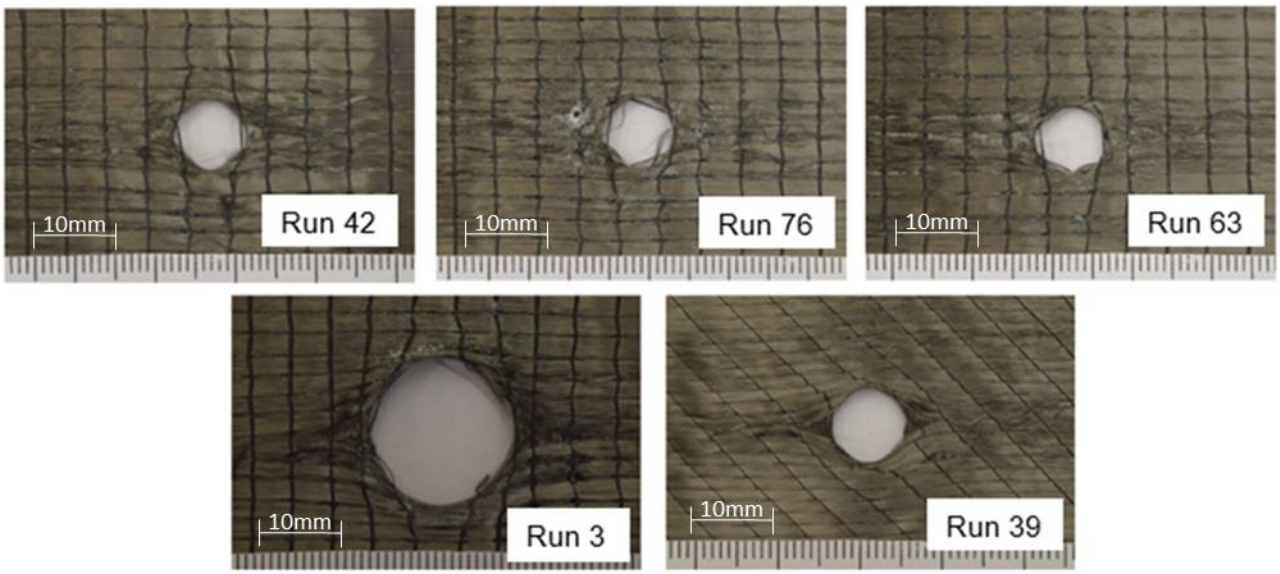

Figure 4.12. Selected images for the regression analysis

.

The analysis consists of searching for the best fit by comparing graphical fit results and comparing numerical fit results including the fitted coefficients and goodness-of-fit statistics. A wide variety of regression models exists, therefore in this work only some polynomial and cosinus shapes are considered.

$f(x) = p_1 \cdot x^7 + p_2 \cdot x^6 + p_3 \cdot x^5 + p_4 \cdot x^4 + p_5 \cdot x^3 + p_6 \cdot x^2 + p_7 \cdot x + p_8$

$f(x) = p_1 \cdot x^6 + p_2 \cdot x^5 + p_3 \cdot x^4 + p_4 \cdot x^3 + p_5 \cdot x^2 + p_6 \cdot x + p_7$

$f(x) = p_1 \cdot x^5 + p_2 \cdot x^4 + p_3 \cdot x^3 + p_4 \cdot x^2 + p_5 \cdot x + p_6$

$f(x) = p_1 \cdot x^4 + p_2 \cdot x^3 + p_3 \cdot x^2 + p_4 \cdot x + p_5$

$f(x) = p_1 \cdot x^3 + p_2 \cdot x^2 + p_3 \cdot x + p_4$

$f(x) = a \cdot \cos(x \cdot b + c) + d$

The known mathematical software Matlab has an app “Curve fitting tool”, which allows made easily comparisons with different kind of curve fittings. However, it is not really efficient to compare a big amount of different data because all the data processing needs to be repeated for each line of each image. This app is used only to find the initial parameter values (a,b,c and d) of the cosinus fit.

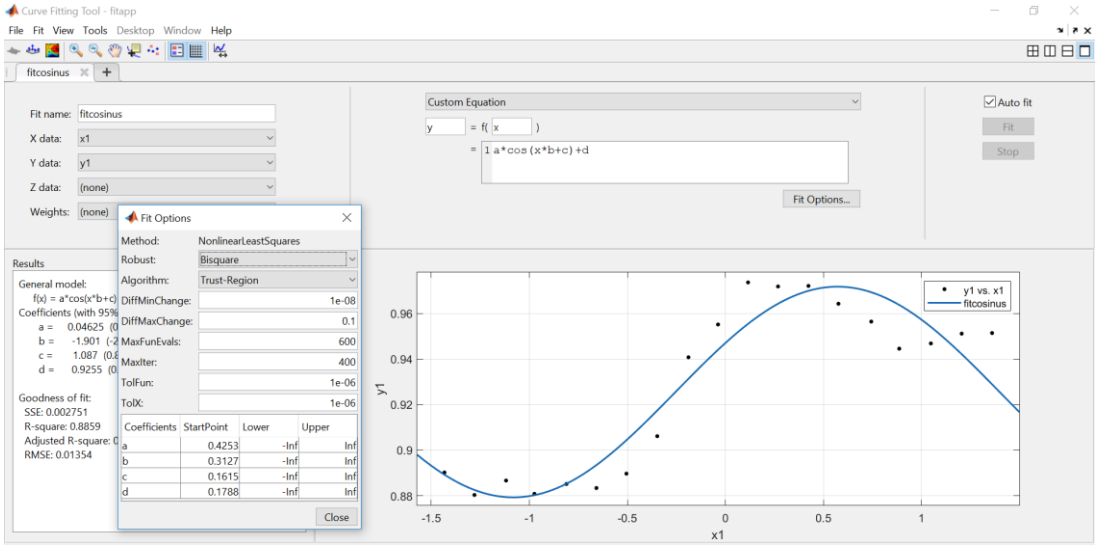

Figure 4.13. Matlab Curve Fitting Tool

The x and y coordinates of the last path, more deformed, are introduced in this app. Then the initial values of a,b, c and d are changed manually to get a size accordantly with the data. Finally, this values are introduced in a self-developed Matlab code, line 196.

A basic code is developed in order to achieve all the fittings plots and goodness of fit values. It allows import data from an excel file, from where the x,y coordinates are read. Only is used the upper half information of each image, it usually means 5-6-7 path lines (10-12-14 rows). In the case that one image has less or more lines, small changes in the code are required.

- Modify range of data
- Increase or decrease variable c, it represents the amount of paths to study, code line 35.
- Increase or decrease cell array size, accordingly the number of paths, code line 39.

For example, for an image with 6 line paths the code will be as is shown in Figure 4.14.

```
35 -  for c=1:6 % c indicates the numer of paths
36 -      x=data(:,2*c-1);
37 -      y=data(:,2*c);
38        %%%%%%%%%%%%%%%%%%
39 -      f=cell(1,6);
40 -      f{c}=createFits(x,y);
41 -      title(['Line' num2str(c)])
42        %%%%%%%%%%%%%%%%%%%%%%%%
43 -  end
```

Figure 4.14. Changes to adapt the code to an image with 6 upper lines.

The code consists of two main functions. The first one, called *importdata(workbookFile,sheetName,startRow,endRow)* allocates column variable names to the information imported, it returns a table with the data read from the excel file, see Figure 4.15.

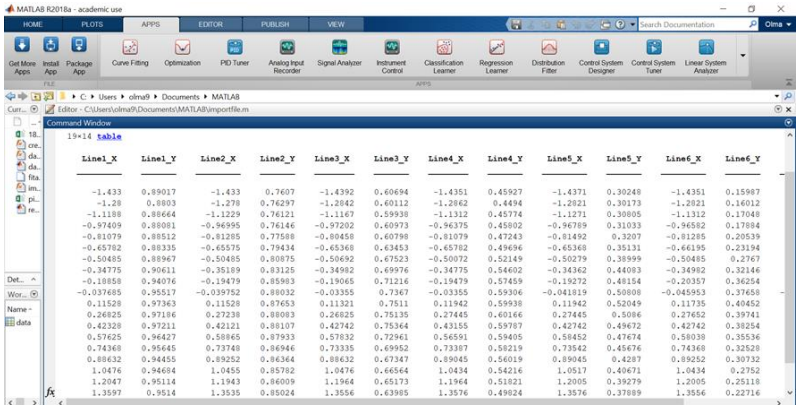

Figure 4.15. Matlab tableout of imported data.

It is employed to check that the data is properly imported. All the regression calculations are performance by a second function called *createFits(x1, y1)*. It creates fits of polynomial from 3th to 7h order and cosine functions. In each iteration it generates a cell array with the goodness of fit values and a plot with all the fits overlapped, there are as iterations as fiber paths in the image.

Before run the code the excel file name and the data range need to be introduced and the cosine initial variables find, if it is required in that point the modifications regarding the amount of paths should be done.

```
25    %% modify if change the name of the woorksheet, sheet or range!!!!
26 -  woorksheetimage='fibrecoordinates_Run 42.xlsx';
27 -  sheet='Sheet1';
28 -  range='B11:M39';
```

Figure 4.16. Data file information

After the Matlab code is performed the outputs are displayed in two different locations:

In the command window:

- Plots of each line with the different fits.
- Table with the data imported from the excel files (x and y data)
- Tables with statistics info, each row one fittype (as tables as paths)

In the workspace:

- Table with the data imported
- cell f. It contains the constant values of each fit of the last evaluated path. If we want to achieve this information of the other paths we need to change the value of c (ex: c=1:2 to know info of path 2) and run again the program.

This procedure is repeated for the five images, selected in the beginning of this subchapter. And then the outputs will be evaluated to take a decision about the main shape and order of the model.

4.2.3 Model creation

In that point the assessment of the project starts. With the knowledge provided in the previous steps the approximated main shape of the real fiberpaths is simplified using the constraints considered in the project definition, chapter 4.2.1.

In addition, the factors to introduced in the model are already known, thus the procedure needs to focused on them. The methodology used is the following:

First, using the data source of the width and height, the deformed area is described mathematically in relation the influence factors. That provides the constraints of the piecewise function of the model, therefore the transition between the straights lines and the curvilinear description is express by the factors values.

Then, the increasing behavior between lines is described. To do this task the real trajectories of the half upper part are evaluated, concretely the y value when x=0. This specific point is the maximum value of the concave shape, so it suggests a growing tendency, which after this procedure is also described using the influence factors.

The last phase of the model creation is figure out the analytical description of the rest of the coefficients. That is not an obvious work, thus the effort is focused only on analyze the data of one quadrant. The curvilinear shape is described separately for each line in relation the main factors and the inflection point of the curve. The values of the points are obtained using a minimization error method.

4.2.4 Model validation

When the model is completely defined a graphical validation is carried out. Using Matlab a basic code to plot the model is performed. It is attached in the appendix of this work.

The input data for the plotting process are the following:

- Excel file information: name, sheet and range where the coefficients are located.
- Radius of the hole in mm
- Coordinates of the deformed region.
- Desired size of the plot
- Desired number of curvilinear paths to be plotted

The output result is a chart of the whole specimen, where the fiberpaths are drawn with space between them of one mm. Moreover, it can be clearly recognized the deformed region and the straight fibers.

The purpose of this drawings is get some conclusions about the accuracy of the model, and make a balance of the weakness and good points of it.

5 Results

This chapter describes the outputs achieved with the methodologies explained in the previous chapter. It aims to report the facts in an objective way with plots, images and tables.

5.1 Measurements and testing results

5.1.1 Real fiber paths

After the postprocessing of the images, an excel file with the coordinates points of each sample were obtained, see 4.1.2. In most of the images were drawn 6 or 7 paths in the upper half and 6 or 7 in the lower part of the image. In the following table is shown one example of the upper half part coordinates. Each line corresponds to the path with the same color of image Table 5.1, where Line1 is the outer one and Line7 the closest to the hole.

Line 1		Line 2		Line 3		Line 4		Line 5		Line 6		Line 7	
X	Y	X	Y	X	Y	X	Y	X	Y	X	Y	X	Y
-19.026	11.068	-18.913	8.063	-18.881	5.057	-18.989	2.235	-19.039	-0.290	-19.128	2.032	-18.967	0.883
-17.983	11.019	-17.991	8.066	-17.978	5.113	-17.966	2.239	-18.037	-0.131	-18.165	2.032	-18.165	0.579
-17.001	11.022	-16.928	8.122	-16.915	5.275	-16.923	2.296	-17.055	-0.052	-16.982	2.093	-17.022	0.395
-15.897	11.132	-15.985	8.178	-15.942	5.371	-15.960	2.510	-16.012	0.133	-16.120	2.153	-16.019	0.493
-14.934	11.293	-14.963	8.156	-15.050	5.519	-14.917	2.593	-15.010	0.238	-15.117	2.456	-14.997	0.913
-13.892	11.297	-13.980	8.265	-13.986	5.760	-13.894	2.702	-14.068	0.608	-14.134	2.759	-14.074	1.273
-12.989	11.511	-12.957	8.347	-12.964	5.684	-12.931	2.732	-13.026	0.872	-12.931	2.961	-13.192	1.592
-11.986	11.567	-11.894	8.298	-12.021	5.556	-11.948	2.788	-12.004	1.083	-11.928	3.365	-12.049	2.072
-10.923	11.571	-10.891	8.407	-11.019	5.296	-11.026	2.765	-10.962	1.532	-11.126	3.688	-11.026	2.311
-9.920	11.654	-10.009	8.358	-10.037	5.194	-10.003	2.927	-10.040	1.770	-10.123	4.092	-10.123	2.550
-8.917	11.763	-9.006	8.467	-8.954	5.224	-8.899	3.247	-9.139	2.034	-9.141	4.516	-8.980	2.909
-7.954	11.766	-8.043	8.523	-7.929	5.887	-7.976	3.567	-8.077	2.536	-7.998	5.121	-7.998	4.335
-6.932	11.770	-6.940	8.580	-6.966	6.365	-6.972	3.939	-7.055	3.011	-7.055	5.868	-7.055	5.841
-5.949	11.958	-5.957	8.583	-5.982	6.922	-5.928	4.444	-5.995	4.121	-6.032	6.938	-6.072	6.945
-4.926	11.882	-4.894	8.587	-4.978	7.400	-5.003	5.218	-5.015	5.098	-5.050	7.685	-5.110	7.607
-3.943	11.912	-3.992	8.669	-3.914	7.661	-3.979	5.973	-3.934	5.811	-3.987	8.271	-3.987	8.368
-3.021	11.916	-3.009	8.805	-2.831	7.828	-2.954	6.590	-2.953	6.445	-3.024	8.594	-3.064	8.809
-1.858	11.814	-1.925	8.967	-1.868	7.912	-1.931	6.857	-2.012	6.762	-2.102	8.998	-2.102	9.027
-0.935	11.870	-1.002	9.128	-0.866	7.784	-0.947	7.098	-0.969	7.052	-1.019	9.260	-1.019	9.226

Table 5.1. Coordinates points of the real paths, Run6.

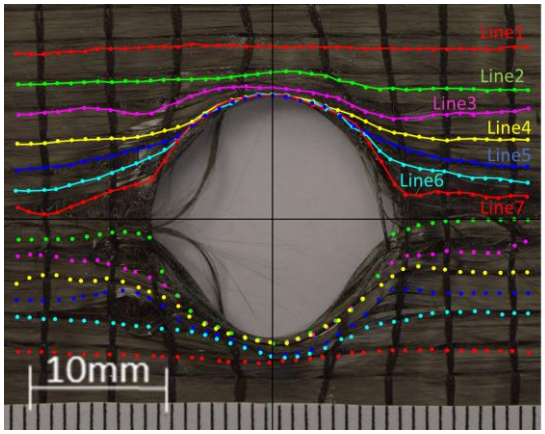

Figure 5.1. Upper half lines, Run6.

5.1.2 Deformed area

Moreover, measures of the deformed area were taken, see 4.1.3.To transform the pixels to mm the following relation was used: 10mm=1200px.

Run	w (px)	h (px)	A [mm2]	Wave	Run	w (px)	h (px)	A [mm2]	Wave
1	4279.000	3207.000	952.969		21	2893.000	1826.000	366.848	
2	3020.000	2173.000	455.726		22	3801.000	2805.000	740.403	
3	5368.000	3223.000	1201.463		23	3784.000	1535.000	403.364	
4	2943.000	1458.000	297.979		24	4147.000	2959.000	852.151	
5	3800.000	2932.000	773.722		25	3999.000	2871.000	797.301	
6	3993.000	3064.000	849.622		26	4114.000	3008.000	859.369	
7	3764.000	2960.000	773.711		27	4389.000	3141.000	957.351	
8	4246.000	2871.000	846.546		28	2211.000	1848.000	283.745	
9	2408.000	1496.000	250.164		29	2178.000	1579.000	238.824	
10	2167.000	1672.000	251.613		30	3999.000	2959.000	821.739	
11	2244.000	1516.000	236.243		31	4609.000	2921.000	934.923	
12	3306.000	2877.000	660.511		32	5517.000	1556.000	596.143	
13	3492.000	2926.000	709.555		33	4571.000	2717.000	862.459	
14	3812.000	2843.000	752.605		34	4702.000	2618.000	854.850	
15	2744.000	1892.000	360.531		35	3537.000	2827.000	694.382	
16	4230.000	3074.000	902.988		36	2414.000	1540.000	258.164	
17	3630.000	3009.000	758.519		37	3751.000	2469.000	643.140	
18	2046.000	1809.000	257.029		38	3856.000	2755.000	737.728	
19	3734.000	2767.000	717.498		39	2761.000	1622.000	310.996	
20	2568.000	1721.000	306.912		40	2783.000	1458.000	281.779	

Run	w (px)	h (px)	A [mm2]	Wave	Run	w (px)	h (px)	A [mm2]	Wave
41	4438.000	2684.000	827.194		61	3223.000	1452.000	324.986	
42	2822.000	2167.000	424.672		62	3756.000	2453.000	639.824	
43	2525.000	1644.000	288.271		63	3559.000	1430.000	353.428	
44	4015.000	3190.000	889.434		64	3702.000	2519.000	647.593	
45	3707.000	2827.000	727.756		65	3894.000	2734.000	739.319	
46	2800.000	1705.000	331.528		66	3839.000	2755.000	734.475	
47	2640.000	1516.000	277.933		67	5055.000	2596.000	911.304	
48	2651.000	1667.000	306.890		68	2536.000	1771.000	311.893	
49	2635.000	1425.000	260.755		69	2382.000	1463.000	242.005	
50	3580.000	2673.000	664.538		70	4725.000	2832.000	929.250	
51	22987.000	1914.000	3055.355		71	3685.000	2915.000	745.957	
52	4081.000	1524.000	431.906		72	2849.000	1408.000	278.569	
53	4158.000	2860.000	825.825		73	4460.000	2690.000	833.153	
54	3602.000	1689.000	422.485		74	2513.000	1507.000	262.992	
55	2673.000	1452.000	269.528		75	3009.000	1507.000	314.900	
56	2744.000	1485.000	282.975		76	2646.000	1733.000	318.439	
57	3245.000	1837.000	413.963		77	4801.000	2964.000	988.206	
58	4329.000	2596.000	780.423		78	4031.000	1826.000	511.153	
59	3894.000	2717.000	734.722		79	3256.000	1634.000	369.466	
60	4136.000	3251.000	933.759		80	2580.000	1831.000	328.054	

Table 5.2. Deformed area calculation and subjective waviness.

5.1.3 Waviness region

In order to analyze statistically the waviness effect in the samples, a numerical response is needed. Using the measure process describe in 4.1.3 the following information of the effected regions is collected.

In the Figure 5.2 is shown one example, for each image were calculated the waviness region as the total of the different waviness areas. The amount of areas depends on each particular image and the shapes are irregular to fit better to the real waviness surface.

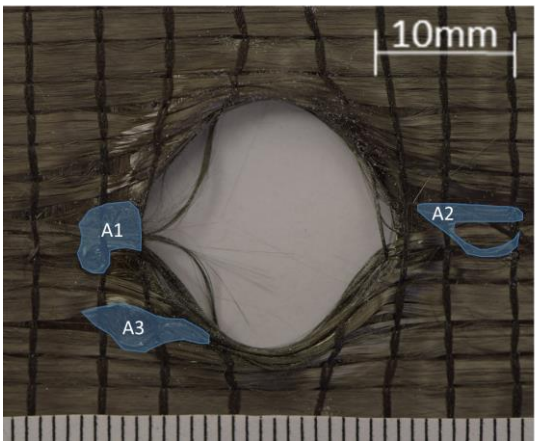

Figure 5.2. Waviness regions, Run6.

Run	A1 (px)	A2 (px)	A3(px)	Total	Run	A1 (px)	A2 (px)	A3(px)	Total
1	1453690	2252682		3706372	21	67955			67955
2	1352677	1577098		2929775	22	138569	510924	366460	1015953
3	364699			364699	23	44574	45200		89774
4	1617614	396780		2014394	24	428432	35034		463466
5	2435242	1708735		4143977	25	296786	177012		473798
6	340133	397291	576280	1313704	26	1220697	182940		1403637
7	1516043	1174291		2690334	27	156042			156042
8	482991			482991	28	1364349	250037	68783	1683169
9	372814	180053	122366	675233	29	1196016	284240		1480256
10	1098959	418045	357769	1874773	30	196455			196455
11	458847	488681		947528	31	355651			355651
12	988227	702108		1690335	32	385747			385747
13	735884	639436		1375320	33	683042			683042
14	90133	259933		350066	34	682036	46777		728813
15	155756			155756	35	147371	66906		214277
16	1249347	80696		1330043	36	445584			445584
17	1189029	1062014		2251043	37	400345			400345
18	1036101	911754		1947855	38	1872927	803065		2675992
19	835953	326223		1162176	39	188090	209106		397196
20	1040343	952631		1992974	40	475961			475961

Run	A1 (px)	A2 (px)	A3(px)	Total	Run	A1 (px)	A2 (px)	A3(px)	Total
41	1634113			1634113	61	146527	117418	285092	549037
42	117131			117131	62	1891630	207602		2099232
43	325468	165295	137360	628123	63	187682			187682
44	871370	365523		1236893	64	1044611	387695	242821	1675127
45	1433058	1444779		2877837	65	2013851	1218645		3232496
46	1015837	103781		1119618	66	897601	378272		1275873
47	476395			476395	67	306990	693681		1000671
48	764260			764260	68	728349	134379		862728
49	1474256	1951743	71477	3497476	69	1218591	708287		1926878
50	947931	288819		1236750	70	811922	131918		943840
51	484572	216688		701260	71	675865	79817		755682
52	41363			41363	72	737594	174973	213244	1125811
53	2067040	140725	126972	2334737	73	1308010	110433	981310	2399753
54	1714633	47323		1761956	74	293308	1213026		1506334
55	1057110	1026025		2083135	75	177727			177727
56	423860			423860	76	50479	83278		133757
57	513016	304433		817449	77	271717			271717
58	29044	80324	128183	237551	78	55617	85620		141237
59	998725	302151	73930	1374806	79	560777			560777
60	220107	60207		280314	80	852805	72498		925303

Table 5.3. Waviness area calculation (px).

5.2 Factorial Design

5.2.1 Response: Deformed area

How is describe in the chapter 4.1.4 a previous treatment of the measured deformed areas is done. In the following table, Table 5.4, is shown for each combination the value of the five repeat trials and the respectively logarithm of the standard deviation. The order of the columns is the standard of a 2^{5-1} experiment, see Table 4.2.

	R1	R2	R3	R4	R5	Std.Dev	log dev
1	250.164	258.164	242.005	262.992	369.466	52.547	1.721
2	952.969	758.519	827.194	664.538	647.593	125.485	2.099
3	236.243	281.779	431.906	282.975	324.986	74.230	1.871
4	849.622	852.151	957.351	821.739	933.759	58.998	1.771
5	251.613	306.912	288.271	306.890	422.485	64.063	1.807
6	660.511	902.988	737.728	825.825	833.153	94.062	1.973
7	846.546	360.531	403.364	424.672	3055.355	1155.670	3.063
8	862.459	694.382	929.250	745.957	988.206	122.884	2.089
9	455.726	257.029	238.824	260.755	269.528	89.781	1.953
10	773.722	859.369	727.756	739.319	911.304	79.810	1.902
11	596.143	277.933	413.963	353.428	311.893	125.563	2.099
12	717.498	797.301	854.850	889.434	780.423	66.880	1.825
13	283.745	310.996	331.528	278.569	328.054	24.541	1.390
14	773.711	740.403	734.722	639.824	734.475	50.121	1.700
15	297.979	366.848	314.900	318.439	511.153	87.299	1.941
16	1201.463	709.555	752.605	934.923	643.140	225.126	2.352

Table 5.4. Standard deviation of the repeat trials.

After the evaluation of the previous table is conclude the high variability between trials, especially in the case 7. This consideration is the reason to make a variability analysis with the standard deviations.

First of all, the analysis of the effects in the response deformed area is done. It is performed using the data of the eighty trials, blue values in Table 5.2. Some tables and graphical information are obtained as a result.

The Pareto chart shows the absolute values of the standardized effects from the largest effect to the smallest effect. The standardized effects are t-statistics that test the null hypothesis that the effect is 0. The chart also plots a reference line to indicate which effects are statistically significant.

The reference line for statistical significance depends on the significance level, denoted by alpha. In our analysis alpha=0,05 is chosen, thus a confidence of 95%.

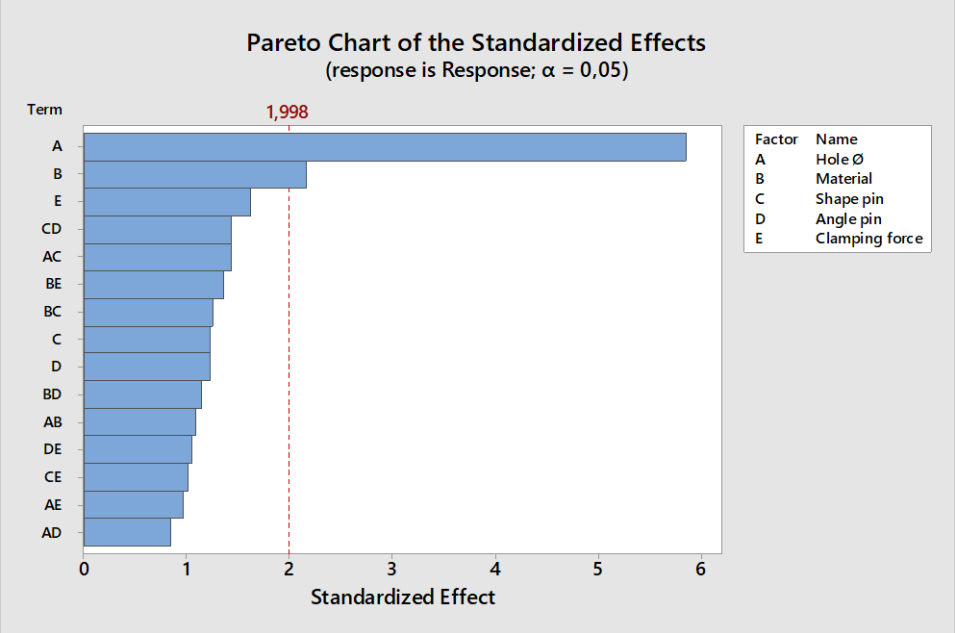

Figure 5.3. Pareto plot of the effect of all the factors.

In Figure 5.3, the bars that represent factors A and B cross the reference line that is at 1,998. These factors are statistically significant at the 0.05 level with the current model terms.

Because the Pareto chart displays the absolute value of the effects, is possible determine which effects are large but not determine which effects increase or decrease the response. In order to examine the magnitude and direction of the effects on one plot the normal probability plot of the standardized effects is the suitable.

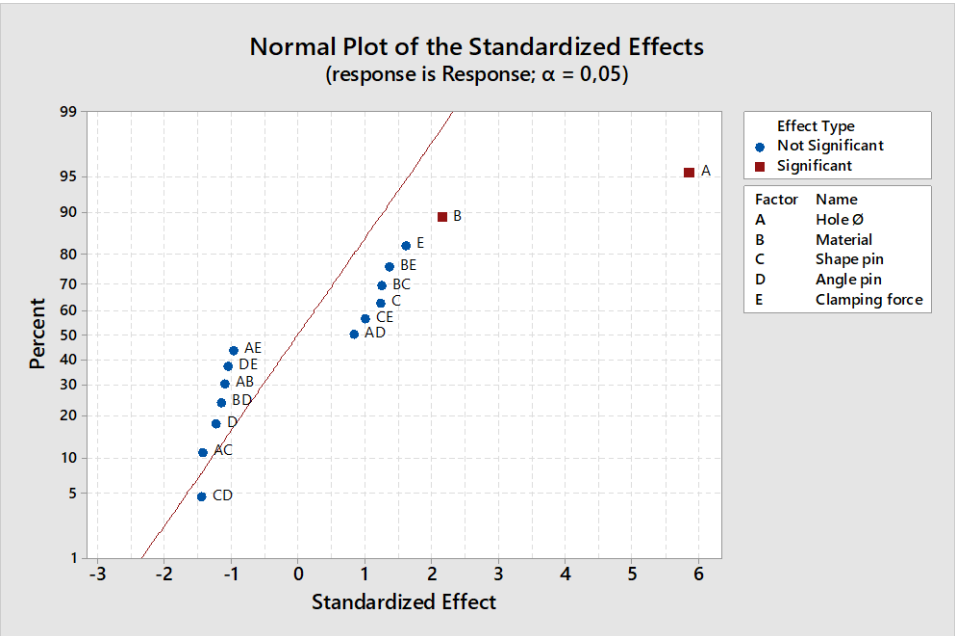

Figure 5.4. Normal plot of the effect of all the factors.

The normal probability plot of the effects, Figure 5.4, is used to determine the magnitude, direction, and the importance of the effects. On the normal probability plot of the effects, effects that are further from 0 are statistically significant. The color and shape of the points differ between statistically significant and statistically insignificant effects. On this plot, the main effects for factors A and B are statistically significant at the 0.05 level.

In addition, the plot indicates the direction of the effect. Hole Ø (A) has a positive standardized effect. When "Hole Ø" changes from the low level to the high level of the factor, the response increases. Material (B) has a positive standardized effects as well. When the material is in high level, ply 0/90, the response increases.

Term	Effect	Coef	SE Coef.	T-Value	P-Value
Constant		609,3	34,1	17,88	0,000
Hole Ø	399,4	199,7	34,1	5,86	0,000
Material	147,7	73,8	34,1	2,17	0,034
Shape pin	84,0	42,0	34,1	1,23	0,222
Angle pin	-84,0	-42,0	34,1	-1,23	0,222
Clamping force	110,7	55,4	34,1	1,62	0,109
Hole Ø*Material	-74,2	-37,1	34,1	-1,09	0,281
Hole Ø*Shape pin	-97,6	-48,8	34,1	-1,43	0,157
Hole Ø*Angle pin	57,5	28,7	34,1	0,84	0,402
Hole Ø*Clamping force	-66,0	-33,0	34,1	-0,97	0,337
Material*Shape pin	85,8	42,9	34,1	1,26	0,213
Material*Angle pin	-78,0	-39,0	34,1	-1,14	0,257
Material*Clamping force	92,9	46,5	34,1	1,36	0,178
Shape pin*Angle pin	-98,0	-49,0	34,1	-1,44	0,155
Shape pin*Clamping force	69,1	34,6	34,1	1,01	0,315
Angle pin*Clamping force	-71,4	-35,7	34,1	-1,05	0,299

.

Table 5.5. Minitab output of the effects of all the factors.

The Table 5.5 has a very useful column, Coeff. The coefficient for a term represents the change in the mean response associated with an increase of one coded unit in that term, while the other terms are held constant. The sign of the coefficient indicates the direction of the relationship between the term and the response. The size of the coefficient is half the size of the effect. The effect represents the change in the predicted mean response when a factor changes from its low level to its high level.

The size of the effect is usually a good way to assess the practical significance of the effect that a term has on the response variable. The size of the effect does not indicate whether a term is statistically significant because the calculations for significance also consider the variation in the response data. To determine statistical significance, examine the p-value for the term or the previous plots.

If the coefficients of the effects are evaluated, it is clearly seen that the “Hole Ø” produces the biggest effect in the response (*199,7*), therefore the diameter which will maximize the deformation area is 18mm.The material has also a significant effect (*73,8*), the coefficient is positive so it means that this effect is produces when the material change from low to high level, ply 0/90.

A second analysis were done in order to study the variability in the response. The methodology used is the same, but now the term of response is the logarithm of the standard deviations, calculated in Table 5.4. The outputs are the following:

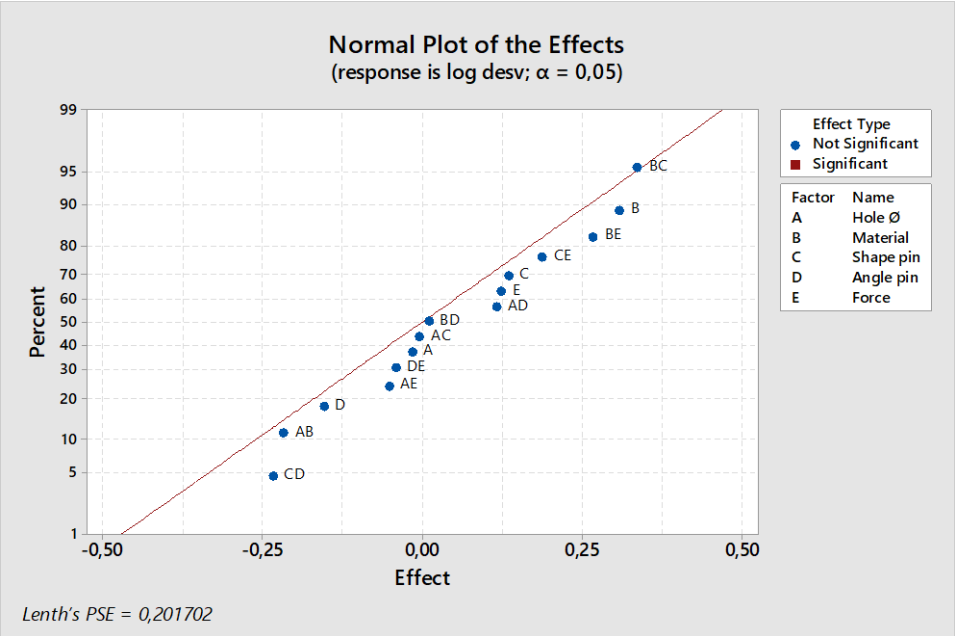

Figure 5.5. Normal plot of the effects over the variability.

In the plot Figure 5.5, the main effects are not clear, there are any statistically significant effect and all the absolute effects values are between 0 and 0,5. Apparently the variability of the standard deviation of the trials, despite applying a logarithm, is still too excessive.

Due to the high effect of the Hole Ø the statistical analysis are repeated using the data of the bigger diameter and the smaller diameter separately. Their objective is compare the factors which have a lower effect and evaluate if they are still statistically insignificant when the factor of the diameter is remove. The study case will be transformed from one 2^{5-1} experiment to two 2^{4-1} experiment. The normal plots resulting are shown below.

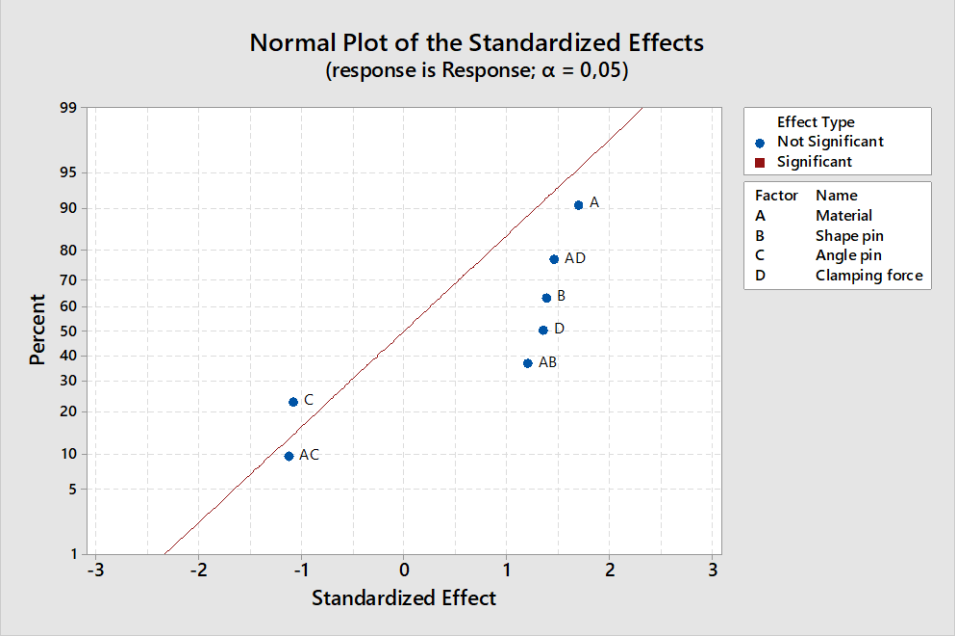

Figure 5.6. Normal plot of the effects when Hole Ø is in low level

Term	Effect	Coef	SE Coef	T-Value	P-Value	VIF
Constant		409,6	65,7	6,24	0,000	
Material	221,9	110,9	65,7	1,69	0,101	1,00
Shape pin	181,6	90,8	65,7	1,38	0,176	1,00
Angle pin	-141,5	-70,7	65,7	-1,08	0,289	1,00
Clamping force	176,7	88,4	65,7	1,35	0,188	1,00
Material*Shape pin	157,2	78,6	65,7	1,20	0,240	1,00
Material*Angle pin	-147,1	-73,5	65,7	-1,12	0,271	1,00
Material*Clamping force	190,9	95,5	65,7	1,45	0,156	1,00

Table 5.6. Minitab output of the effects of the factors when Hole Ø is in low level.

The Figure 5.6 shows the normal plot of the effects when the data with the smaller diameter are introduced. Any factor has an effect statistically significant. However, the size of the effect coefficients, Table 5.6, is slightly bigger for the Material term (*110,9*) and the interaction Material*Clamping force term (*95,5*).

When the data of the higher diameter is used the normal plot of the effects and the coefficient values are the shown below.

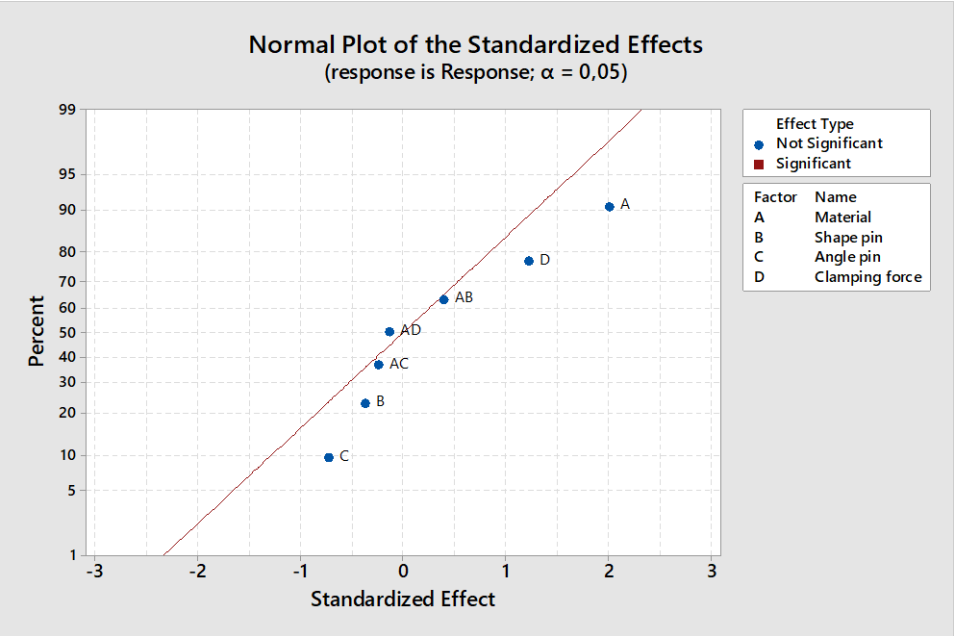

Figure 5.7. Normal plot of the effects when Hole Ø is in high level

Term	Effect	Coef	SE Coef	T-Value	P-Value	VIF
Constant		809,0	18,3	44,20	0,000	
Material	73,5	36,8	18,3	2,01	0,053	1,00
Shape pin	-13,6	-6,8	18,3	-0,37	0,714	1,00
Angle pin	-26,5	-13,3	18,3	-0,72	0,474	1,00
Clamping force	44,7	22,4	18,3	1,22	0,231	1,00
Material*Shape pin	14,3	7,2	18,3	0,39	0,698	1,00
Material*Angle pin	-8,9	-4,4	18,3	-0,24	0,810	1,00
Material*Clamping force	-5,1	-2,5	18,3	-0,14	0,891	1,00

Table 5.7. Minitab output of the effects of the factors when Hole Ø is in high level.

In that case the effects have a different behavior, although there are not significant factors. Most of the factors and the interactions have a low absolute standardized effect and small coefficients size, (<*15*). Then the coefficient effect of the Clamping force has a value slightly higher (*22,4*) and finally the coefficient of the Material is the highest with a value of *36,8*.

5.2.2 Response: Waviness

In the following subchapter the results of the factorial design analysis with the response waviness are shown. The data introduced is the displayed in the Table 5.3, for details about how was collected see chapter 4.1.3.

As in the previous statistical analysis the confidence used is 95%.

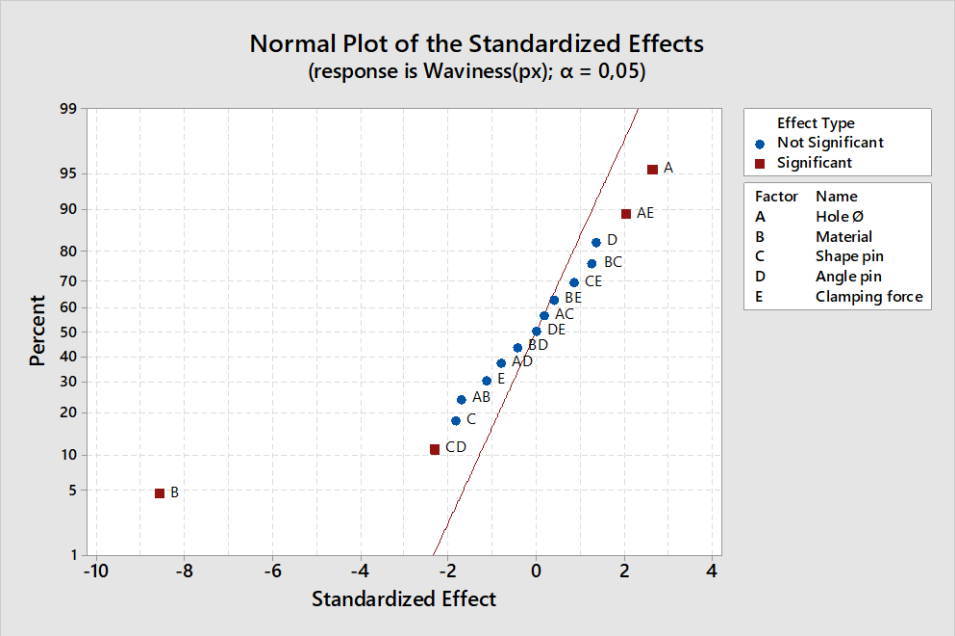

Figure 5.8. Normal plot effect of all factors with response waviness.

Term	Effect	Coef	SE Coef	T-Value	P-Value	VIF
Constant		1157364	73140	15,82	0,000	
Hole Ø	385918	192959	73140	2,64	0,010	1,00
Material	-1254050	-627025	73140	-8,57	0,000	1,00
Shape pin	-266886	-133443	73140	-1,82	0,073	1,00
Angle pin	198011	99005	73140	1,35	0,181	1,00
Clamping force	-165311	-82655	73140	-1,13	0,263	1,00
Hole Ø*Material	-250212	-125106	73140	-1,71	0,092	1,00
Hole Ø*Shape pin	26409	13204	73140	0,18	0,857	1,00
Hole Ø*Angle pin	-118645	-59322	73140	-0,81	0,420	1,00
Hole Ø*Clamping force	299218	149609	73140	2,05	0,045	1,00
Material*Shape pin	185869	92934	73140	1,27	0,208	1,00
Material*Angle pin	-63652	-31826	73140	-0,44	0,665	1,00

Material*Clamping force	57929	28965	73140	0,40	0,693	1,00
Shape pin*Angle pin	-337009	-168505	73140	-2,30	0,024	1,00
Shape pin*Clamping force	124963	62481	73140	0,85	0,396	1,00
Angle pin*Clamping force	1151	576	73140	0,01	0,994	1,00

Table 5.8. Minitab output of the effects of all factors with response waviness.

Both in the chart, Figure 5.8, and in the Minitab output, Table 5.8 the factors more significant in relation to the response waviness, are the Material and the Hole Ø. This experiment has considered all the possible interactions of a design 2^{5-1}, and the interactions Shape pin-Angle pin and Hole Ø-Clamping force result as statistical significant.

The Material term is the one that has a more significant effect on the response. In addition, the coefficient of the effect has a negative sign (*-627025*), this means that if the variable increases, the response decreases. If the aim of the analysis is minimize the response waviness, this variable should be in the highest value, which corresponds to the carbon fiber 0/90 ply.

The variable Hole Ø, also has a significant effect on the response. In this case the effect coefficient is positive (*192959*), which means that when the variable increases, the response increases as well. Therefore, it is interesting to keep the variable in its minimum value corresponding to 9mm.

Moreover, there are the interactions Shape pin-Angle pin and Hole Ø-Clamping force with a statistical significant effect. The first with a negative coefficient (*-168505*) and the second one with a positive coefficient (*149609).*

To understand the behavior of the response in relation the interested interactions, a cube plot to show the relationship between the pair factors and a response is used.

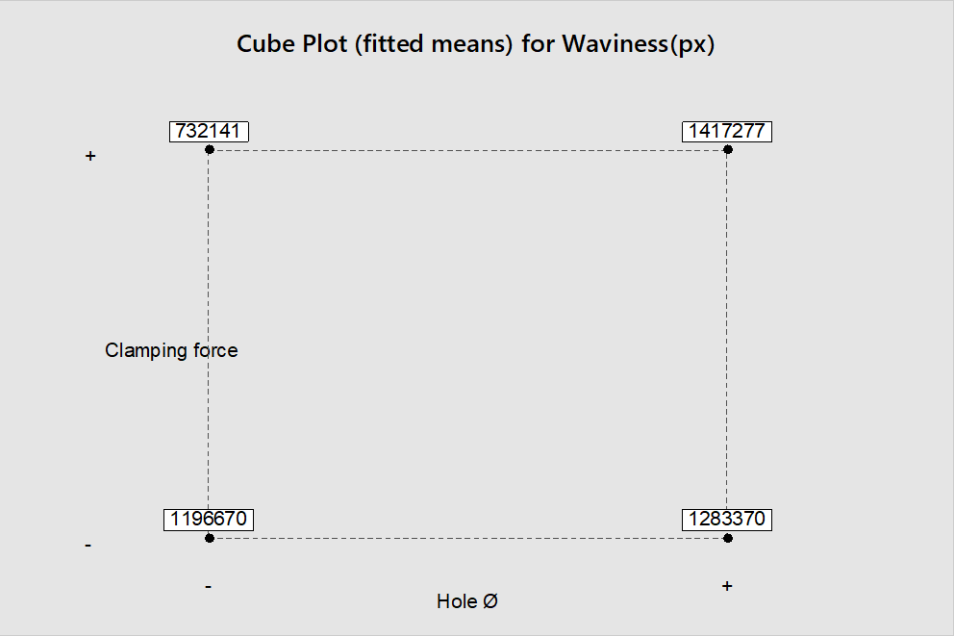

Figure 5.9. Interaction between Hole Ø and Clamping force.

For the waviness data, one square displays all combinations of factor settings for the two factors involved in the interactions and the fitted mean for each combination. Fitted means are useful for assessing response differences due to changes in factor levels rather than differences due to the unbalanced experimental conditions. It is generally good practice to use the fitted means, instead of the data means, to obtain more precise results.

The Figure 5.9 displays the cube plot for the factors Hole Ø and Clamping force. The minimum fitted mean takes place when the factor Hole Ø is in low level and the Clamping force in high level.

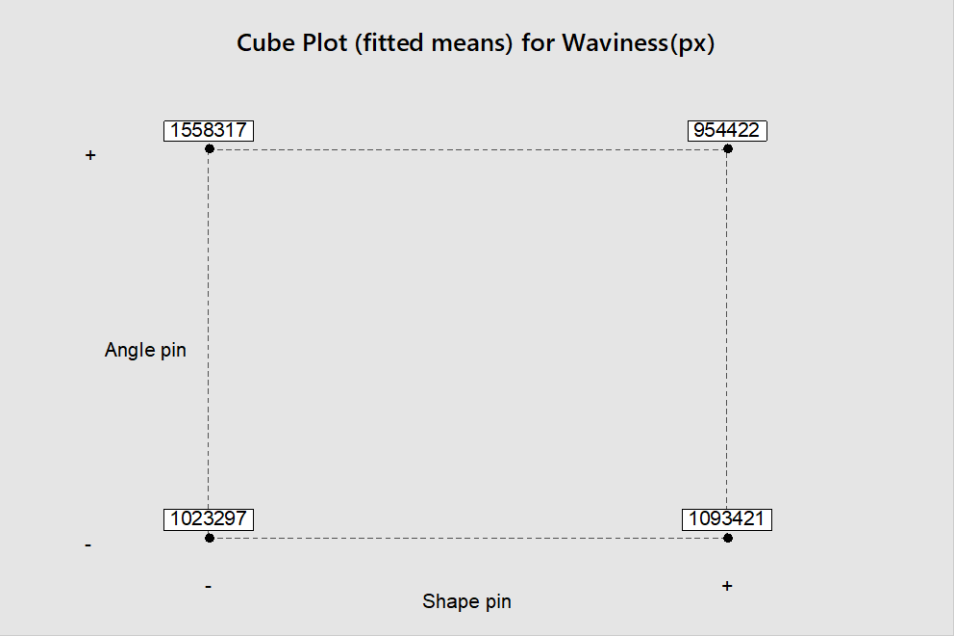

Figure 5.10. Interaction between Angle pin and Shape pin

The second cube plot, Figure 5.10, represents the relationship between the factor Angle pin, Shape pin and the response. In that case, the fitted mean is lower when the Shape and Angle pin are in high level. It has sense with the previous analysis, which determined a negative effect coefficient.

5.3 Regression analysis

The point trajectories images of Run3, Run39, Run42, Run63 and Run76 were selected to decide the main shape of the model. The methodology used is described in chapter 4.2.2.

One of the input information needed is the range of data, which will be imported by the code. In order to achieve a higher accuracy in the fitting, this will be chosen for each image. The aim is to avoid the information of straight fibers due to the distortion of the fitted curve. This effect is illustrated with yellow marks in Figure 5.11, the points of these regions are not included in any fitting because of the amount of horizontal points in both ends. In that situations the criteria of removed some initial and final points was taken.

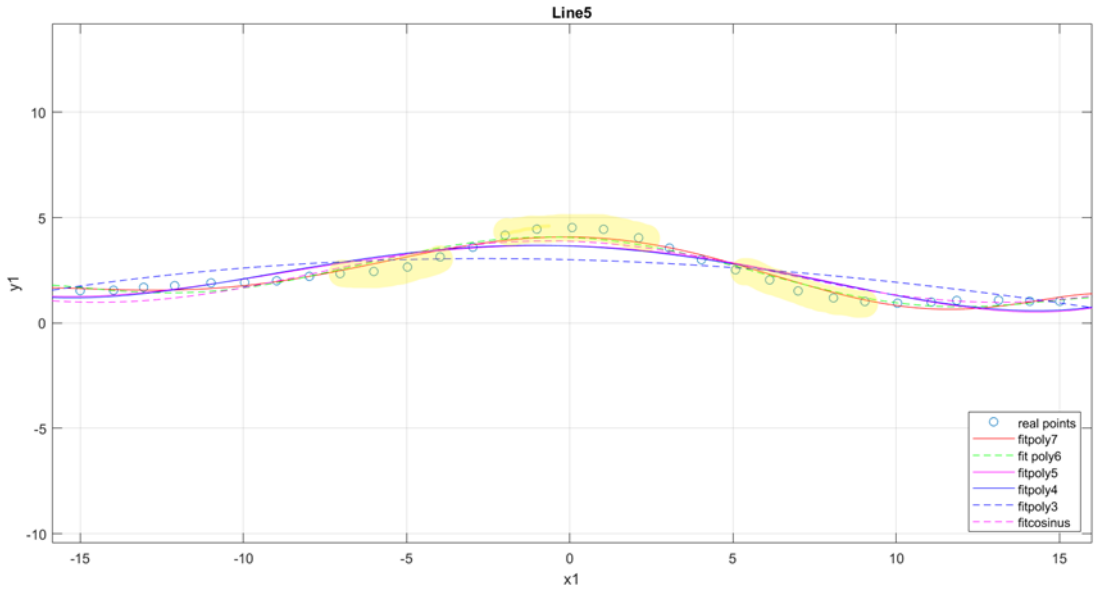

Figure 5.11. Fitting with all the points, distortion effect.

The criteria to decide how much points should be removed is the following. The path closer to the hole, the waviest, is plotted with all the points, moreover two red straight lines, which begin in the end points, are drawn overlapping the chart, see Figure 5.12. Then the two half of the curve, left and right, are evaluate separately. The y coordinate difference between the left endpoint and the rest of the left half part are calculated, the same procedure with the right half part is repeated. The remove points are the ones with a difference value lower than 0,1.

When a value above or equal than 0,1 is find the following dots are counted. This constraint is taken, because some curves cross the red straight lines. In that intersection the difference value is close to 0, however it does not mean that these dots belong to a straight line of the fiber.

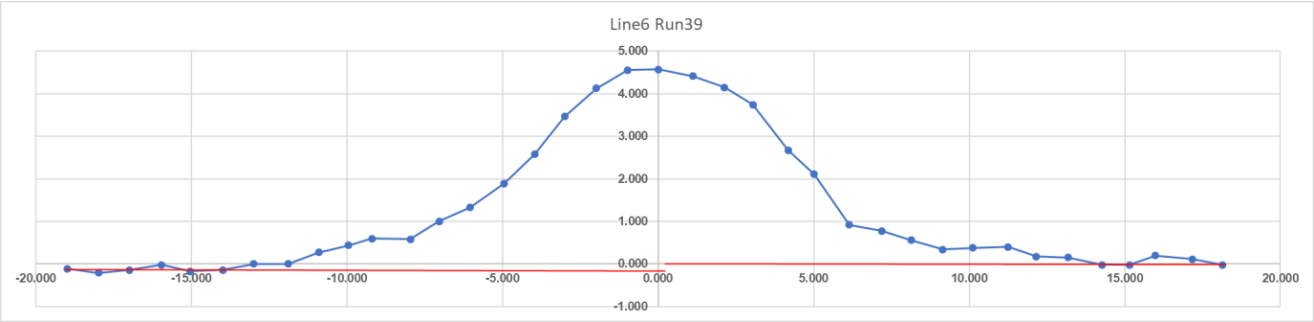

0.000	4.5991
0.094	4.4376
0.032	4.1751
0.091	3.7713
0.059	2.7012
0.032	2.1359
0.115	0.9447
0.115	0.8033
0.390	0.5812
0.551	0.3591
0.713	0.3995
0.692	0.4197
1.116	0.1976
1.439	0.1774
2.005	0.0003
2.691	0.0003
3.580	0.2178
4.246	0.137
4.670	0.0003
4.690	0.0003

Figure 5.12. Range data selection and y coordinates difference.

The previous methodology was performed in the five runs and they conclude in the following data ranges,

Table 5.9.

Moreover, in the table is given information about the amount of studied lines of each run and number of points per line. According to the criteria used, the number of points eliminated is not always the same at both ends of the curve. That is the reason why in some situations the number of points is even and in other odd.

	Data range	Nº lines	Nº points per line
Run3	B5:O41	7	37
Run39	B11:M41	6	31
Run42	B11:M39	6	29
Run63	B15:K38	5	24
Run76	B10:M32	6	23

Table 5.9. Range of coordinates used to generate the fits.

When the coordinates' data ranges were known, the next step was find accurately initial values for the fitting of cosine, $a \cdot \cos(b \cdot x + c) + d$, the ones used are shown in the

Table 5.10. Different values can conclude in different curves.

	a	b	c	d
Run3	1	0.1	0.1	0.1
Run39	1	0.1	0.1	0.1
Run42	1	0.1	0.1	0.1
Run63	1	0.1	0.1	1
Run76	1	0.1	0.1	0.1

Table 5.10. Initial values of the cosine function parameters.

Then, all the fittings were obtained with the Matlab code attached in the appendix. One example of the outputs is shown in the following figures.

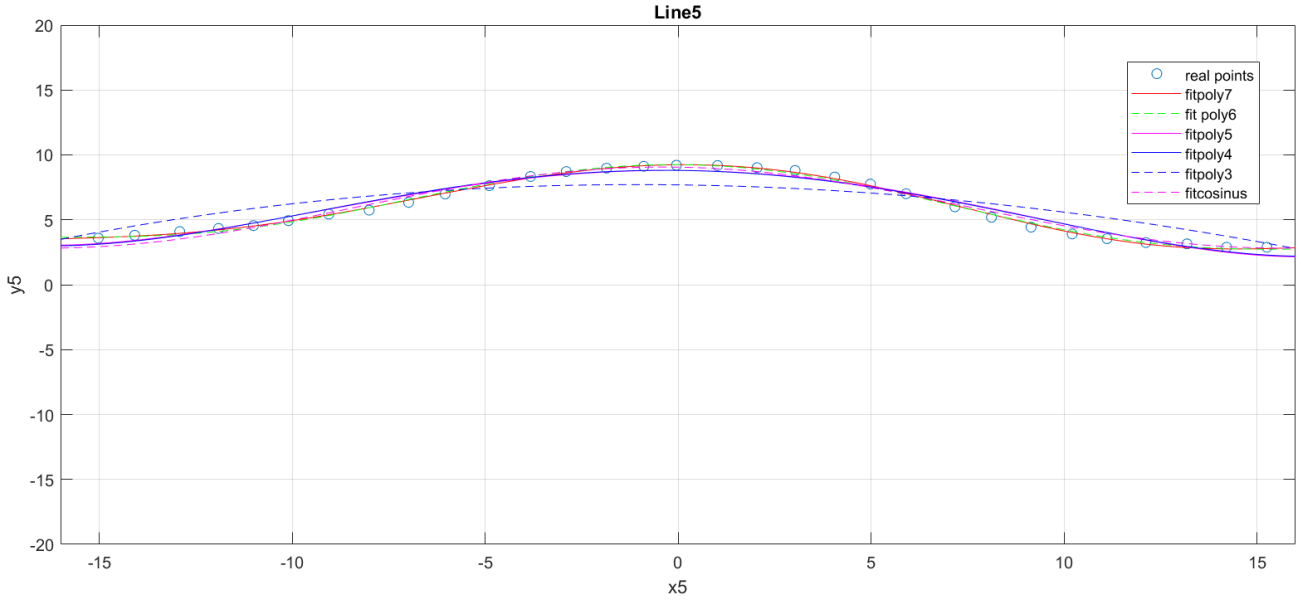

Figure 5.13. Fitting plot Line 5 of Run3.

Figure 5.13 represents the different studied fittings for one fiber path. Each fitting curve is displayed in a different color and overlapped with the measured points. The aim of this plot is by a visual evaluation reject the fittings which differ a lot of the real points, in the example figure is clear that fitpoly3, discontinues blue line, is not a good candidate to describe this path. Moreover, the

graphical representation helps to detect any anomaly point or errors produced in the collecting data process from the real images.

The plots axis' lengths are [x_{min} x_{max} y_{min} y_{max}]=[-20 20 16 16], the same size of the points plotting images. On the one hand, it gives a good overview of the plotted curve's shape, but due to the amount of lines makes harder the visual interpretation. For this reason, all the output plots are saved as Matlab figure file, hence it is able to zoom in. The same image showed before is amplified in Figure 5.14.

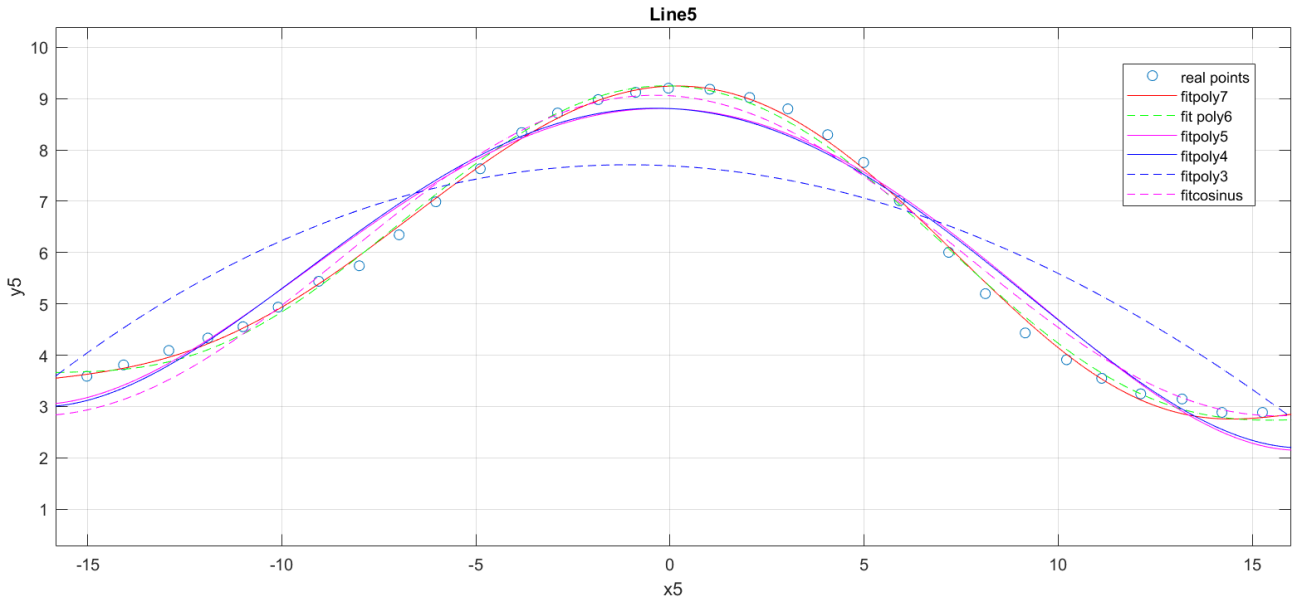

Figure 5.14. Amplified fitting plot Line 5 of Run3.

During the evaluation is important pay special attention to the center region of the last path, Line5, Line6 or 7 depends on the image, since it is the location of the hole and future insert. The real points with x coordinate between -4,5 and 4,5 in the case of images Ø9mm or between -9 and 9 images Ø18mm are considered a border, all the fitting curves under them will be reject as a possible candidate.

After using graphical methods to evaluate the goodness of fit, can happens that is no possible the elimination of more fits examining them graphically. Then is useful the use of the numerical fit results, the parameters of the goodness-of-fit (gof) statistics are the following:

- **SSE** is the sum of squares due to error of the fit. A value closer to zero indicates a fit that is more useful for prediction.
- **R-square** is the square of the correlation between the response values and the predicted response values. A value closer to 1 indicates that a greater proportion of variance is accounted for by the model.
- **DFE** is the degree of freedom in the error.
- **Adj R-sq** is the degrees of freedom adjusted R-square. A value closer to 1 indicates a better fit.

- **RMSE** is the root mean squared error or standard error. A value closer to 0 indicates a fit that is more useful for prediction.

Of all the gof parameters, the sum of squares due to error (SSE) and the adjusted R-square statistics are examined to help to determine the best fit.

The SSE is a measure of the discrepancy between the data and an estimation model. It is the sum of the squares of residuals, see right image of Figure 5.15. The areas of the blue squares represent the squared residuals with respect to the fit regression.

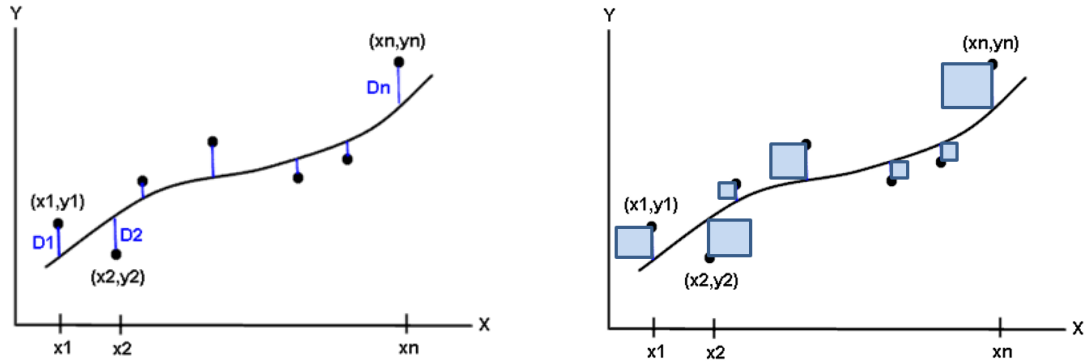

Figure 5.15. Residuals on the right and square residuals on the right.

The statistic R-square measures how successful the fit is in explaining the variation of the data. It can take on any value between 0 and 1, with a value closer to 1 indicating that a greater proportion of variance is accounted for by the model. For example, an R-square value of 0.9987 means that the fit explains 99.87% of the total variation in the data about the average.

If the number of fitted coefficients increases, R-square will increase as well. Although the fit may not improve in a practical sense. To avoid this situation, the Adjusted R-Square is used. This statistic uses the R-square statistic defined above, and adjusts it based on the residual degrees of freedom.

For each fit, the goodness-of-fit (gof) statistics are calculated. Compare all fits of the same path simultaneously helps to determine which expression and how well it fits the data. The gof parameters referred the example of the previous plots are calculated, Table 5.11, and the SSE and Adj.R-Square are analyzed in the following paragraphs.

Line5

	sse	rsquare	dfe	adjrsquare	rmse
Polyfit7	0.24737	0.99873	29	0.99842	0.092359
Polyfit6	0.97635	0.99497	30	0.99397	0.1804
Polyfit5	4.0012	0.9794	31	0.97608	0.35926
Polyfit4	5.9028	0.96961	32	0.96581	0.42949
Polyfit3	37.811	0.80536	33	0.78766	1.0704
Cosinusfit	187.78	0.033326	33	-0.054553	2.3855

Table 5.11. Goodness of fit statistics Line 5 of Run3.

The largest SSE for *Polyfit3* indicates it is a poor fit, which was already determined by examining the plotting fit. The lowest SSE value is associated with *Polyfit7*. However, the behavior of this fit beyond the data range is closer of *Polyfit6*, which needs less coefficients. The next best SSE value is associated with the sixth-degree polynomial fit, *Polyfit6*, suggesting it might be the best fit.

However in other gof tables, such as Table 5.12 , the SSE and adjusted R-square values for the polynomial fits from fifth to seventh-degree are all very close to each other.

Line5

	sse	rsquare	dfe	adjrsquare	rmse
Polyfit7	0.12375	0.99671	15	0.99517	0.090829
Polyfit6	0.88588	0.97644	16	0.9676	0.2353
Polyfit5	0.89188	0.97628	17	0.9693	0.22905
Polyfit4	4.2243	0.88765	18	0.86268	0.48444
Polyfit3	4.9946	0.86716	19	0.84619	0.51271
Cosinusfit	37.185	0.011021	19	-0.14513	1.399

Table 5.12. Goodness of fit statistics Line 5 of Run76.

Resolve the best fit issue by examining the confidence bounds for the remaining fits provide information of their accuracy. The coefficients information is generated in a cell array, *f*, in the workspace of Matlab. It contains the coefficients values and bounds of each fit of the last path. If the data of other paths is required, the value of c needs to be changed, in the example c=1:5 to know information of line 5. Then run the program again.

For example to read the data of seventh-degree polynomial is needed type `f{1,5}{1,1}` in the command window. See Figure 5.16Figure 5.16. Cell array call to get fit coefficients data. to know how to get the rest of cells information.

f{1,3}{1,1}
f{1,3}{2,1} Line
f{1,3}{3,1} Curve fitting type
f{1,3}{4,1}

1	Seventh-degree polynomial
2	Sixth-degree polynomial
3	fifth-degree polynomial
4	fourth-degree polynomial
5	third-degree polynomial
6	Cosinus fitting

Figure 5.16. Cell array call to get fit coefficients data.

To get the coefficients bounds first the data was normalized, it is done why the y values differ several orders of magnitude from x. The operation $X = \frac{x - mean}{St.dsv.}$ is made automatically with the option Normalize in the Matlab code.

```
[fitresult{5}, gof(5)] = fit( xData, yData, ft, 'Normalize', 'on' )
```

Regarding the Line5 of Run76, the bounds of the coefficients are shown in the figure below.

```
Linear model Poly7:
ans(x) = p1*x^7 + p2*x^6 + p3*x^5 + p4*x^4 + p5*x^3 +
             p6*x^2 + p7*x + p8
  where x is normalized by mean -2.976 and std 6.812
Coefficients (with 95% confidence bounds):
  p1 =     -0.5257  (-0.6422, -0.4091)
  p2 =      0.0428  (-0.05207, 0.1377)
  p3 =       3.123  (2.587, 3.658)
  p4 =      0.1218  (-0.2513, 0.4948)
  p5 =      -6.308  (-7.028, -5.587)
  p6 =       -1.53  (-1.914, -1.146)
  p7 =       4.472  (4.195, 4.75)
  p8 =       3.354  (3.266, 3.443)
```

```
Linear model Poly6:
ans(x) = p1*x^6 + p2*x^5 + p3*x^4 + p4*x^3 + p5*x^2 +
             p6*x + p7
  where x is normalized by mean -2.976 and std 6.812
Coefficients (with 95% confidence bounds):
  p1 =     0.03797  (-0.2065, 0.2824)
  p2 =      0.7335  (0.5331, 0.934)
  p3 =      0.1388  (-0.8223, 1.1)
  p4 =      -3.266  (-3.918, -2.613)
  p5 =      -1.546  (-2.536, -0.5568)
  p6 =       3.532  (3.059, 4.004)
  p7 =       3.359  (3.132, 3.587)
```

```
Linear model Poly5:
ans(x) = p1*x^5 + p2*x^4 + p3*x^3 + p4*x^2 + p5*x + p6
  where x is normalized by mean -2.976 and std 6.812
Coefficients (with 95% confidence bounds):
  p1 =      0.7335  (0.5394, 0.9277)
  p2 =      0.2859  (0.1239, 0.4478)
  p3 =      -3.265  (-3.898, -2.633)
  p4 =      -1.685  (-2.099, -1.27)
  p5 =       3.531  (3.073, 3.988)
  p6 =       3.378  (3.19, 3.566)
```

Figure 5.17. Matlab output of confidence bounds and coeffcients, Line5 Run76.

The bounds cross zero on the p2 and p4 coefficients for the seventh-degree polynomial and on the p1 and p3 coefficients for the sixth-degree polynomial. This means it cannot be sure that these coefficients differ from zero. If the higher order model terms may have coefficients of zero, they are not helping with the fit, which suggests that this model overfits the studied data.

However, the small confidence bounds do not cross zero on p1, p2, p3, p4, p5 and p6 for the fifth-degree polynomial fit, Poly5, indicate that the fitted coefficients are known fairly accurately. Therefore, the fifth-degree polynomial will be selected as the best fit to extrapolate the data.

This procedure of analysis was done in all the studied paths of the five images. Given the following results, Table 5.13.

	Run3	Run39	Run42	Run63	Run76
Line1	Overfitted	Poly3 or cos	Poly3 or cos	Poly5,Poly4, Poly3 or cos	Poly4, Poly3 or cos
Line2	Overfitted: Poly7, Poly6, Poly5 and Poly4	Poly6	Poly3	Overfitted: Poly7, Poly6, Poly5 and Poly4	Poly4
Line3	Poly7 or Poly6	Overffited: Poly7, Poly6, Poly5 and Poly4	Poly7, Poly6, Poly5	Poly6	Poly5 or cos
Line4	Poly7 or Poly6	Poly7, Poly6, Poly5	Overfitted:Poly7 or Poly6	Overffited:Poly7 orPoly6	Poly5
Line5	Poly7 or Poly6	Poly7	Poly6	Overffited:Poly7 or Poly6	Poly5
Line6	Poly7 or Poly6	Poly7 or Poly6	Poly7 or Poly6	-	Poly5
Line7	Poly6	-	-	-	-

Table 5.13. Results after confidence bounds analysis

If the results are analyzed, three situations can be described. The simplest scene is the one when only one candidate is chosen, it means that only one fit satisfies the graphical, gof parameters and bounds coefficients evaluation. The next case is when more than one fit is selected, that happens when is not possible discard more fits, more than one satisfy the bounds evaluation. Finally, in some cases, after the confidence interval evaluation all the candidate's bounds cross the 0, thus the overfitting can occur.

In order to simplify the shape of the model, in the cases which there are more than one candidate, the lowest polynomial degree is chosen. About the cosine function it is only suitable in some outer lines, thus it was dismissed. In the following table, the selected polynomial and the respectively SSE are shown in bold letters. Information about the closest polynomial are also display, therefore it makes easier the comparison to decide the main shape.

	Run3		Run39		Run42		Run63		Run76	
	Fit	SSE	Fit	SSE	Fit	SSE	Fit	SSE	Fit	SSE
Line1										
	Poly3	**0.33355**	**Poly3**	**0.14305**	**Poly3**	**0.027956**	**Poly3**	**0.038814**	**Poly3**	**0.031643**
	Poly4	0.30502	Poly4	0.14297	Poly4	0.027672	Poly4	0.025398	Poly4	0.013805
Line2	Poly3	1.4881	Poly5	0.090337			Poly3	0.056016	Poly3	0.035066
	Poly4	**0.54037**	**Poly6**	**0.037683**	**Poly3**	**0.017684**	**Poly4**	**0.042737**	**Poly4**	**0.01235**
	Poly5	0.54028	Poly7	0.032396	Poly4	0.017086	Poly5	0.041528	Poly5	0.011659
Line3	Poly5	1.1036	Poly3	0.96912	Poly4	0.37464	Poly5	0.54493	Poly4	0.17265
	Poly6	**0.35117**	**Poly4**	**0.23427**	**Poly5**	**0.14425**	**Poly6**	**0.1863**	**Poly5**	**0.074417**
	Poly7	0.21523	Poly5	0.19163	Poly6	0.089023	Poly7	0.1619	Poly6	0.072795
Line4	Poly5	2.0012	Poly4	0.29618	Poly5	2.5854	Poly5	7.5623	Poly4	1.3458
	Poly6	**0.93377**	**Poly5**	**0.22061**	**Poly6**	**0.56508**	**Poly6**	**2.794**	**Poly5**	**0.3492**
	Poly7	0.19178	Poly6	0.15306	Poly7	0.019485	Poly7	2.725	Poly6	0.3474
Line5	Poly5	4.0012	Poly6	0.345	Poly5	3.1152	Poly5	8.9564	Poly4	4.2243
	Poly6	**0.97635**	**Poly7**	**0.20263**	**Poly6**	**0.5487**	**Poly6**	**2.6949**	**Poly5**	**0.89188**
	Poly7	0.24737			Poly7	0.53099	Poly7	2.5993	Poly6	0.88588
Line6	Poly5	6.9961	Poly5	6.4566	Poly5	6.8864			Poly4	6.9121
	Poly6	**2.6288**	**Poly6**	**1.6758**	**Poly6**	**1.6246**			**Poly5**	**1.1704**
	Poly7	2.1667	Poly7	1.3235	Poly7	1.0344			Poly6	1.1343
Line7	Poly5	10.348								
	Poly6	4.8298								
	Poly7	4.5856								

Table 5.14. Best fit for each studied path and respectively SSE.

Analyzing the previous table some conclusions can be taken. There is a relevant difference between the values of SSE of outer and inner paths. From Line1 to Line3 the residual sum of squares is lower than 0,5 in almost all situations, therefore all the polynomials are suitable candidates. However, in the inner paths the values of SSE increase reaching values around 10 in the worst situation. In that point is still hard decide a polynomial degree to describe all the paths.

Thus a deep analysis of the residuals of the inner lines were done. The residuals from a fitted model are defined as the differences between the response data and the fit to the response data at each predictor value, $residual = data - fit$, see Figure 5.15. This procedure is considered a good way to figure out in which regions the error is higher, especially in that situations where the SSE is high. From Line4 to 7 the residual plots of each run were calculated using the Curve Fitting app of Matlab, one example is explained below in Figure 5.18.

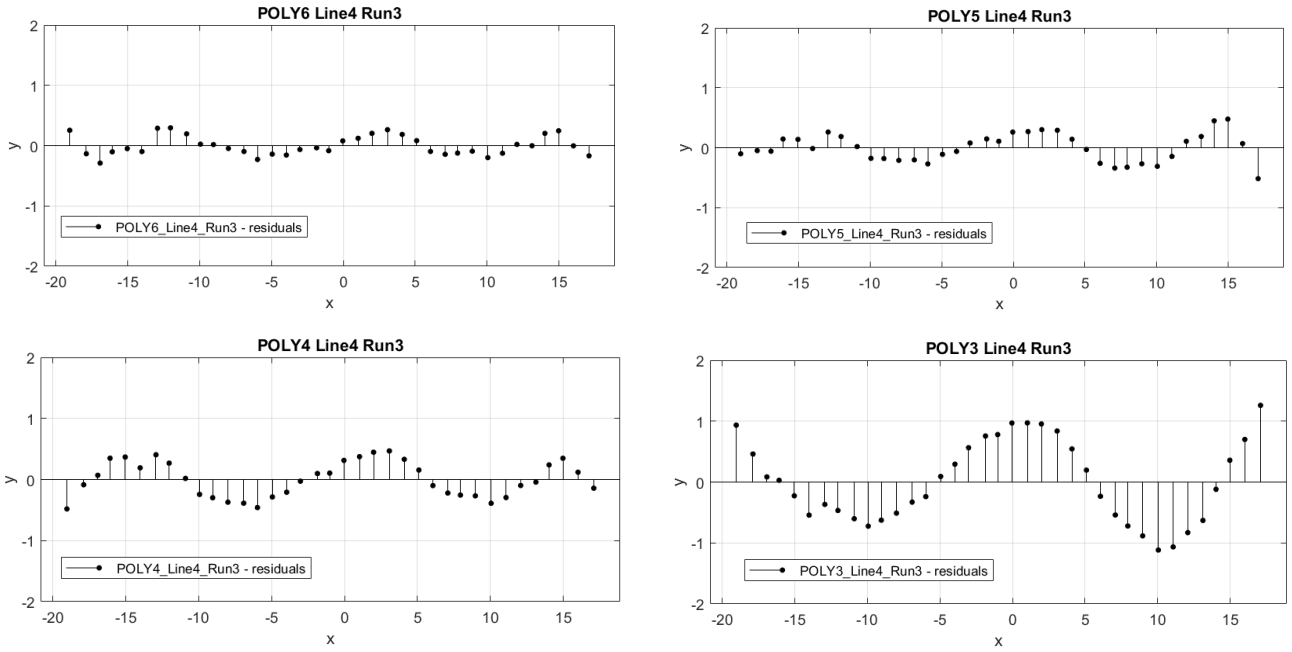

Figure 5.18. Residuals Line4 Run3.

A graphical display of the residuals for a third-degree polynomial to sixth-degree fit is shown. The plots display the residuals relative to the fit, which is the zero line. If the residuals appear to behave randomly around zero, it suggests that the model fits the data well.

In addition, the residual values were collected and classified in relation to the degree-polynomial and line. The different values of each polynomial were treated independently, in Table 5.15 is shown the data of the sixth-degree polynomial from Run39.

Line4_Run39			Line5_Run39			Line6_Run39		
Real x	Region	residuals	Real x	Region	residuals	Real x	Region	residuals
-13.121	-14.000	0.507	-13.070	-14.000	0.694	-12.991	-13.000	-2.033
-12.115	-13.000	0.147	-12.035	-13.000	0.341	-11.888	-12.000	-1.994
-11.110	-12.000	-0.108	-11.130	-12.000	0.187	-10.905	-11.000	-1.685
-10.084	-11.000	-0.126	-10.084	-11.000	-0.015	-9.943	-10.000	-1.489
-9.049	-10.000	-0.255	-9.099	-10.000	-0.571	-9.201	-10.000	-1.301
-8.134	-9.000	-0.335	-8.154	-9.000	-0.894	-7.958	-8.000	-1.277
-7.068	-8.000	-0.344	-7.309	-8.000	-0.677	-7.035	-8.000	-0.821
-6.103	-7.000	-0.297	-6.143	-7.000	-0.632	-6.052	-7.000	-0.463
-5.097	-6.000	-0.164	-4.997	-5.000	-0.436	-4.949	-5.000	0.142
-4.152	-5.000	-0.114	-3.992	-4.000	-0.105	-3.967	-4.000	0.863
-3.006	-4.000	0.068	-3.006	-4.000	0.130	-3.004	-4.000	1.786
-2.041	-3.000	0.231	-2.001	-3.000	0.521	-1.981	-2.000	2.488
-1.036	-2.000	0.372	-0.995	-1.000	0.669	-0.979	-1.000	2.948
-0.041	-1.000	0.441	-0.096	-1.000	0.726	0.013	1.000	3.003
1.015	2.000	0.272	1.015	2.000	0.575	1.127	2.000	2.881
2.001	3.000	0.261	2.021	3.000	0.468	2.130	3.000	2.654
2.966	3.000	0.192	3.107	4.000	0.373	3.052	4.000	2.283
3.992	4.000	0.082	4.132	5.000	0.191	4.175	5.000	1.253
5.097	6.000	-0.005	5.097	6.000	0.038	5.017	6.000	0.718
6.123	7.000	-0.104	6.033	7.000	-0.037	6.140	7.000	-0.434
6.927	7.000	-0.176	7.008	8.000	-0.219	7.183	8.000	-0.538
8.063	9.000	-0.241	7.933	8.000	-0.352	8.146	9.000	-0.726
8.958	9.000	-0.045	8.978	9.000	-0.463	9.149	10.000	-0.913
9.944	10.000	-0.095	9.944	10.000	-0.485	10.111	11.000	-0.838
11.029	12.000	-0.226	11.029	12.000	-0.411	11.254	12.000	-0.777
12.035	13.000	-0.144	12.055	13.000	-0.294	12.157	13.000	-0.967
13.040	14.000	-0.142	13.020	14.000	-0.094	13.179	14.000	-0.951
14.066	15.000	-0.097	14.126	15.000	0.050	14.262	15.000	-1.090
15.071	16.000	0.043	15.152	16.000	0.145	15.145	16.000	-1.059
16.097	17.000	0.181	16.217	17.000	0.261	15.987	16.000	-0.811
17.042	18.000	0.222	17.022	18.000	0.317	17.170	18.000	-0.850

Table 5.15. Residual values Line4,5 and 6 of Run39

The goal of collect the residual values is compare how well each degree-polynomial fits all the paths. In order to analyze it graphically, the x coordinate is rounded to the upper value. This step is needed, due to the fact the coordinate points were taking manually, chapter 4.1.2, therefore the x values are close but not identical. So the x range take integer values from -20 to 20. Then the data of the different runs were join. As the residuals can be positive or negative, the addition of the values is done like a sum square operation. Moreover, it has to be keep in mind that the runs have different x ranges, which produces plots with more information in the central region, which is also the most critical.

The following plots, one from each polynomial degree, show in different colors the residuals from each line. The comparison between the four plots gives information about which fit is the more suitable and in which regions the error is higher.

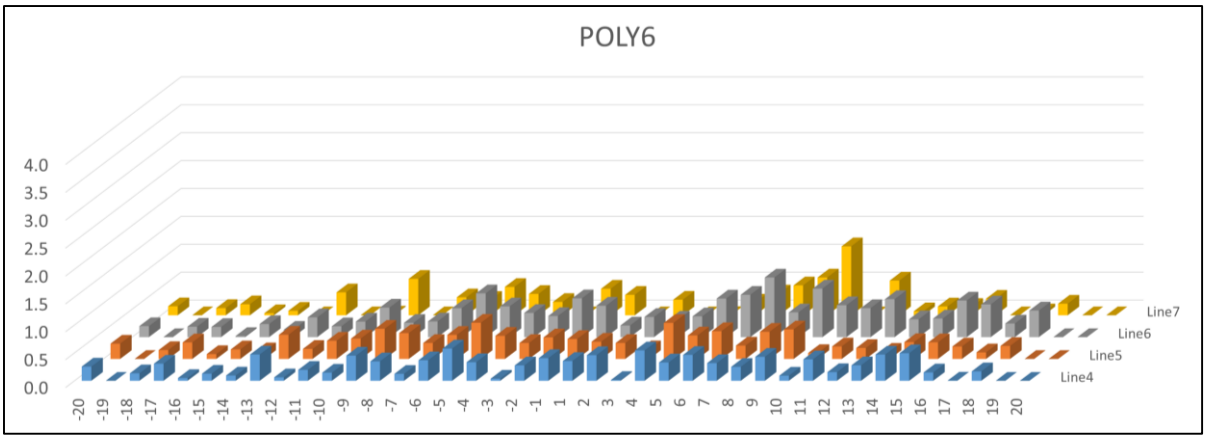

Figure 5.19. Residuals of sixth-degree polynomial

The residuals of the sixth-degree polynomial have low values, less than 1, in almost all the x range. The data are concentrate mostly in the center and left region with a peak value of a little more than 1 in the region 9 of Line7. About the central part, from -5 to 5, the residuals have a maximum value around 0,7 in the region -2 of Line2 and an average value of 0,360. The values in detail are attached in the appendix.

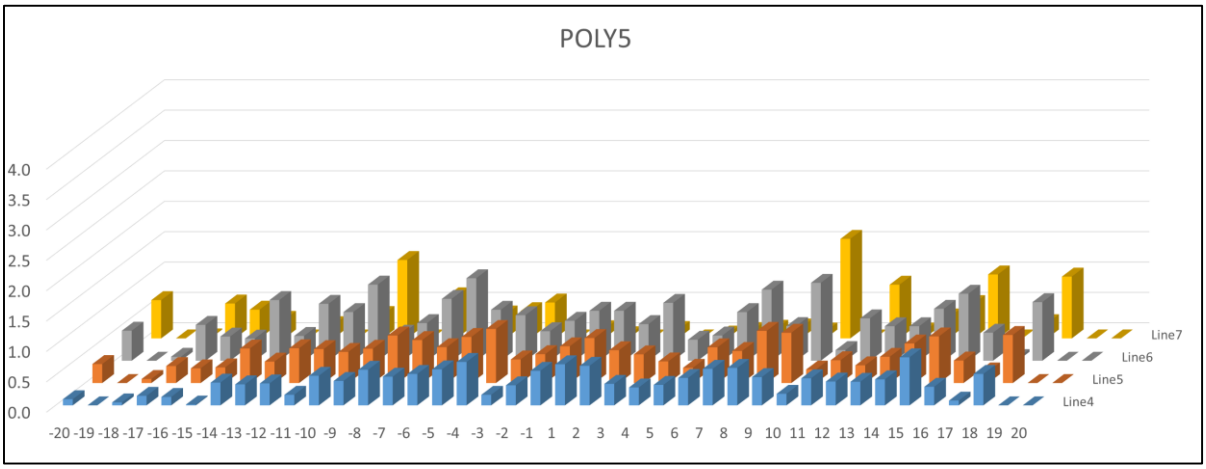

Figure 5.20. Residuals of fifth-degree polynomial.

The residuals of the fifth-polynomial are distributed through all the x range. It is noticed an increase between lines, being the Line4 the one with smaller values. Moreover, in Lines 6 and 7 there are several peaks with values above 1. However, the central part of the chart describes always below residuals, being the maximal value 0,890.

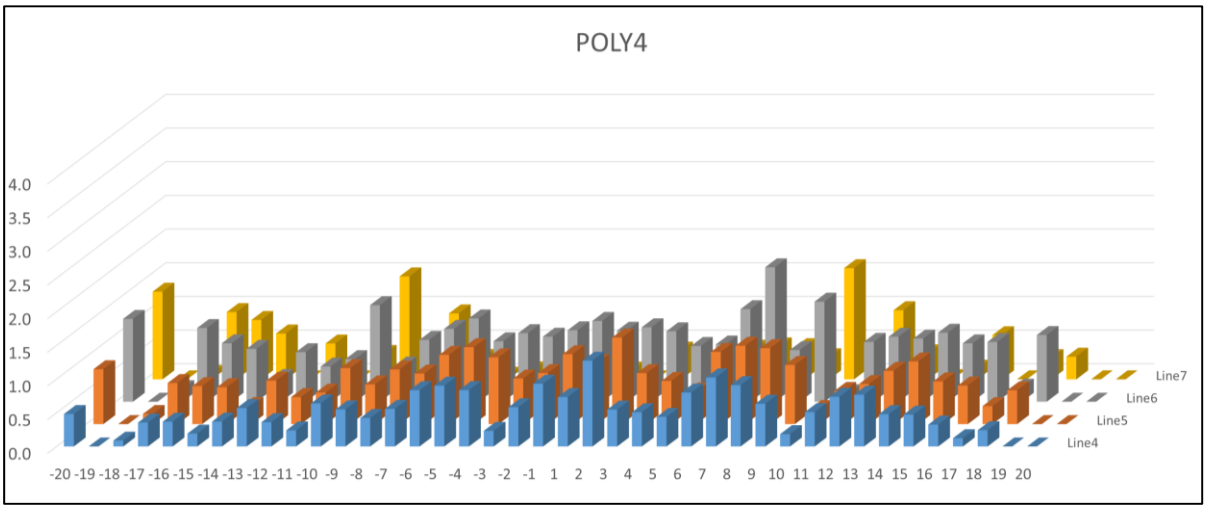

Figure 5.21. Residuals of fourth-degree polynomial.

The bar chart above shows the residuals of the fourth-degree polynomial. The growing tendency is clearer than the fifth polynomial. An important fact is that in every line there are at least one peak with values higher than 1, even in the middle zone.

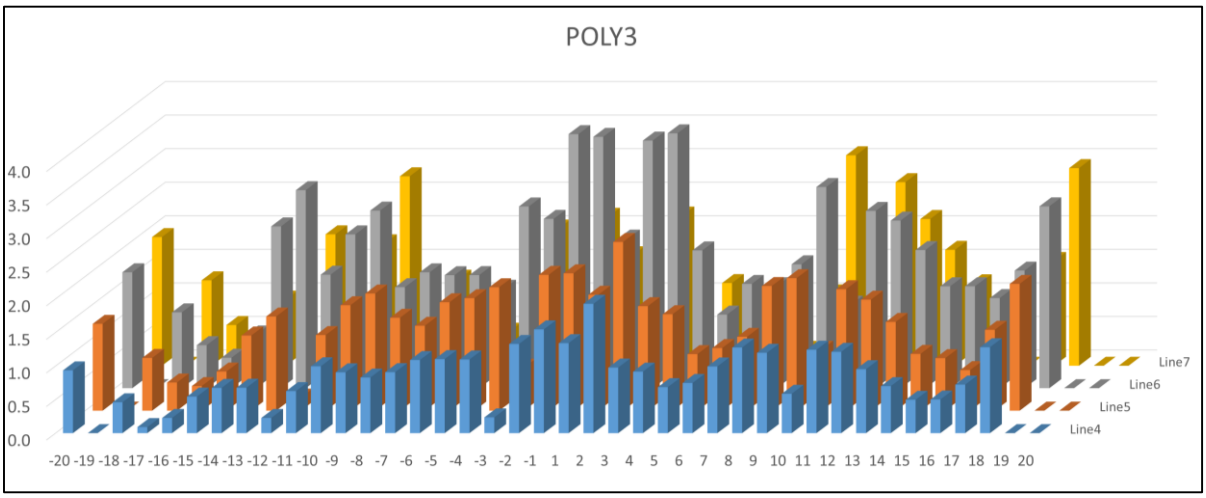

Figure 5.22. Residuals of third-degree polynomial.

Eventually, in the third-degree plot there is a sharp increase in relation the previous ones, achieving values near or over 2 in all the lines. Moreover, the peaks are located in the central

range of the chart, with a maxim value of 3,785. Owing to the higher values and their distribution the third polynomial is dismissed.

After the evaluation of the four plots, the polynomials with sixth, fifth and fourth are considered possible candidates. Although, if the general behavior of the polynomials is studied, the fifth polynomial would be remove as well. Big differences between odd or even degrees exist, in Table 5.16 the main properties are described.

	Odd degree		**Even degree**	
Sign of leading coeff.	Positive	Negative	Positive	Negative
End behaviour				
Nº of turning points	n-1 at most; local (or global) max or min			

Table 5.16. Polynomial main behavior properties.

In the studied case, the polynomial has to describe paths which go around one hole, thus even degrees-polynomial seem to fit better owing to the end behavior, same direction in both sides. Due to the small dimensions the fifth degree fits the analyzed paths quite well. Nevertheless, with other size sample or with different hole's diameter it is possible that the fitting describes a different end direction between the both sides of the sample. In order to avoid this phenomena, the odd degrees will be dismissed.

Between both sixth and fourth, it is evident that the sixth-polynomial gives the best accuracy to describe the real paths, therefore this is selected as the model's main shape. Nevertheless, in an ideal situation the paths would be symmetric, therefore lower degree polynomial could fit the paths with smaller residuals than the ones described in the previous bar plots. That is the reason why in the following chapters it will be necessary to evaluate if all the coefficients are needed.

$$f(x) = a_0 + a_1 \cdot x + a_2 \cdot x^2 + a_3 \cdot x^3 + a_4 \cdot x^4 + a_5 \cdot x^5 + a_6 \cdot x^6$$

6 Assessment

This chapter sets to show the reader the model creation steps. In the following subchapters the previous results will be used to reach an expression, which describes the fibre paths close the joining area.

6.1 Influence factors

The purpose of the chapters 4.1 and 5.2 was provide enough information to define the influencing factors to introduce in the analytical model.

After the analysis of the standarized effects, the factors Hole Ø and Material were found as a statistically significant. The rest of the factors and interactions had lower and similar effect coefficients, resulting as statistically insignificant.

With these arguments, the variables which will be introduced in the analytical model are: Hole Ø, and Material.

- Hole Ø

  This feature will be used to find geometrical relations.

- Material

  Physical properties of the material are unknown. To introduce this factor, a comparison between the data of the studied materials will be done and the observed tendencies will be described by coefficients, which the values depends on the material.

6.2 Waviness

During the testing process the phenomenon of the waviness highly appeared in some samples. That is the reason why a study to demonstrate which factors produce this behaviour were done, chapter 5.2.2. The regions affected by this wave presence are considered as anomaly trajectory paths, because they are not predictive, therefore it is not introduced to the developed model.

However, it was evaluated in order to choose or define the best conditions to avoid this phenomenon and produce knowledge for further experiments.

The waviness was analysed as a response in a factorial design in the same way as the deformed area. The results, explained in detail in the chapter 5.2.2, conclude that the best combination to minimize the wave behaviour is:

Factor	Level	Value	Influence order
Hole Ø	low	9mm	2
Material	high	0/90 ply	1
Angle pin	high	20º	3
Shape pin	high	Cone	3
Clamping Force	high	30kg	4

Table 6.1. Factors conditions to minimize the waviness.

The previous table presents, according to the statistical analysis, that the best procedure to minimize the waviness is punching the carbon fiber 0/90 ply with the pin (Ø9mm, 20º, cone) and applying a clamping force of 30 kg.

It should keep in mind that not all the factors have the same influence. The material is the most relevant, although maybe others facts as the mechanical properties have to be considered for a specific application.

About the hole diameter, one should choose the smallest that satisfies the requirements of the application. It was seen that a bigger hole increases the probabilities of waviness.

Regarding the pin, there is an interaction between the angle and the shape. Apparently the cone shape has a good effect to minimize the waviness and the manufacturing process is simpler as the bullet shape, in that case is clear that the cone shape will be select in further experiments. The chosen sharpness is 20º, this value could be increases and then evaluate. In that case considerations about manufacturing and handle performance should be done.

On the other hand, it would be interesting study different systems to apply force and figure out the perfect clamping force. The method employed was by weights, probably with a little press, screws or springs the applied force could increase.

6.3 Deformed area description

The development of the model starts for define the piecewise function constraints. In each sample a deformed and non-deformed regions exist. The non-deformed area is considered the one where the path becomes straight line. The approximation that the deformed area is rectangular region defined by the width length and the height length, $deformed\ area = w \cdot h$, is taken. In previous chapters, 4.1.3 and 5.1.2, measures of the width and height were done.

First of all, a small reminder of the testing runs is shown. In the Table 6.2 the 16 combinations and the respectively runs which satisfied them are displayed.

Std.order	Hole Ø	Material	Shape pin	Angle pin	Force	R1	R2	R3	R4	R5
1	-	-	-	-	+	Run9	Run36	Run69	Run74	Run79
2	+	-	-	-	-	Run1	Run17	Run41	Run50	Run64
3	-	+	-	-	-	Run11	Run40	Run52	Run56	Run61
4	+	+	-	-	+	Run6	Run24	Run27	Run30	Run60
5	-	-	+	-	-	Run10	Run20	Run43	Run48	Run54
6	+	-	+	-	+	Run12	Run16	Run38	Run53	Run73
7	-	+	+	-	+	Run8	Run15	Run23	Run42	Run51
8	+	+	+	-	-	Run33	Run35	Run70	Run71	Run77
9	-	-	-	+	-	Run2	Run18	Run29	Run49	Run55
10	+	-	-	+	+	Run5	Run26	Run45	Run65	Run67
11	-	+	-	+	+	Run32	Run47	Run57	Run63	Run68
12	+	+	-	+	-	Run19	Run25	Run34	Run44	Run58
13	-	-	+	+	+	Run28	Run39	Run46	Run72	Run80
14	+	-	+	+	-	Run7	Run22	Run59	Run62	Run66
15	-	+	+	+	-	Run4	Run21	Run75	Run76	Run78
16	+	+	+	+	+	Run3	Run13	Run14	Run31	Run37

Table 6.2. Trials table.

The second and third columns of the table are the most relevant, since they contain the information of the chosen factors. A color code is defined for each combination: blue when diameter and material are in high level, green when diameter is in high level and material is low, red when diameter is in low level and material in high and yellow when both are in low level. In the table below the measures of width and high of each run are displayed. In addition, the average and mean values of repeat the trials are calculated.

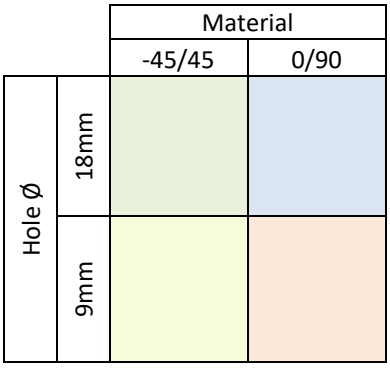

Figure 6.1. Color code

	w (mm)							h (mm)						
Std.order	R1	R2	R3	R4	R5	mean	average	R1	R2	R3	R4	R5	mean	average
1	20.067	20.117	19.850	20.942	27.133	20.117	21.622	12.467	12.833	12.192	12.558	13.617	12.558	12.733
2	35.658	30.250	36.983	29.833	30.850	30.850	32.715	26.725	25.075	22.367	22.275	20.992	22.367	23.487
3	18.700	23.192	34.008	22.867	26.858	23.192	25.125	12.633	12.150	12.700	12.375	12.100	12.375	12.392
4	33.275	34.558	36.575	33.325	34.467	34.467	34.440	25.533	24.658	26.175	24.658	27.092	25.533	25.623
5	18.058	21.400	21.042	22.092	30.017	21.400	22.522	13.933	14.342	13.700	13.892	14.075	13.933	13.988
6	27.550	35.250	32.133	34.650	37.167	34.650	33.350	23.975	25.617	22.958	23.833	22.417	23.833	23.760
7	35.383	22.867	31.533	23.517	25.342	25.342	27.728	23.925	15.767	12.792	18.058	15.950	15.950	17.298
8	38.092	29.475	39.375	30.708	40.008	38.092	35.532	22.642	23.558	23.600	24.292	24.700	23.600	23.758
9	25.167	17.050	18.150	21.958	22.275	21.958	20.920	18.108	15.075	13.158	11.875	12.100	13.158	14.063
10	31.667	34.283	30.892	32.450	42.125	32.450	34.283	24.433	25.067	23.558	22.783	21.633	23.558	23.495
11	45.975	22.000	27.042	29.658	21.133	27.042	29.162	12.967	12.633	15.308	11.917	14.758	12.967	13.517
12	31.117	33.325	39.183	33.458	36.075	33.458	34.632	23.058	23.925	21.817	26.583	21.633	23.058	23.403
13	18.425	23.008	23.333	23.742	21.500	23.008	22.002	15.400	13.517	14.208	11.733	15.258	14.208	14.023
14	31.367	31.675	32.450	31.300	31.992	31.675	31.757	24.667	23.375	22.642	20.442	22.958	22.958	22.817
15	24.525	24.108	25.075	22.050	33.592	24.525	25.870	12.150	15.217	12.558	14.442	15.217	14.442	13.917
16	44.733	29.100	31.767	38.408	31.258	31.767	35.053	26.858	24.383	23.692	24.342	20.575	24.342	23.970

Table 6.3. Mean and average width and high values of each combination.

For the next steps the values of the averages will be used, thus they give more accuracy. However, if both values, mean and average, are compared it is seen that they are very close in almost all situations. It suggests that with a higher amount of samples, mean and average statically should have the same value.

With the purpose of seeing easier a pattern between the different combinations, the calculated averages are classified by the influence factors, diameter and material. The resulting matrix is shown below, where the four categories can be distinguished.

		Material					
		-45/45			0/90		
		Std.order	Width [mm]	Height [mm]	Std.order	Width [mm]	Height [mm]
Hole Ø	18mm	2	32.715	23.487	4	34.440	25.623
		6	33.350	23.760	8	35.532	23.758
		10	34.283	23.495	12	34.632	23.403
		14	31.757	22.817	16	35.053	23.970
	9mm	1	21.622	12.733	3	25.125	12.392
		5	22.522	13.988	7	27.728	17.298
		9	20.920	14.063	11	29.162	13.517
		13	23.008	14.023	15	25.870	13.917

Table 6.4. Repeat trials width and height average values classified by Ø and material.

In each category it is seen that the values of width and height between runs are very close. In addition, as was determined in the previous statistical analysis, the diameter has a bigger effect, since, as is shown by the values the ones of diameter 18mm are higher than the diameter 9mm. Moreover, it is noticed that for the same diameter the width and height take maximum values when the material is the ply 0/90.

In order to find a numerical expression that describes the deformed area, the average of the values is calculated, obtaining a value of width and height for each combination,

Table 6.5.

w1	33.026	w2	34.914
w3	22.018	w4	26.971
h1	23.390	h2	24.189
h3	13.702	h4	14.281

Table 6.5. Width and height averages values of each category

In Figure 6.2 are shown the geometrical descriptions of the height, left image, and width, right image. The height is defined as the distance between the first straight paths, thus the half value can be express as the sum of the radius and a distance, called *d*. In the case of width, the measure is taken horizontally between the straight fibers and the half value corresponds to the sum of the radius and a distance named *s*.

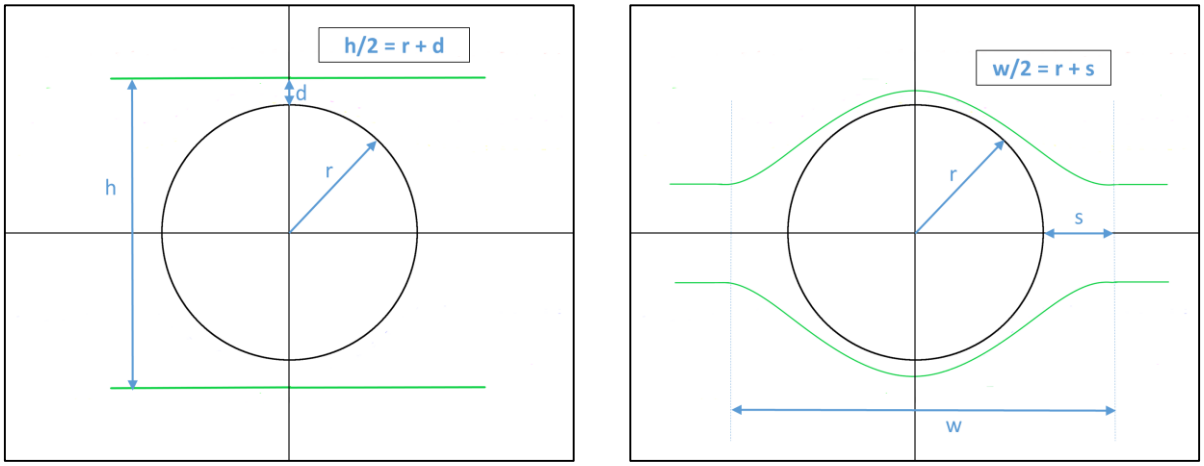

Figure 6.2. Geometrical definition of height and width.

The geometrical description can be applied to the values of the averages and the respectively radius. This procedure is done analyzing the results of the same material.

Width constraint of textile ply -45/45

$$\left.\begin{aligned}\frac{w_1}{2} &= r_+ + d_1\\ \frac{w_3}{2} &= r_- + d_3\end{aligned}\right\} \quad \left.\begin{aligned}\frac{33{,}026}{2} &= 9 + s_1\\ \frac{22{,}018}{2} &= 4{,}5 + s_3\end{aligned}\right\} \quad \boxed{\begin{aligned}s_1 &= 7{,}513\\ s_3 &= 6{,}509\end{aligned}}$$

For a concise representation of the deformed area of fibers in relation to the material, the distance *s* is defined as $s = C_1 \cdot r + C_2$. At least two coefficients are needed to express the width, because of the difference between the *s* values of the same material ($s_1 \neq s_3$).

$$\left.\begin{aligned} s_1 &= c_1 \cdot r_+ + c_2 \\ s_3 &= c_1 \cdot r_- + c_2 \end{aligned}\right\} \quad \left.\begin{aligned} 7{,}513 &= c_1 \cdot 9 + c_2 \\ 6{,}509 &= c_1 \cdot 4{,}5 + c_2 \end{aligned}\right\} \quad \boxed{\begin{aligned} c_1 &= \frac{251}{1125} \approx 0{,}223 \\ c_2 &= 5{,}505 \end{aligned}}$$

The calculations of *s* and the coefficients C_1 and C_2 are repeated for the other material, ply 0/90.

Width constraint of textile ply 0/90

$$\left.\begin{aligned} \frac{w_2}{2} &= r_+ + s_2 \\ \frac{w_4}{2} &= r_- + s_4 \end{aligned}\right\} \quad \left.\begin{aligned} \frac{34{,}914}{2} &= 9 + s_2 \\ \frac{26{,}971}{2} &= 4{,}5 + s_4 \end{aligned}\right\} \quad \boxed{\begin{aligned} s_2 &= 8{,}457 \\ s_4 &= 8{,}9855 \end{aligned}}$$

$$\left.\begin{aligned} s_2 &= c_1 \cdot r_+ + c_2 \\ s_4 &= c_1 \cdot r_- + c_2 \end{aligned}\right\} \quad \left.\begin{aligned} 8{,}457 &= c_1 \cdot 9 + c_2 \\ 8{,}9855 &= c_1 \cdot 4{,}5 + c_2 \end{aligned}\right\} \quad \boxed{\begin{aligned} c_1 &= \frac{-1057}{9000} \approx -0{,}117 \\ c_2 &= 9{,}514 \end{aligned}}$$

Height constraint of textile ply -45/45

In the height description is also needed the use of two coefficents, C_3 and C_4, of each material.

$$\left.\begin{aligned} \frac{h_1}{2} &= r_+ + d_1 \\ \frac{h_3}{2} &= r_- + d_3 \end{aligned}\right\} \quad \left.\begin{aligned} \frac{23{,}390}{2} &= 9 + d_1 \\ \frac{13{,}702}{2} &= 4{,}5 + d_3 \end{aligned}\right\} \quad \boxed{\begin{aligned} d_1 &= 2{,}695 \\ d_3 &= 2{,}351 \end{aligned}}$$

$$\left.\begin{aligned} d_1 &= c_3 \cdot r_+ + c_4 \\ d_3 &= c_3 \cdot r_- + c_4 \end{aligned}\right\} \quad \left.\begin{aligned} 2{,}695 &= c_3 \cdot 9 + c_4 \\ 2{,}351 &= c_3 \cdot 4{,}5 + c_4 \end{aligned}\right\} \quad \boxed{\begin{aligned} c_3 &= \frac{86}{1125} \approx 0{,}076 \\ c_4 &= 2{,}007 \end{aligned}}$$

Height constraint of textile ply 0/90

$$\left.\begin{aligned}\frac{h_2}{2} &= r_+ + d_2\\ \frac{h_4}{2} &= r_- + d_4\end{aligned}\right\} \quad \left.\begin{aligned}\frac{24{,}189}{2} &= 9 + d_2\\ \frac{14{,}281}{2} &= 4{,}5 + d_4\end{aligned}\right\} \quad \boxed{\begin{aligned}d_2 &= 3{,}0945\\ d_4 &= 2{,}6405\end{aligned}}$$

$$\left.\begin{aligned}d_2 &= c_3 \cdot r_+ + c_4\\ d_4 &= c_3 \cdot r_- + c_4\end{aligned}\right\} \quad \left.\begin{aligned}3{,}0945 &= c_3 \cdot 9 + c_4\\ 2{,}6405 &= c_3 \cdot 4{,}5 + c_4\end{aligned}\right\} \quad \boxed{\begin{aligned}c_3 &= \frac{227}{2250} \approx 0{,}101\\ c_4 &= 2{,}1865\end{aligned}}$$

After the evaluation of the geometrical descriptions, the resulting conclusion is that four coefficients, which depend of the material, are needed. In the Table 6.6 the coefficients of the two studied materials are shown. It is noticed that the values of C_3 and C_4 are really close between the both materials. That is an interesting fact, thus it suggests that might be a constant value. However, only two materials were studied and it is not considered a sample big enough to be representative.

	C1	C2	C3	C4
Ply -45/45	0,223	5,505	0,076	2,007
Ply 0/90	-0,117	9,514	0,101	2,186

Table 6.6. Values of material coefficients.

In case that another material wants to be used, it will be necessary to test two samples with different diameters, measure the respectively width and height and proceed in the same way as was explained above to figure out the new C_1, C_2, C_3 and C_4.

Following the mentioned design rule of symmetry about x-axis, the curves for the upper and lower half plane are assumed by separately piecewise functions. The respectively constraints of x and y, x_{def} and y_{def}, are defined below, the first one represents the upper half plane and the second one the lower half plane.

$$\boldsymbol{x \in}\ [\,-|\boldsymbol{r} + (\boldsymbol{C_1} \cdot \boldsymbol{r} + \boldsymbol{C_2})|\,, |\boldsymbol{r} + (\boldsymbol{C_1} \cdot \boldsymbol{r} + \boldsymbol{C_2})|\,] \cap \boldsymbol{y \in}\ [\,\boldsymbol{0}, |\,\boldsymbol{r} + (\boldsymbol{C_3} \cdot \boldsymbol{r} + \boldsymbol{C_4})|\,] \qquad \text{Formula 6.1}$$

$$\boldsymbol{x \in}\ [\,-|\boldsymbol{r} + (\boldsymbol{C_1} \cdot \boldsymbol{r} + \boldsymbol{C_2})|\,, |\boldsymbol{r} + (\boldsymbol{C_1} \cdot \boldsymbol{r} + \boldsymbol{C_2})|\,] \cap \boldsymbol{y \in}\ [\,\boldsymbol{0}, -|\boldsymbol{r} + (\boldsymbol{C_3} \cdot \boldsymbol{r} + \boldsymbol{C_4})|\,] \qquad \text{Formula 6.2}$$

Where:

$r\ is\ the\ radius\ of\ the\ hole\ in\ mm.$

$C_1\ and\ C_2\ are\ the\ height\ coeffcients\ of\ the\ material.$

$C_3\ and\ C_4\ are\ the\ width\ coeffcients\ of\ the\ material.$

6.4 Model description

After the regression analysis in chapter 5.3, a sixth-degree polynomial was chosen as the main shape to describe the real trajectories.

$$f(x) = a_0 + a_1 \cdot x + a_2 \cdot x^2 + a_3 \cdot x^3 + a_4 \cdot x^4 + a_5 \cdot x^5 + a_6 \cdot x^6 \qquad \text{Formula 6.3}$$

However, in the definition of the project, hypothesis of symmetry were assumed. In the ideal model the upper and lower half part are symmetric about x-axis, therefore if the upper half can be described the lower part expression will be the same, but with opposite signs.

Moreover, the ideal model has symmetry about the y-axis. It means that the polynomial has to be an even function. By definition an even function is the one which satisfies $f(x) = f(-x)$ in all x range, see Figure 6.3.

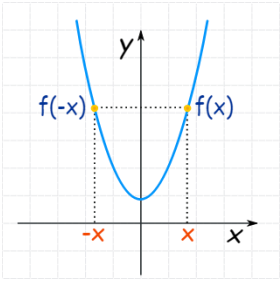

Figure 6.3. Even function

For a polynomial expression the behavior of an even term , $(-x)^n = x^n$, only occurs when *n* is an even number. The considered polynomial expression is the addition of the different degree terms; the adding properties of the polynomials are the following:

- The sum of two even functions is even.
- The sum of two odd functions is odd.
- The sum of an even and odd function is neither even nor odd (unless one function is zero).

Regarding these properties to get a symmetric function about y, the only way is adding even functions. Therefore, x^5, x^3 and x terms are dismissed. Insert this constraint in Formula 6.3 gives the polynomial with the terms shown below and it satisfies $f(x) = f(-x)$.

$$f(x) = a_0 + x^2 + x^4 + x^6 \qquad \text{Formula 6.4}$$

$$f(-x) = a_0 + (-x)^2 + (-x)^4 \cdot + (-x)^6 = a_0 + x^2 + x^4 + x^6 = f(x)$$

6.4.1 Final shape and signs

To fit the real fiberpaths a sixth-degree polynomial were chosen as the best candidate. Despite this fact, the ideal model could be described with a lower degree. In that point three candidates can be obtained from Formula 6.4.

1. $f(x) = a_0 + a_2 \cdot x^2 + a_4 \cdot x^4 + a_6 \cdot x^6$
2. $f(x) = a_0 + a_2 \cdot x^2 + a_4 \cdot x^4$
3. $f(x) = a_0 + a_2 \cdot x^2$

In order to choose the most accurate expression, avoiding underfitting and overfitting, a practical example is analysed. The fitting using the three expressions above were done in just one fiberpath, concretely Line5 of Run76. The resulting expressions of the fitting are:

1. $f(x) = 4{,}5 - 0{,}1125 \cdot x^2 + 0{,}001 \cdot x^4 - 0{,}000003 \cdot x^6$
2. $f(x) = 4{,}5 - 0{,}1125 \cdot x^2 + 0{,}00083 \cdot x^4$
3. $f(x) = 4{,}5 - 0{,}04 \cdot x^2$

Some valuable information is obtained from the previous functions. It is seen that the sign of the terms has a big influence in the shape of the curve, being negative in the second and sixth degree term. Moreover, the magnitude of the coefficients differs in function of the amount of terms. A plot is done to compare the behaviours of the three functions, shown in Figure 6.4.

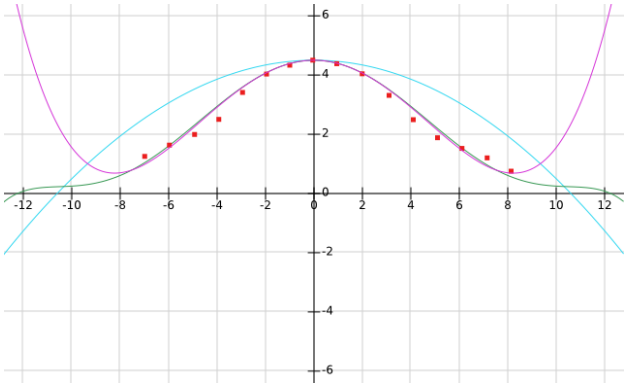

Figure 6.4. Final shape selection.

In the graphic the sixth-degree polynomial are drawn in green, the fourth-degree in pink and the quadratic in blue. In addition, the real points of the deformed region are plotted in red color. It is clearly that the quadratic expression has not the desired behaviour, only the maximum value is described by the function. Regarding the sixth and fourth-degree expressions both have a similar behaviour in the region, which concern the real points. Hence the simplest expression between both, the fourth-degree, is chosen. The generic expression, with the suitable signs, will be:

$$f(x) = a_0 - a_2 \cdot x^2 + a_4 \cdot x^4$$

6.4.2 Constant coefficient a_0

In this subchapter the constant term of the model is studied. A graphical interpretation of this value is illustrated in Figure 6.5. a_0 corresponds to the relative maximum value of the function, due to the symmetry and the polynomial behaviour the highest value always occurs when the x value is zero.

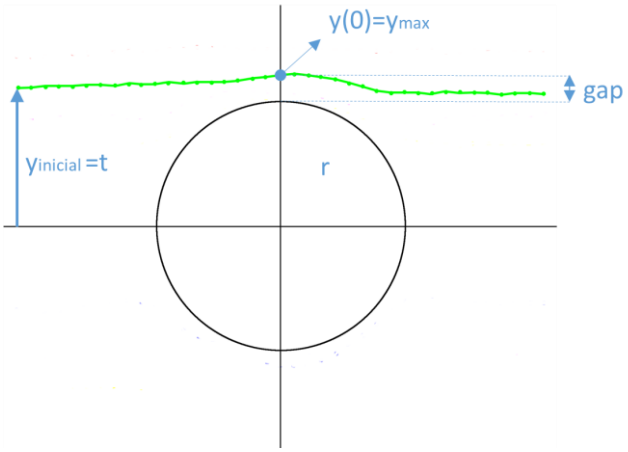

Figure 6.5. Geometrical description of a_0.

With other words, the maximum value of y is the addition of the radius of the hole and a gap, $a_0 = y(0) = r + gap$. The gap distance is not a constant value; it depends of the line. To describe the family of curves the variable t is defined. It represents the initial value of y, when the straight line ends and starts the curve trajectory.

Std.order	R3
1	Run69
2	Run41
3	Run52
4	Run27
5	Run43
6	Run38
7	Run23
8	Run70
9	Run29
10	Run45
11	Run57
12	Run34
13	Run46
14	Run59
15	Run75
16	Run14

Line 1		Line 2		Line 3		Line 4		Line 5		Line 6	
X	Y	X	Y	X	Y	X	Y	X	Y	X	Y
-19.12	10.06	-19.02	7.98	-19.03	5.95	-19.03	3.98	-19.00	1.97	-19.06	0.94
-18.06	10.00	-18.09	7.97	-18.02	5.97	-18.03	3.95	-18.07	2.01	-18.03	0.92
-17.02	10.00	-17.00	7.98	-17.04	6.03	-17.03	3.95	-17.02	2.00	-16.93	0.94
-15.97	9.95	-16.03	8.01	-16.05	6.11	-15.99	3.95	-16.09	1.95	-16.03	0.99
-14.96	10.01	-14.96	7.93	-15.04	6.11	-15.06	3.95	-14.96	1.96	-14.94	0.98
-13.91	10.03	-13.95	7.99	-14.07	6.17	-14.07	3.97	-14.01	1.98	-14.02	1.08
-13.06	10.01	-13.01	7.96	-12.99	6.11	-12.98	4.00	-12.96	1.99	-13.05	1.09
-11.92	9.98	-11.94	8.03	-12.03	6.09	-11.92	4.00	-11.95	1.95	-12.05	0.91
-10.97	10.00	-10.95	8.07	-11.04	6.16	-11.05	4.00	-11.07	1.98	-11.05	0.66
-10.05	10.06	-10.03	8.08	-9.97	6.26	-10.00	3.98	-9.98	1.95	-10.02	0.47
-9.00	10.01	-8.93	8.12	-8.98	6.30	-8.94	4.03	-8.91	1.85	-8.98	0.24
-7.88	10.06	-7.97	8.14	-7.99	6.33	-7.93	4.05	-8.07	1.79	-8.01	0.04
-7.01	10.06	-7.03	8.14	-6.92	6.38	-7.03	4.05	-7.01	1.86	-7.05	0.07
-6.00	10.12	-5.98	8.14	-5.99	6.37	-6.02	4.14	-5.92	1.96	-6.00	0.27
-4.97	10.13	-4.98	8.16	-4.99	6.41	-4.99	4.29	-4.99	2.34	-4.99	0.72
-3.97	10.12	-3.90	8.21	-3.92	6.52	-3.96	4.43	-4.01	2.84	-4.00	2.14
-3.03	10.16	-2.95	8.29	-2.86	6.63	-2.95	4.64	-3.03	3.57	-2.99	3.36
-2.02	10.15	-1.93	8.32	-1.81	6.65	-1.87	4.97	-2.00	4.22	-1.96	4.02
-1.00	10.16	-0.90	8.26	-0.97	6.66	-0.92	5.22	-0.92	4.65	-0.96	4.40
0.10	10.16	0.00	8.23	-0.01	6.63	0.13	5.32	0.17	4.76	0.06	4.52
1.05	10.19	1.01	8.20	1.07	6.63	1.06	5.29	1.13	4.69	1.02	4.46
2.09	10.18	2.06	8.26	2.05	6.60	2.10	5.13	2.06	4.36	2.03	4.05
3.07	10.19	3.01	8.25	3.05	6.61	3.06	4.91	3.06	3.79	3.08	3.29
4.08	10.12	4.08	8.18	4.09	6.55	4.10	4.77	4.01	3.34	4.04	2.16
4.94	10.09	5.12	8.18	5.08	6.55	5.07	4.64	5.08	2.91	5.03	-0.18
6.08	10.12	6.03	8.14	6.05	6.58	6.05	4.62	6.04	2.68	6.10	0.04
7.07	10.14	7.13	8.19	7.10	6.50	7.02	4.53	6.96	2.51	7.08	0.48
8.05	10.14	8.11	8.22	8.07	6.56	8.09	4.13	8.03	2.37	8.00	0.92
9.09	10.10	9.10	8.17	9.13	6.50	8.98	3.80	8.96	2.35	9.03	1.31
10.13	10.06	10.04	8.21	10.06	6.54	10.02	3.88	10.07	2.51	10.15	1.51
11.12	10.04	11.12	8.15	11.18	6.49	11.13	4.16	11.06	2.58	11.07	1.54
12.09	10.10	12.03	8.09	12.12	6.45	12.06	4.25	12.13	2.42	12.05	1.49
13.12	10.11	13.06	8.12	13.10	6.42	13.18	4.18	13.13	2.25	13.08	1.37

Figure 6.6. Data used to describe the constant coefficient a_0

To describe the tendency of the gap distance the coordinates of one trial are studied. In Figure 6.6 the runs which belongs to the third trial are displayed, they are also classified by the color code defined in chapter 6.3. For each run and line the values of the initial y and the y when x is near zero are collected.

The values of y(0) are classified by the color category and *t*, from 0 to 10. As it was explained before, the variable *t* represents the distance between the x axis and the initial value of y. In the collected data the values of $y_{initial}$ are not integer numbers, therefore in order to classify them the criteria of assign the nearest t value is taken. In the Appendix of this work the classification table is attached.

After the classification, the average values are calculated for each category and then by linear interpolation the values for all the studied range of t are obtained. The result is shown in Table 6.7.

	0	1	2	3	4	5	6	7	8	9	10
Ø18mm ply 0/90	9.277	9.250	9.223	9.195	9.226	9.227	9.330	9.153	9.801	10.333	11.133
Ø9mm ply 0/90	4.576	4.595	4.606	4.669	4.859	4.690	5.951	6.976	7.834	-	-
Ø18mm ply 45/45	9.072	9.063	9.055	9.120	9.150	9.123	9.293	9.546	9.704	10.071	10.635
Ø9mm ply 45/45	4.645	4.819	5.041	4.878	5.241	5.724	6.640	7.838	8.297	9.514	10.287

Table 6.7. Values of a_0 or y_{max} for different values of t and category.

If an inspection of the last table is done, it is obvious that the categories with the bigger diameter, Ø18, have a higher value of a_0. If a comparison between the both cases with the same diameter is done, it is realized that in the case of diameter 18mm the material ply 0/90 presents higher values than ply -45/45 in all the studied t values, expect in t=7. In the other hand, when the diameter is 9mm the highest a_0 takes place when the material is ply -45/45. That facts suggests that the gap distance has an important effect to determine the constant term a_0 and it depends of the kind of material.

In the beginning of this chapter, the gap was defined as $gap = y_{max} - radius$. Thus using the results of the table above the gap is calculated. To evaluate the increase behavior, the gap values are plotted, see Figure 6.7 and Figure 6.8.

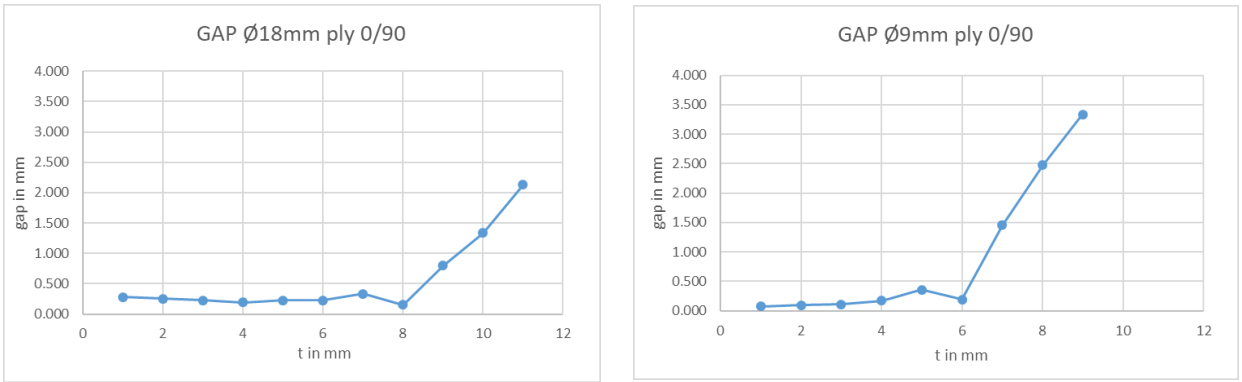

Figure 6.7. Gap plots of material ply 0/90

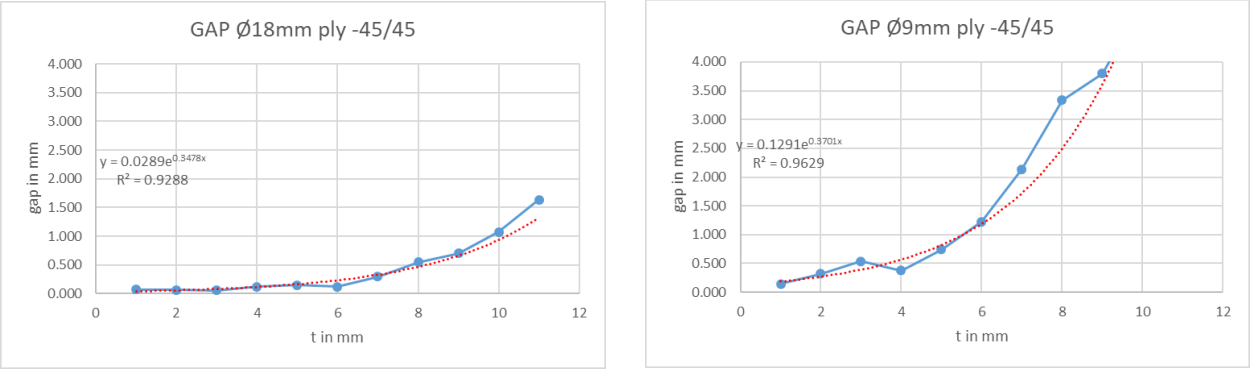

Figure 6.8. Gap plots of material ply -45/45

As it was expected the material has a big relationship with the behaviour of the gap distance. In one situation, when the ply is 0/90, the plot is described as a piecewise function with a first part with more or less a constant value and a second part with a linear increase. The second situation, with material -45/45, the tendency is completely different; it can be described as a curvilinear shape, approximately exponential, in all the range. In that point the gap distance and consequently the coefficient a_0 will be described separately for each material.

6.4.2.1 Ply 0/90 a_0 definition

The piecewise function to describe the gap increase in the material with ply 0/90 looks like the Figure 6.9.

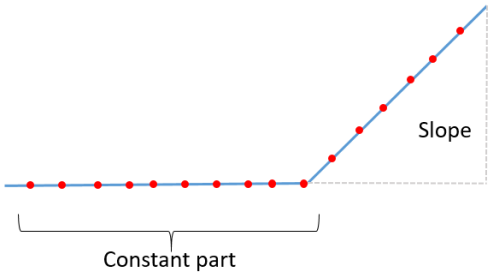

Figure 6.9. Gap increase behavior of ply 0/90

However, it can be seen in the previous plots that the number of lines with more or less no increase and the slope magnitude differs between the diameters. So both properties are dependent from the hole size.

In order to describe it, first the constant part of the gap piecewise function is studied. Since only the value of two diameters are available, the behavior is approximated by linear interpolation. The Table 6.8 shows until which *t* the slope is 0, referred the plots of Figure 6.7.

Radius (Ø/2)	Last t with constant value ($\boldsymbol{slope = 0}$)
4,5	6 (4,5)
9	8

Table 6.8. Constant part range

The *t* which have a gap lower than 0,1 are considered in the constant part. In the numbers showed in the table above, concretely the situation of diameter 4,5, show a fact that it is not representative with the hypothesis formulated in the chapter 4.2.1. The t is higher than the radius, it refers a convex shape. To solve this situation the restriction that the constant part include a maximum value of $t = r$ is taken.

Therefore, the constrain in function of the radius is given by the following expression:

$$constraints(r) = t_{cst}(r_1) + \frac{t_{cst}(r_2) - t_{cst}(r_1)}{(r_2 - r_1)} \cdot (r - r_1) \quad \text{Formula 6.5}$$

$$constraints(r) = 4{,}5 + \frac{8 - 4{,}5}{(9 - 4{,}5)} \cdot (r - 4{,}5) = 1 + 0{,}777 \cdot \mathrm{r} \quad \text{Formula 6.6}$$

The other part of the gap piecewise function is the linear increase part. A linear line is expressed as $gap = m * t + n$. In the table below the results of the two studied situations are displayed.

Radius (Ø/2)	Slope	Constant
4,5	1,05	-4,93
9	0,66	-4,40

Table 6.9. Slopes (m) and constant term (n) in relation to the diameter.

As it was done to get the constraint expression, the interpolation method is chosen to figure out the linear increase part in relation the radius.

$$slope(r) = slope(r_1) + \frac{slope(r_2) - slope(r_1)}{(r_2 - r_1)} \cdot (r - r_1) \quad \text{Formula 6.7}$$

$$constant(r) = constant(r_1) + \frac{constant(r_2) - constant(r_1)}{(r_2 - r_1)} \cdot (r - r_1) \quad \text{Formula 6.8}$$

$where$:

$r_1 \; and \; r_2 \; are \; known \; radius, with \; r_1 < r_2$

$slope(r_1) \; and \; slope(r_2) \; are \; known \; slope \; values$

$constant(r_1) \; and \; constant(r_2) \; are \; known \; constat \; term \; (n) \; values$

Inserting the slope and constant values from Table 6.9 in the middle and final linear gap's expression are obtained:

$$slope(r) = 1{,}05 + \frac{0{,}66-1{,}05}{(9-4{,}5)} \cdot (r - 4{,}5) = 1{,}44 - 0{,}0867 \cdot r$$

$$constant(r) = -4{,}93 + \frac{-4{,}4-(-4{,}93)}{(9-4{,}5)} \cdot (r - 4{,}5) = -5{,}46 + 0{,}1177 \cdot r$$

$$gap(r,t) = (1{,}44 - 0{,}0867 \cdot r) \cdot t + (-5{,}46 + 0{,}1177 \cdot r) \qquad \text{Formula 6.9}$$

When the gap is described, the coefficient a_0 can be formulated, $a_0(r,t) = r + gap$.

$$a_0(r,t) = r\ ; \qquad 0 \le t \le 1 + 0{,}777 \cdot r$$
$$a_0(r,t) = r + (1{,}44 - 0{,}0867 \cdot r) \cdot t + (-5{,}46 + 0{,}1177 \cdot r); \qquad t > 1 + 0{,}777 \cdot r$$

Formula 6.10. a_0 expression for material ply 0/90.

With the purpose of know how close the approximated value is to the true value, the percent error is calculated with both diameters.

Ø18mm ply0/90

t	real a0	a0(r,t)	error(%)
0	9.277	9.000	2.987
1	9.250	9.000	2.706
2	9.223	9.000	2.422
3	9.195	9.000	2.122
4	9.226	9.000	2.447
5	9.227	9.000	2.463
6	9.330	9.000	3.542
7	9.153	9.000	1.674
8	9.801	9.877	0.776
9	10.333	10.537	1.970
10	11.133	11.196	0.571

Ø9mm ply0/90

t	real a0	a0(r,t)	error(%)
0	4.576	4.500	1.660
1	4.595	4.500	2.061
2	4.606	4.500	2.302
3	4.669	4.500	3.624
4	4.859	4.500	7.382
5	4.690	4.819	2.743
6	5.951	5.869	1.383
7	6.976	6.919	0.821
8	7.834	7.968	1.717

Table 6.10 Percent error a_0 coefficient for material ply 0/90

With the bigger diameter the maximum error is around 3,5% and with the smaller around 7,4%. Both are located in a t value which belongs to the constant behavior. More data should be analyzed to figure out is the consideration of a constant region is accurate enough. For this work the previous expression of a_0 is accepted and will be used for the model.

6.4.2.2 Ply -45/45 a_0 definition

The tendency of the gap distance in the textile with ply -45/45 can be approximated to an exponential curve, $gap = a * e^{b*t}$. The values obtained for the data are shown in the table below.

Radius (Ø/2)	Coefficient (a)	Exponential (b)
4,5	0,129	0,348
9	0,029	0,370

Table 6.11. Coefficients of the exponential curve (a and b) in relation the radius.

In Table 6.11 it is clearly that for this concrete material the gap distance depends on the radius as well. The same methodology used in the previous material is applied in this situation. Using linear interpolation, the coefficients *a* and *b* are described in relation the radius.

$$a(r) = a(r_1) + \frac{a(r_2)-a(r_1)}{(r_2-r_1)} \cdot (r - r_1) = 0{,}2293 - 0{,}0223 \cdot \mathrm{r} \qquad \text{Formula 6.11}$$

$$b(r) = b(r_1) + \frac{b(r_2)-b(r_1)}{(r_2-r_1)} \cdot (r - r_1) = 0{,}348 + 0{,}0049 \cdot \mathrm{r} \qquad \text{Formula 6.12}$$

$$gap(r,t) = (0{,}2293 - 0{,}0223 \cdot \mathrm{r}) \cdot \ e^{(0{,}348+0{,}0049 \cdot \mathrm{r}) \cdot \mathrm{t}} \qquad \text{Formula 6.13}$$

By the definition considered the coefficient a_0 can be formulated, $a_0(r,t) = r + gap$. Using the last equation, $gap(r,t) = (0{,}2293 - 0{,}0223 \cdot \mathrm{r}) \cdot \ e^{(0{,}348+0{,}0049 \cdot \mathrm{r}) \cdot \mathrm{t}}$ Formula 6.13, the expression for the material ply -45/45 is achieved:

$$a_0(r,t) = r + (0{,}2293 - 0{,}0223 \cdot \mathrm{r}) \cdot \ e^{(0{,}348+0{,}0049 \cdot \mathrm{r}) \cdot \mathrm{t}}$$

Formula 6.14. a_0 expression for material ply -45/45.

In the table the percent calculation for this expression is obtained.

Ø18mm ply-45/45

t	real a0	a0(r,t)	error(%)
0	9.072	9.029	0.484
1	9.063	9.042	0.230
2	9.055	9.063	0.086
3	9.120	9.093	0.299
4	9.150	9.137	0.135
5	9.123	9.203	0.879
6	9.293	9.301	0.083
7	9.546	9.445	1.053
8	9.704	9.659	0.464
9	10.071	9.975	0.959

Ø9mm ply-45/45

t	real a0	a0(r,t)	error(%)
0	4.645	4.629	0.348
1	4.819	4.687	2.753
2	5.041	4.770	5.364
3	4.878	4.891	0.283
4	5.241	5.067	3.331
5	5.724	5.320	7.055
6	6.640	5.688	14.346
7	7.838	6.219	20.650
8	8.297	6.989	15.764
9	9.514	8.104	14.820

Table 6.12. Percent error a_0 coefficient for material ply -45/45.

The percent error of Ø18 mm has a maximum value of 1,8% and almost all the situations have an error below 1. That suggests that this expression gives an accurate description of this material and diameter. However, for the Ø9mm the performance is clearly worst, the error reaches values of 20%, especially in high values of *t*. Although with small diameters the high of deformed area could be lower than t=10, the error is considered too high also in the initial values of t.

Future test using the material ply -45/45 and more sizes of punches should be performance and evaluate in order to find an improved way to describe the behavior of this textile. For example, more complex expressions could be proposed.

6.4.3 Dependent terms: coefficients a_2 and a_4

In the previous chapter a geometrical interpretation was used to describe the constant term a_0 in relation the material, the radius and the vertical distance from the origin *t*. This chapter focuses on describe the two coefficients left, a_2 and a_4, which belong to the dependent terms of the x variable.

$$f(x) = a_0(r,t)_{material} + (-a_2) \cdot x^2 + a_4 \cdot x^4 \qquad \text{Formula 6.15}$$

The value of a0 is the particular case when $x = 0$. Moreover, another point f(x) is known; the transition between the straight line and the curvature is considered in $x = r + (C_1 \cdot r + C_2)$, see chapter 6.3, and has a value equal a t.

$$f(0) = a_0(r,t)_{material} \qquad \text{Formula 6.16}$$

$$f\big(r + (C_1 \cdot r + C_2)\big) = a_0 + a_2 \cdot \big(r + (C_1 \cdot r + C_2)\big)^2 + a_4 \cdot \big(r + (C_1 \cdot r + C_2)\big)^4 = t \qquad \text{Formula 6.17}$$

To short the equations from here on $r + (C_1 \cdot r + C_2)$ will be mentioned as ψ.

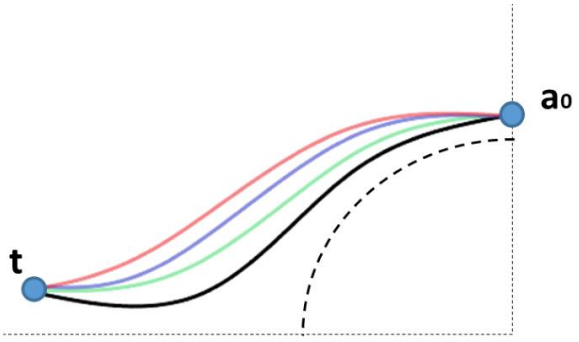

Figure 6.10. Curve's known points.

Despite the both ends of the curve are already defined, is not enough to predict his shape. A wide range of curves are still possible between points (0, a_0) and (-ψ,t). Thus, an extra equation is

required to defined the curve completely. In Figure 6.10 the issue is illustrated by a drawing, the differences between curve geometries are strictly in the coordinates of their inflection point, therefore this feature will be used to find the third constraint.

An inflection or transition point is a point on a curve at which the sign of the curvature, the concavity, changes. Inflection points may be stationary points, but are not local maximum or local minimum values. Thus the second derivative test is useful to find them. A necessary condition for x to be an inflection point is $f''(x) = 0$. The resulting expression of applying this condition to $f(x) = a_0(r,t)_{material} + (-a_2) \cdot x^2 + a_4 \cdot x^4$ Formula 6.15 is:

$$f''(x) = 2 \cdot a_2 + 12 \cdot a_4 \cdot {x_P}^2 = 0 \qquad \text{Formula 6.18}$$

$where\ x_P\ is\ the\ x\ coordinate\ of\ the\ inflection\ point$

Combining Formula 6.17 and Formula 6.18 $f''(x) = 2 \cdot a_2 + 12 \cdot a_4 \cdot {x_P}^2 = 0$ Formula 6.18 the generic expressions of a_2 and a_4 can be found in relation the x_P.

$$a_2(\psi, x_P, t, a_0) = \frac{-6 \cdot {x_P}^2 \cdot (-t + a_0)}{\psi^4 - 6 \cdot \psi^2 \cdot x_P^2}$$

$$a_4(\psi, x_P, t, a_0) = \frac{t - a_0}{\psi^4 - 6 \cdot \psi^2 \cdot x_P^2}$$

Formula 6.19. Generic expressions of coefficients a_2 i a_4.

6.4.3.1 Inflection points calculation

With the purpose of finding the numeric values of the coefficients, the third repeat trial's data is used, the same data was used to define the coefficient a_0. For each category, material and diameter combinations, the data is treated independently.

First of all, using the equations defined in the previous chapters ψ or x_{def}, y_{def} and t_{limit} are calculated. Both depend on the radius and the material. The obtained values are:

	x_{def} (mm)	y_{def} (mm)	t_{limit} (mm)
Ø18mm ply 0/90	17,461	12,095	7,993
Ø9mm ply 0/90	13,487	7,1405	4,496
Ø18mm ply -45/45	16,512	11,691	-
Ø9mm ply -45/45	11,009	6,849	-

Table 6.13. x_{def}, y_{def} and t_{limit} for the studied case.

Using the extreme values of x and y the data is filtered, only the data which belongs to the second quadrant of the deformed region, $-x_{def} \leq x \leq 0 \ \cup 0 \leq y \leq y_{def}$,is collected. Moreover, the lines of each run are tagged with the nearest t value. Then is proceeded with the average coordinates calculation, it is performed between the runs of the same category and t classification.

On the other hand, using an excel file the coefficients a_0, a_2 and a_4 are calculated with the expressions developed before, Formula 6.10, Formula 6.14 and Formula 6.19. For the expressions of a_2 and a_4 an initial value of x_P equal to the radius is taken.

After that, the y for x data point is calculated using the polynomial expression. To check the accuracy, the error between the obtained values and the data is evaluated for each t respectively. A process of error minimization is carried out changing the value of x_P, using Formula 6.20.

$$E(x_P) = \sum_{i=1}^{n} [y_i - f(x, x_P)]^2; \ with \ n \ the \ number \ of \ data \ points$$
$$e = \sqrt{E}$$

Formula 6.20. Sum squared residuals and error formula.

The real points and the curves are plotted as well, so a graphic validation is done simultaneously. That's important in some situations where more than one solution is possible, concave or convex shapes. Mostly concave behavior fits better the model. Figure 6.11 illustrates one example of the chart employed in this step.

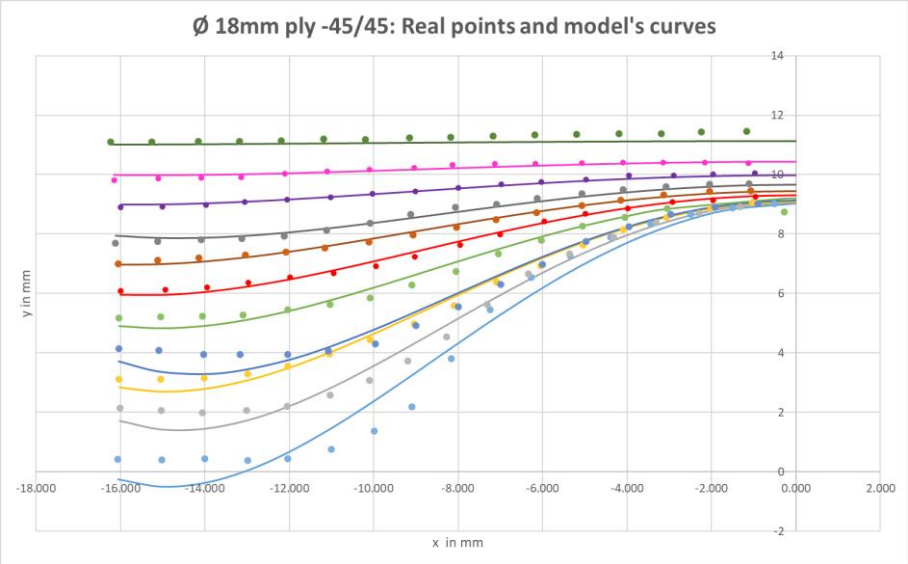

Figure 6.11. Plot of the average points and the model's curves.

The iterative process of minimization ends with an inflection point candidate for each curve and the numerical value of the coefficients. In the following lines the error results and transition points for each configuration are described. The error is the accumulative for each residual, thus is not comparable between categories, because of the different amount of data points used.

In Figure 6.12 the obtained plots for the Ø18mm and ply 0/90 study are shown. In the left figure, it can clearly be seen that the lines near the origin, low values of *t*, have a worst fitting, while the upper lines have an error with half values.

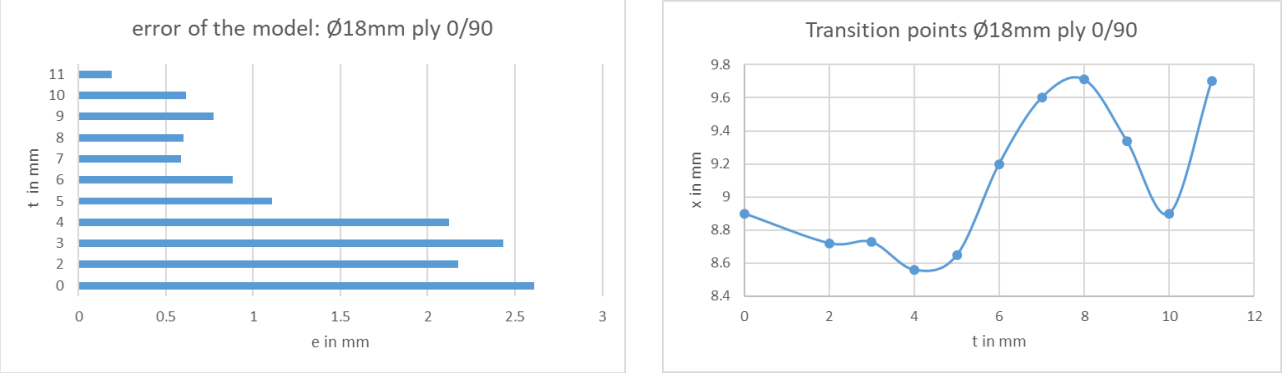

Figure 6.12. Error and inflection points for Ø18mm ply 0/90.

The figure of the transition points does not show any apparent trend. In the beginning the inflection points have *x* values under 9, but then they rise considerably up near 10 and decrease again.

The results with the same material but smaller diameter, Ø9 mm, shows the same error pattern. The maximum errors take place in the lower part and decrease dramatically in the upper part, achieving values around 0,5mm, see Figure 6.13.

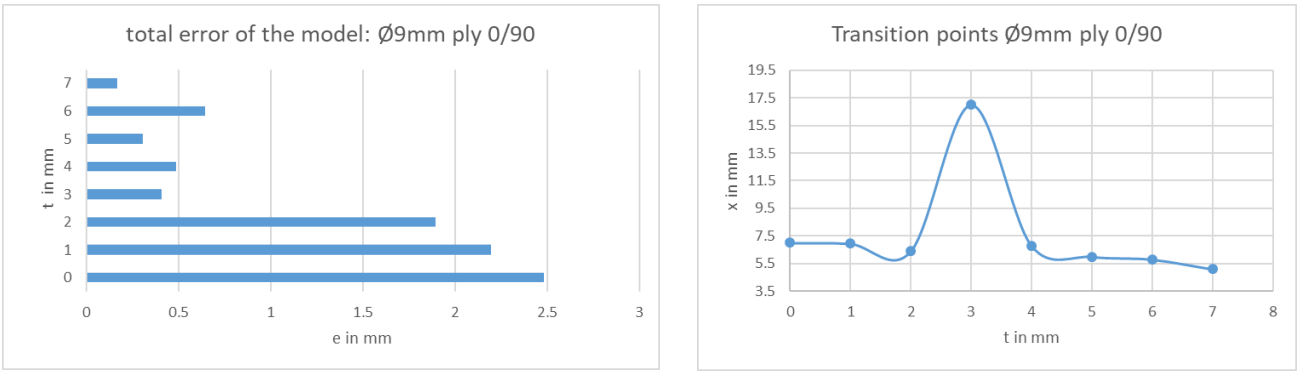

Figure 6.13. Error and inflection points for Ø9mm ply 0/90.

The right graph shows the transition points in each *t*, almost all the values are between six and seven, but in $t = 3$ shows a peak value. After this fluctuation the values are fairly static again. Therefore, there is not a common pattern with the situation seen before.

As can be seen from the error graphs from Figure 6.14 and Figure 6.15 the tendency is to concentrate the error in lower values of t as well. During the post processing of the test images it was seen that near the hole the waviness is more frequent, moreover the polynomial is not able to achieve the desired curvature with only one inflection point. The increase in the numbers

indicates that different sources of errors are produced in the explanation of this part of the fiber textiles.

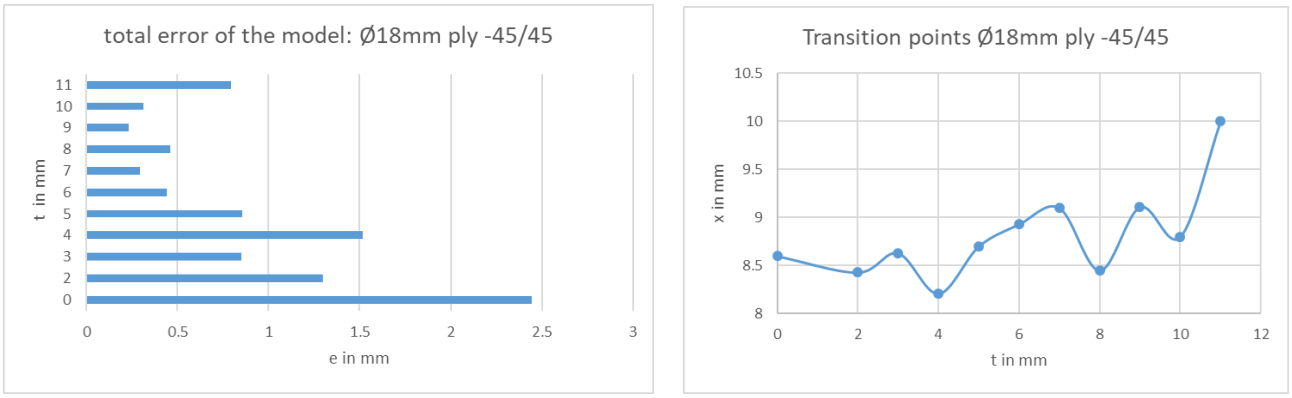

Figure 6.14. Error and inflection points for Ø18mm ply -45/45.

The transition points in the bigger diameter of the textile with ply .45/45 go up and down widely over almost all the t range and increase rapidly in the end.

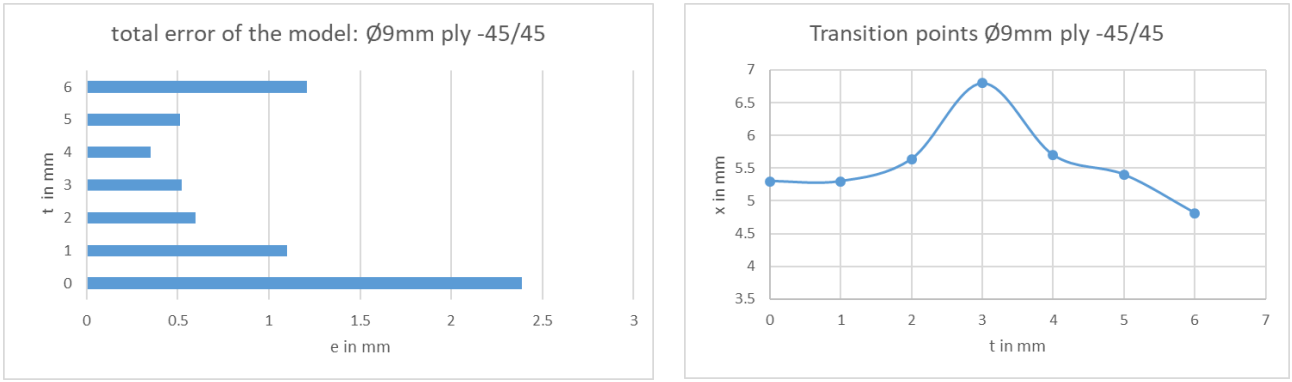

Figure 6.15. Error and inflection points for Ø9mm ply -45/45.

Finally, the transition points' figure with diameter 9mm shows a similar trend with the case Ø9mm and 0/90 ply. Both has a peak value in $t = 3mm$, although the magnitude is lower in this situation and this is follow by a downward trend.

To sum up, in all the cases the error is focus on the lower part, concretely near the axis. In material ply -45/45 there is also remarkable error values in higher distances, due to the inaccuracy of the a_0 coefficient. Regarding the transition points, the ones from the bigger hole does not present a clear trend. However, in the smaller diameter both situations perform a peak in t=3. That fact suggests that might be a relationship between x_P and the diameter, more analysis using the data of the rest of trials or tests using different diameters should be performed to achieve more details about.

6.4.4 Model expression

To end the subchapter, the values of the coefficients of the four studied cases are shown and the generic expression of the model is written below, Formula 6.21.

18 ply0/90				
t	a0	a2	a4	xP
0	9.000	-8.234E-02	1.733E-04	8.900
2	9.000	-6.921E-02	1.517E-04	8.720
3	9.000	-5.913E-02	1.294E-04	8.727
4	9.000	-5.353E-02	1.218E-04	8.559
5	9.000	-4.097E-02	9.134E-05	8.646
6	9.000	-2.462E-02	4.848E-05	9.200
7	9.000	-1.462E-02	2.644E-05	9.600
8	9.879	-1.336E-02	2.362E-05	9.710
9	10.538	-1.208E-02	2.309E-05	9.340
10	11.198	-1.096E-02	2.306E-05	8.900
11	11.858	-6.116E-03	1.083E-05	9.700
12	12.517	-4.554E-03	9.370E-06	9.000

9 ply0/90				
t	a0	a2	a4	xP
0.000	4.500	-6.488E-02	2.207E-04	7.000
1.000	4.500	-5.193E-02	1.797E-04	6.940
2.000	4.500	-5.290E-02	2.152E-04	6.400
3.000	4.500	-9.212E-03	5.313E-06	17.000
4.000	4.500	-7.983E-03	2.877E-05	6.800
5.000	4.794	7.162E-03	-3.316E-05	6.000
6.000	5.840	8.909E-03	-4.414E-05	5.800
7.000	6.886	-3.796E-03	2.433E-05	5.100

Table 6.14. Coefficients values and transition point of ply 0/90.

18 ply-45/45				
t	a0	a2	a4	xP
0	9.029	-8.588E-02	1.935E-04	8.600
2	9.063	-7.184E-02	1.685E-04	8.430
3	9.093	-5.732E-02	1.283E-04	8.630
4	9.137	-5.783E-02	1.430E-04	8.210
5	9.203	-3.857E-02	8.494E-05	8.700
6	9.301	-2.814E-02	5.882E-05	8.930
7	9.445	-1.987E-02	4.000E-05	9.100
8	9.659	-1.673E-02	3.906E-05	8.450
9	9.975	-7.902E-03	1.587E-05	9.110
10	10.443	-3.931E-03	8.461E-06	8.800
11	11.136	-9.116E-04	1.519E-06	10.000

9 ply-45/45				
t	a0	a2	a4	xP
0	4.629	-1.360E-01	8.068E-04	5.300
1	4.687	-1.083E-01	6.425E-04	5.300
2	4.770	-6.263E-02	3.281E-04	5.640
3	4.891	-2.771E-02	9.988E-05	6.800
4	5.067	-2.326E-02	1.193E-04	5.700
5	5.320	-8.601E-03	4.916E-05	5.400
6	5.688	2.031E-02	-1.463E-04	4.810

Table 6.15. Coefficients values and transition point of ply -45/45.

$$f(x) = \begin{cases} y, & x \notin [-\psi, \psi] \cup y \notin [0, |r + (C_3 \cdot r + C_4)|] \\ a_0 + \left[\frac{-6 \cdot {x_P}^2 \cdot (-t + a_0)}{\psi^4 - 6 \cdot \psi^2 \cdot x_P^2}\right] \cdot x^2 + \left[\frac{t - a_0}{\psi^4 - 6 \cdot \psi^2 \cdot x_P^2}\right] \cdot x^4, & x \in [-\psi, \psi] \cap y \in [0, |r + (C_3 \cdot r + C_4)|] \end{cases}$$

$$f(x) = \begin{cases} -y, & x \notin [-\psi, \psi] \cup y \notin [-|r + (C_3 \cdot r + C_4)|, 0] \\ -a_0 - \left[\frac{-6 \cdot {x_P}^2 \cdot (-t + a_0)}{\psi^4 - 6 \cdot \psi^2 \cdot x_P^2}\right] \cdot x^2 - \left[\frac{t - a_0}{\psi^4 - 6 \cdot \psi^2 \cdot x_P^2}\right] \cdot x^4, & x \in [-\psi, \psi] \cap y \in [-|r + (C_3 \cdot r + C_4)|, 0] \end{cases}$$

with:

$$\psi = r + C_1 \cdot r + C_2$$

$$a_0(r,t)_{ply\ 0/90} = \begin{cases} r, & t \in [0, 1 + 0{,}777 \cdot r] \\ r + (1{,}44 - 0{,}0867 \cdot r) \cdot t + (-5{,}46 + 0{,}1177 \cdot r), & t \notin [0, 1 + 0{,}777 \cdot r] \end{cases}$$

$$a_0(r,t)_{ply-45/45} = r + (0{,}2293 - 0{,}0223 \cdot r) \cdot e^{(0{,}348 + 0{,}0049 \cdot r) \cdot t}$$

where:

r *is the radius of the hole in mm.*

C_1 *and* C_2 *are the height coeffcients of the material.*

C_3 *and* C_4 *are the width coeffcients of the material.*

t *is the distance between the straight fiber and the origin in mm.*

x_P *is the x coordinate of the inflexion point for a specific t in mm.*

Formula 6.21. Final model expression

The model consists in two functions, the first one describes the half upper part, positive y, and the second one the lower half part, negative y. Due to the symmetry by x axis, the lower part has the same structure that the upper one but with opposite signs. Both functions are piecewise functions, where the constraints that delimited the straight fiberpaths from the curvilinear trajectories depend on the radius and four coefficients: C_1, C_2, C_3 and C_4. These coefficients have a specific value for each material.

Moreover, the coefficient a_0 is also described for each material in particular. Being a piecewise function for the carbon fiber with ply 0/90 and an exponential for the carbon fiber ply -45/45.

The expressions of a_2 and a_4 have the special feature that they depend on the x coordinate of the inflection point. That's the parameter which provides the concavity of the curve.

As a last comment, it is important notice that the model is related to a variable called *t*, which is defined as the distance between the x axis and the straight fiber. Changing this variable, the family of curves is obtained.

6.5 Conclusions

6.5.1 Validation

The last step of this project is the evaluation of the obtained model. Using the expression formulated in the last chapter, the plots for the four studied cases will be obtained as it is explained in the chapter 4.2.4. In the Figure 6.16 the results are shown.

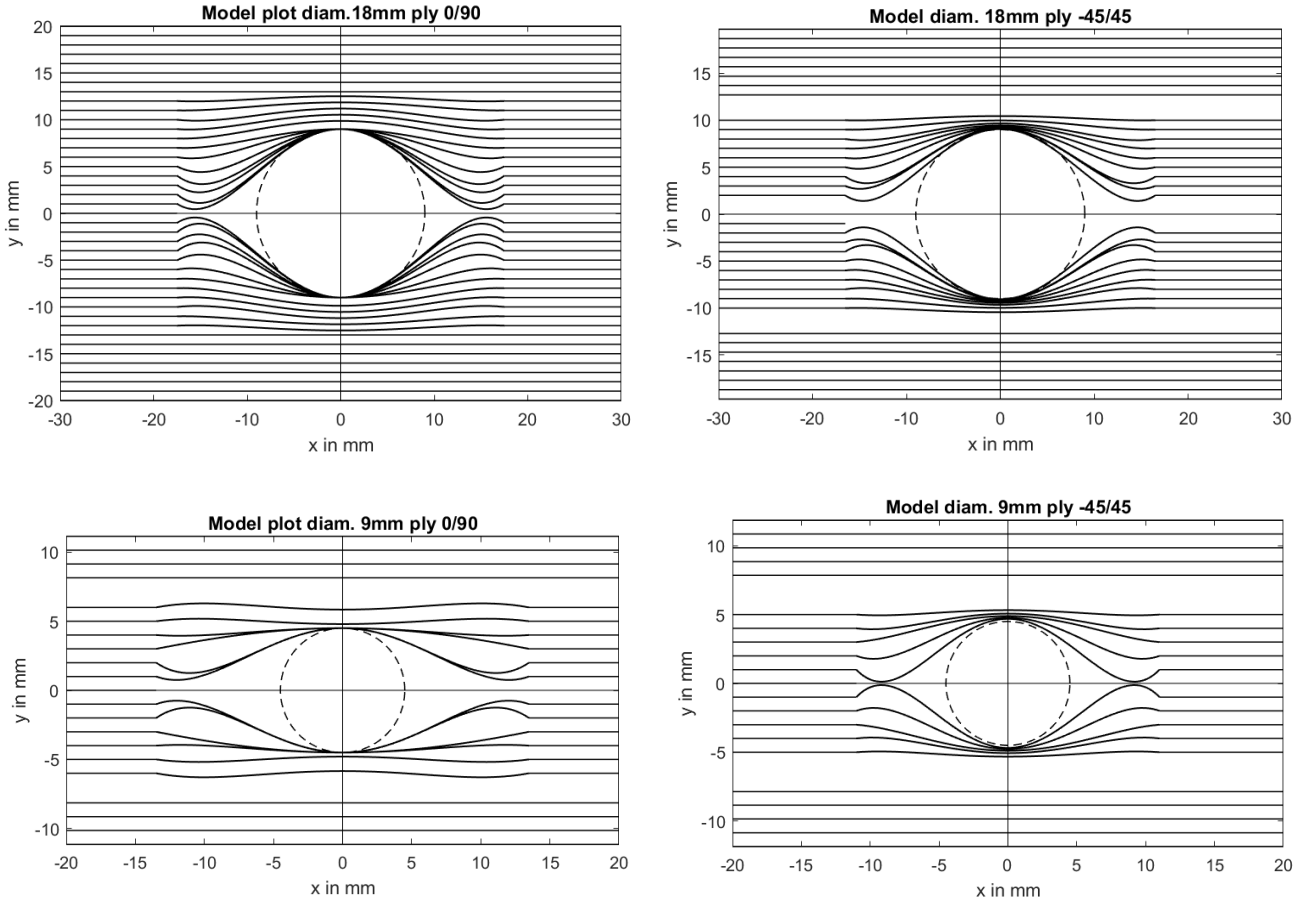

Figure 6.16. Model plots of the 4 studied situations.

If the different situations are observed, it is clear that the diameter has a big effect on the main shape of the curves. Moreover, it is noticed the difference between materials, concretely in the increasing behavior.

After analyzing them an important conclusion can be taken, the model does not describe a soft transition between the deformed and non-deformed regions. That fact suggest that more than one inflection point is required.

To validate the fiberpaths in the following lines a visual evaluation of the models overlapped with the real images, from which the coefficients were predicted, is done.

- **Carbon fiber ply 0/90 Ø 9mm.**

The first situation illustrated in Figure 6.17 is the carbon fiber with ply0/90 and the centered hole of diameter 9mm.

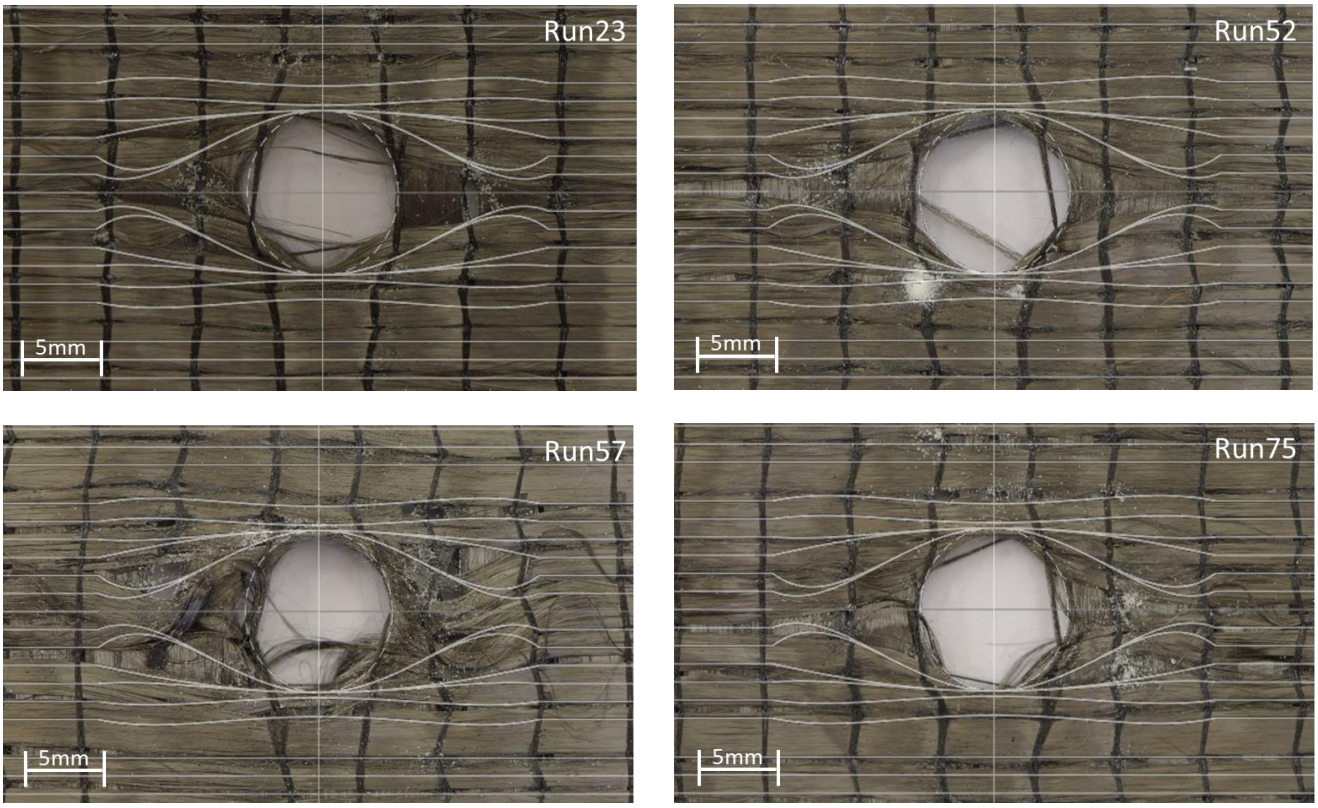

Figure 6.17. Overlapped model with real images Ø9mm ply 0/90.

The four images have the influencing factors in the same level. However, variability between them are observed. If we analyzed each image separately, another issues appear: unsymmetry and waviness. For example, the image of Run57 is not a good resource to validate the model, because of the wave presence in the central region. Using the images Run23, Run52 and Run75 it is seen that the model describes with more accuracy the fiberpaths with y values over the radius. Regarding the central regions seems to describe better the upper half part.

- **Carbon fiber ply -45/45 Ø 9mm.**

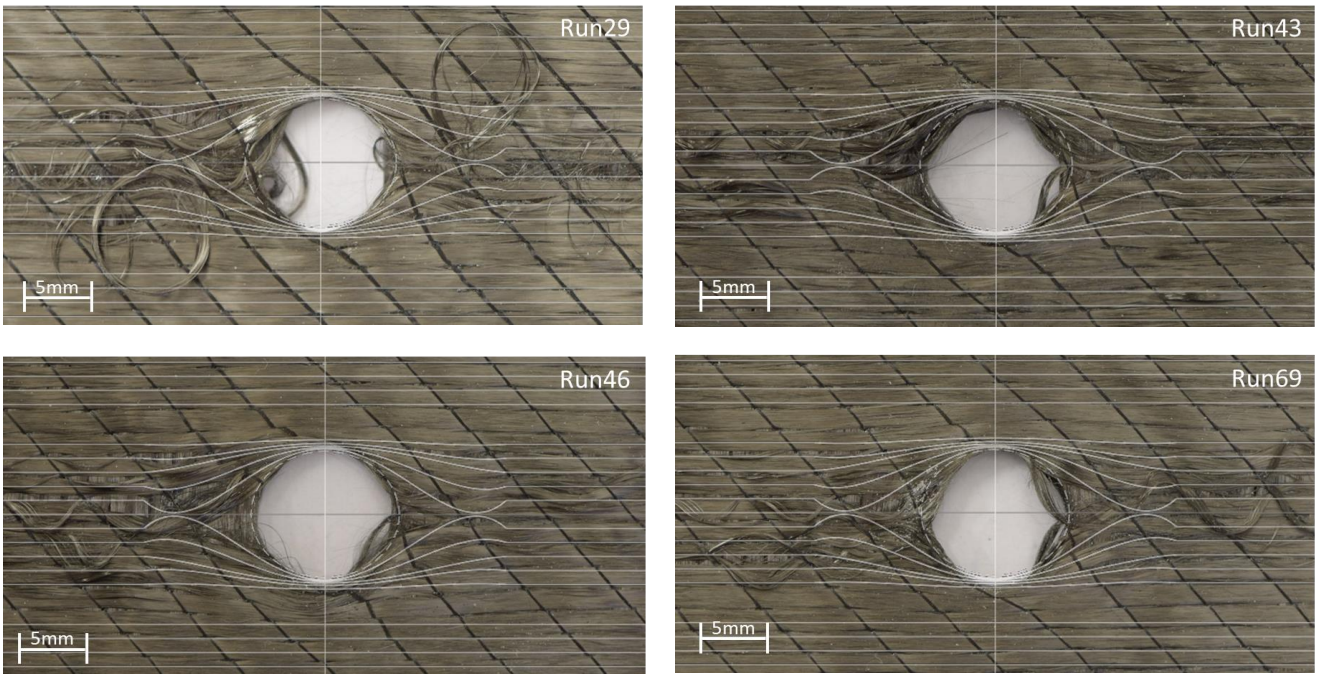

Figure 6.18. Overlapped model with real images Ø9mm ply -45/45.

The second case is with the same size of the hole but of the other fabric, ply -45/45 Figure 6.18. Although in this situation the presence of waviness is higher, it seems to be more symmetric by the y axis than the last one. The accuracy still seems to be worst in the paths near the x axis, however the prediction is apparently better than the first situation.

- **Carbon fiber ply 0/90 Ø 18mm**

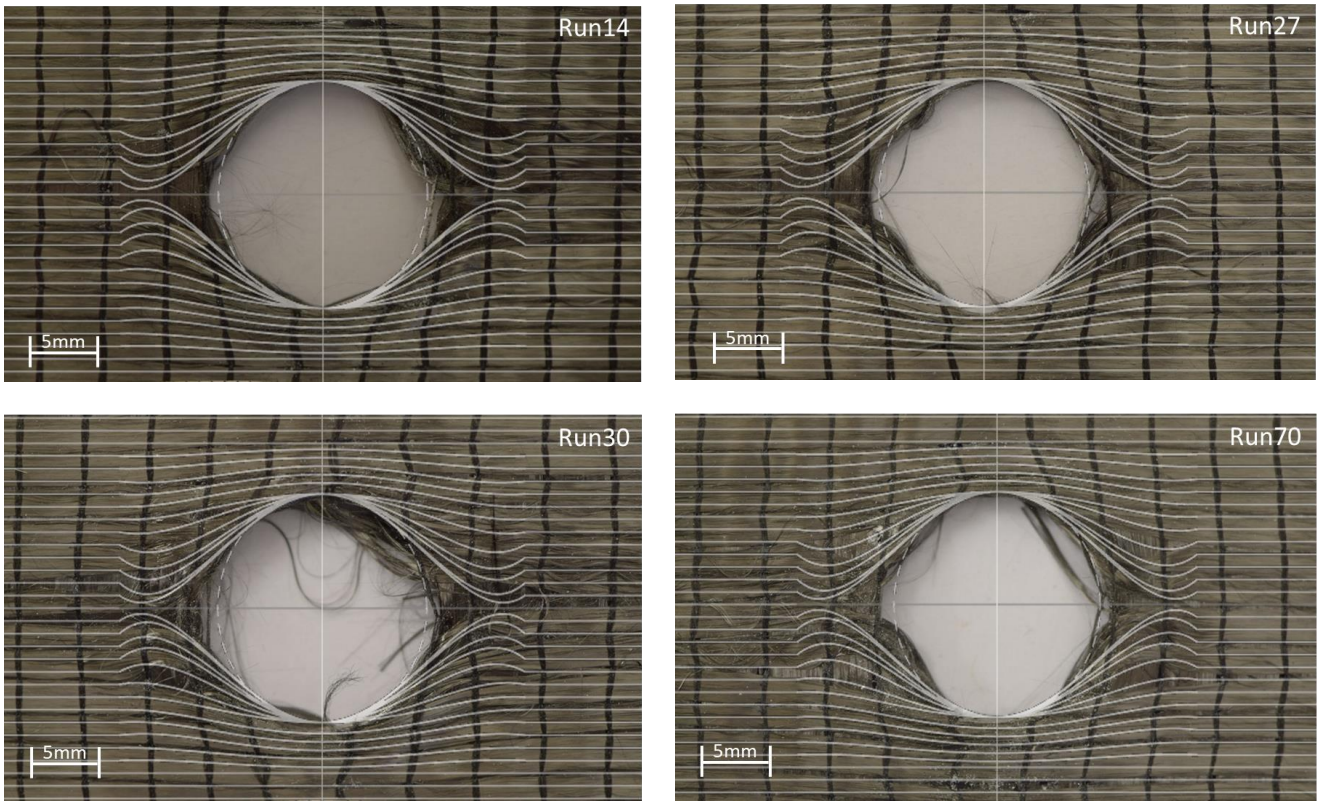

Figure 6.19. Overlapped model with real images Ø18mm ply 0/90.

The image above shows the case with a bigger diameter and textile with ply 0/90. Even though the deformed area is bigger, the model describes quite well the increasing behavior of the material. As it was mentioned in the previous cases, there is still issues in describe the trajectories in the laterals of the hole. However, the waviness is lower than the samples already analyzed.

- **Carbon fiber ply -45/45 Ø 18mm**

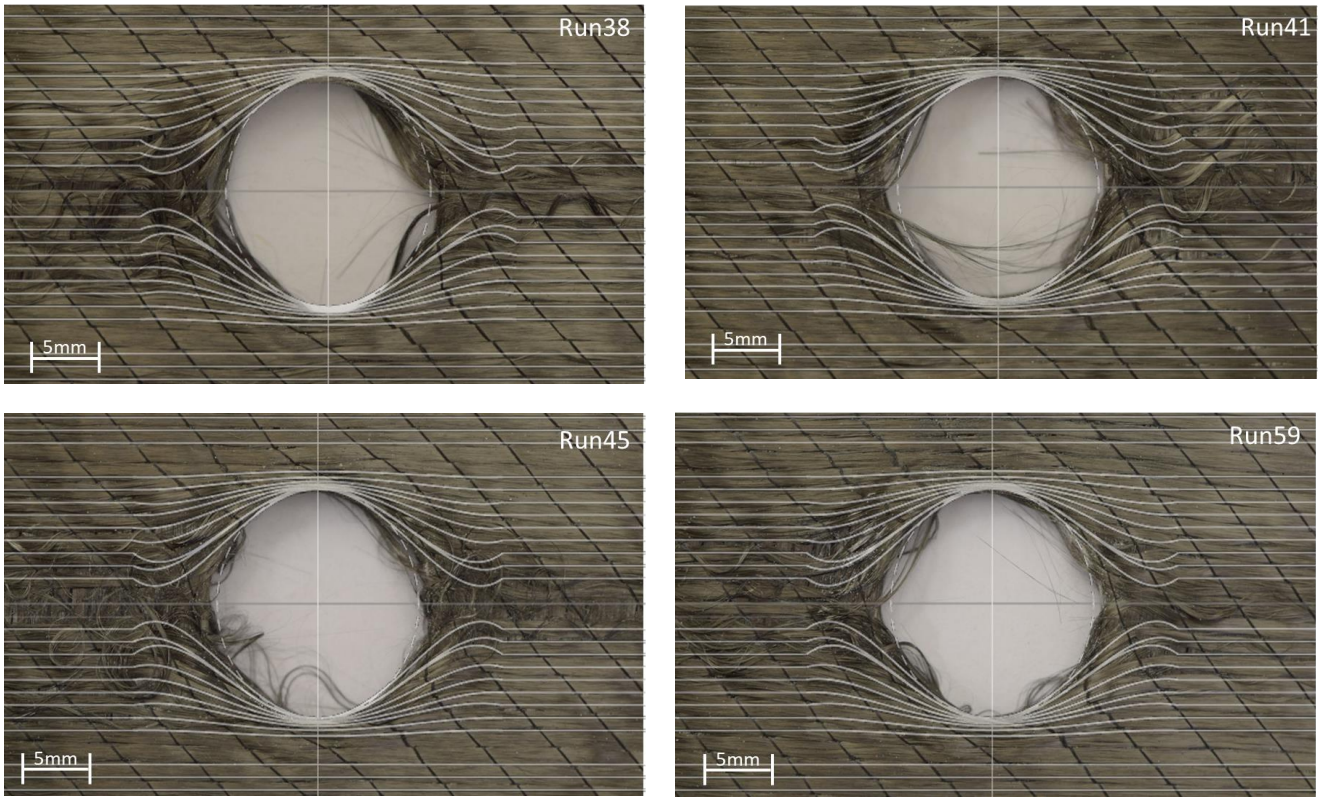

Figure 6.20. Overlapped model with real images Ø18mm ply -45/45.

In the last situation, the conclusions are similar. The waviness and unsymmetry makes harder validate the model using visual methods. So it seems that the best way to quantify the results is the error minimization performed in the last chapter.

6.5.2 Sources of error

Throughout the work different error sources were found:

The first one is already mentioned, the model described by the fourth-degree polynomial is not enough to fit the real data and define the transition area. The proposed model has got a unique inflection point concerning the data region, more degrees of freedom are needed to adjust better the curve and the straight path.

Moreover, the variability in the tested samples is high. Defects such as the waviness and the unsymmetry increase the error of the model. These defects also introduced unreliable data in the model, due to the uncertain in the manually plotting.

Regarding the manually plotting of the real trajectories, it is considered a source of error as well. Most of the collected data required the accuracy of the human eye, that means that these values are subjective and the values proposed in this work, should be validated with more information.

7 Summary and Outlook

7.1 Summary

This work was done to create knowledge about the prediction of the trajectories of the fiberpaths when an insert is located using RTM. It was noticed that the consistence of the fibers has a positive effect in the mechanical performance in the joining area. However, there is very little research in this field.

One of the main objectives was to study deeply about the influencing factors, that might produce the curvilinear behaviors. A design of experiments was proposed and simple punch process were performed in order to analyze the effects of the possible influencing factors. After the statistical evaluation of the samples, the material and the hole diameter were chosen as a responsible of the fiberpaths relocation.

The goal was use these factors and the information provided by the tested samples to develop an analytical model. The main expression of the model was chosen after the approximation and description of the real trajectories of the samples. In order to realize this description, a manually plotting was performed and then a regression analysis by fitting different curves shapes to the approximated paths was done. The resulting polynomial expression was simplified with symmetry constraints and a fourth-degree polynomial with three coefficients was proposed as a model.

The next objective was the formulation of the deformed area boundaries. In order to do that some measures were taken from the tested images and by geometrical descriptions the constraints of a piecewise function were obtained in relation the radius of the hole and four coefficients, which the value depends on the material.

More geometrical descriptions were used to define the mathematical expressions of the three coeffcients. Regarding the increasing behavior, distance between fiberpaths, it was noticed and described different behaviors for the both studied materials. Then, the coefficients of the dependent terms of the function were expressed in relation the inflection point, point where the concavity of the curve changes. In the end, the numerical values were found by an iterative process of error minimization.

During the process some error sources were found. Concretely the phenomenon of waviness and unsymmetry of the samples made harder achieve a good accuracy. Another issue was found related to the performance of the model, the transition between the deformed and non-deformed area was not softly enough, fact that suggests that more than one inflection point is needed.

Even though the presence of errors, after this project, the following steps to improve in this research topic are clearer.

7.2 Outlook

Research on the prediction of the trajectories of the fiberpaths located in the joining area have been done to further improvements in the fibers optimization that allows an increase of the mechanical performance of the multi material assemblies. However, further studies should be made in order to optimize the definition of the model and describe better the different behaviors of the materials.

In the case of the curve definition, further investigations may be done to describe the transition between the deformed and non-deformed region, using splines instead of one polynomial could be the following step.

Another issue that may be tackled is the need to conduct more experimental studies with more diameters and materials, the aim should be the validation of the expressions and coefficients proposed in this work.

Moreover, the methodology used is too subjective in some points, thus further steps to improve the collect process of the data could help to reduce the error of the model significantly.

List of Figures

List of Tables

Appendix

In the appendix, the resulting from the work of larger tables, lists, layouts, program code, etc. are included.

A. Experiment design and measures
B. Regression analysis results
C. Assessment tables
D. Matlab code

A. Experiment design and measures

Run	Hole Ø	Material	Shape pin	Angle pin	Clamping force	Deformed area (mm^2)	Waviness(px)
1	+	-	-	-	-	952.969	3706372
2	-	-	-	+	-	455.726	2929775
3	+	+	+	+	+	1201.463	364699
4	-	+	+	+	-	297.979	2014394
5	+	-	-	+	+	773.722	4143977
6	+	+	-	-	+	849.622	1313704
7	+	-	+	+	-	773.711	2690334
8	-	+	+	-	+	846.546	482991
9	-	-	-	-	+	250.164	675233
10	-	-	+	-	-	251.613	1874773
11	-	+	-	-	-	236.243	947528
12	+	-	+	-	+	660.511	1690335
13	+	+	+	+	+	709.555	1375320
14	+	+	+	+	+	752.605	350066
15	-	+	+	-	+	360.531	155756
16	+	-	+	-	+	902.988	1330043
17	+	-	-	-	-	758.519	2251043
18	-	-	-	+	-	257.029	1947855
19	+	+	-	+	-	717.498	1162176
20	-	-	+	-	-	306.912	1992974
21	-	+	+	+	-	366.848	67955
22	+	-	+	+	-	740.403	1015953
23	-	+	+	-	+	403.364	89774
24	+	+	-	-	+	852.151	463466
25	+	+	-	+	-	797.301	473798
26	+	-	-	+	+	859.369	1403637
27	+	+	-	-	+	957.351	156042
28	-	-	+	+	+	283.745	1683169
29	-	-	-	+	-	238.824	1480256
30	+	+	-	-	+	821.739	196455
31	+	+	+	+	+	934.923	355651
32	-	+	-	+	+	596.143	385747
33	+	+	+	-	-	862.459	683042
34	+	+	-	+	-	854.85	728813
35	+	+	+	-	-	694.382	214277
36	-	-	-	-	+	258.164	445584
37	+	+	+	+	+	643.14	400345
38	+	-	+	-	+	737.728	2675992
39	-	-	+	+	+	310.996	397196
40	-	+	-	-	-	281.779	475961

41	+	-	-	-	-	827.194	1634113
42	-	+	+	-	+	424.672	117131
43	-	-	+	-	-	288.271	628123
44	+	+	-	+	-	889.434	1236893
45	+	-	-	+	+	727.756	2877837
46	-	-	+	+	+	331.528	1119618
47	-	+	-	+	+	277.933	476395
48	-	-	+	-	-	306.89	764260
49	-	-	-	+	-	260.755	3497476
50	+	-	-	-	-	664.538	1236750
51	-	+	+	-	+	3055.355	701260
52	-	+	-	-	-	431.906	41363
53	+	-	+	-	+	825.825	2334737
54	-	-	+	-	-	422.485	1761956
55	-	-	-	+	-	269.528	2083135
56	-	+	-	-	-	282.975	423860
57	-	+	-	+	+	413.963	817449
58	+	+	-	+	-	780.423	237551
59	+	-	+	+	-	734.722	1374806
60	+	+	-	-	+	933.759	280314
61	-	+	-	-	-	324.986	549037
62	+	-	+	+	-	639.824	2099232
63	-	+	-	+	+	353.428	187682
64	+	-	-	-	-	647.593	1675127
65	+	-	-	+	+	739.319	3232496
66	+	-	+	+	-	734.475	1275873
67	+	-	-	+	+	911.304	1000671
68	-	+	-	+	+	311.893	862728
69	-	-	-	-	+	242.005	1926878
70	+	+	+	-	-	929.25	943840
71	+	+	+	-	-	745.957	755682
72	-	-	+	+	+	278.569	1125811
73	+	-	+	-	+	833.153	2399753
74	-	-	-	-	+	262.992	1506334
75	-	+	+	+	-	314.9	177727
76	-	+	+	+	-	318.439	133757
77	+	+	+	-	-	988.206	271717
78	-	+	+	+	-	511.153	141237
79	-	-	-	-	+	369.466	560777
80	-	-	+	+	+	328.054	925303

B. Regression analysis results

- **Range data selection**

Run3: B5:041

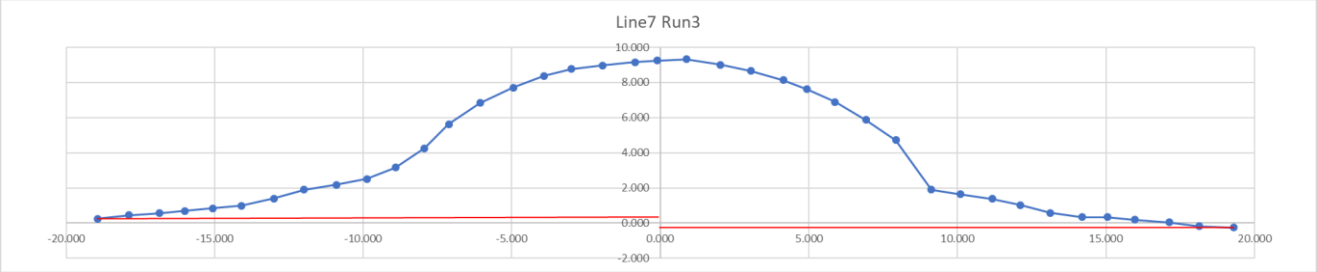

0.000	9.502
0.201	9.562
0.322	9.260
0.443	8.897
0.605	8.373
0.746	7.869
1.149	7.143
1.653	6.116
1.935	4.967
2.257	2.145
2.923	1.883
4.011	1.621
5.382	1.278
6.591	0.835
7.458	0.593
8.123	0.593
8.526	0.431
8.728	0.281
8.909	0.071
9.010	0.000

Run39: B11:M41

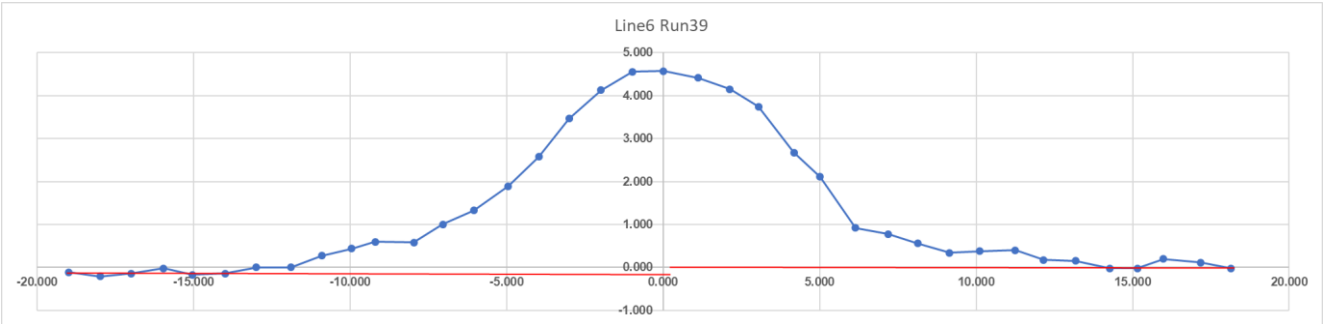

0.000	4.599
0.094	4.438
0.032	4.175
0.091	3.771
0.059	2.701
0.032	2.136
0.115	0.945
0.115	0.803
0.390	0.581
0.551	0.359
0.713	0.400
0.692	0.420
1.116	0.198
1.439	0.177
2.005	0.000
2.691	0.000
3.580	0.218
4.246	0.137
4.670	0.000
4.690	0.000

Run42: B11:M39

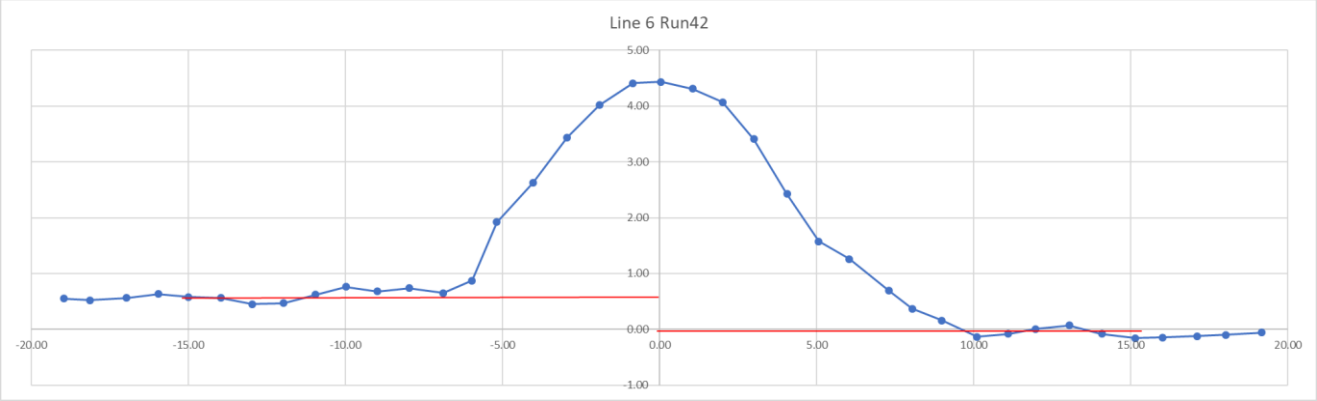

0.000	4.492
0.030	4.371
0.010	4.130
0.080	3.468
0.030	2.485
0.010	1.633
0.100	1.322
0.080	0.750
0.070	0.429
0.211	0.219
0.130	0.073
0.190	0.020
0.100	0.063
0.321	0.133
1.374	0.020
2.076	0.100
2.888	0.089
3.470	0.064
3.861	0.037
	0.002

Run63: B15:K38

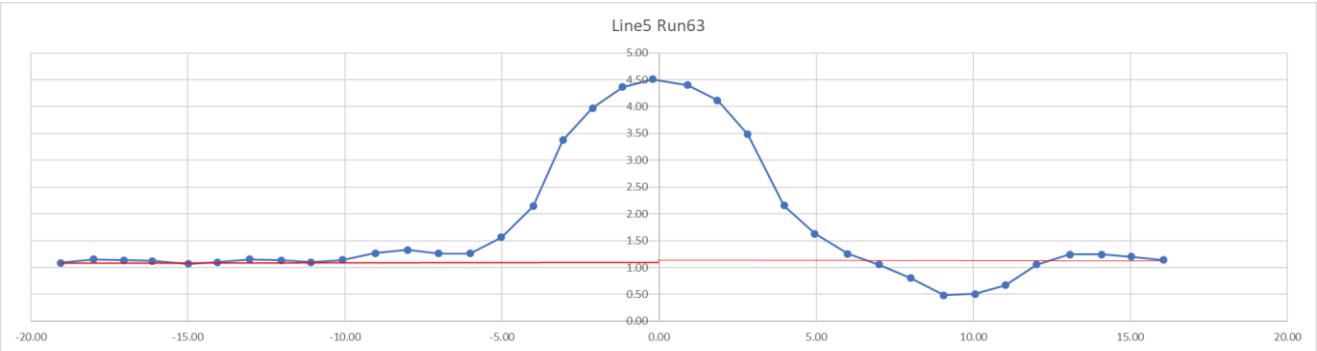

0.001	3.371
0.067	3.259
0.045	2.978
0.033	2.344
0.019	1.017
0.009	0.494
0.067	0.12
0.045	0.082
0.013	0.335
0.051	0.658
0.18	0.63
0.238	0.471
0.176	0.082
0.174	0.107
0.473	0.105
1.052	0.063
2.283	0
2.883	
3.272	
3.421	

Run76: B10:M32

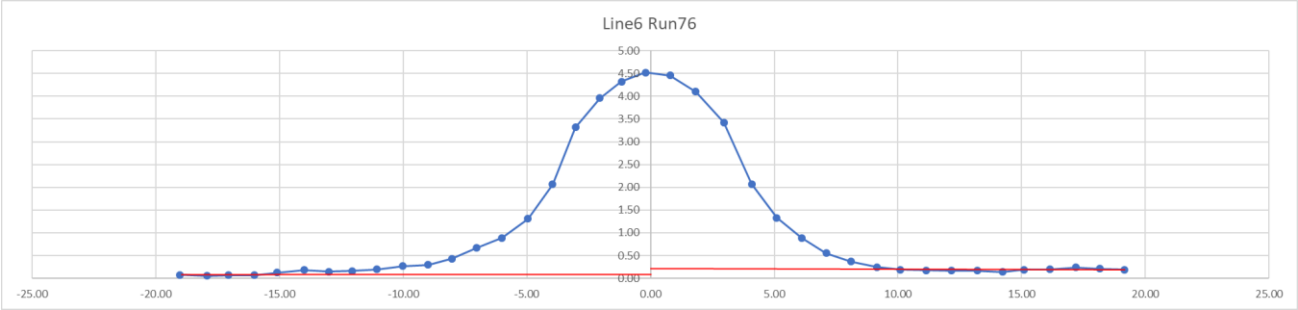

0.004	4.332
0.019	4.271
0.002	3.910
0.002	3.237
0.059	1.884
0.114	1.142
0.079	0.701
0.089	0.360
0.129	0.179
0.199	0.059
0.229	0.001
0.360	0.011
0.600	0.021
0.821	0.021
1.242	0.051
1.994	0.001
3.248	0.009
3.890	0.049
4.251	0.019
4.452	0.001

- **Goodness of fit parameters**

Run3

Line1

	sse	rsquare	dfe	adjrsquare	rmse
Polyfit7	0.26938	0.88312	29	0.8549	0.09638
Polyfit6	0.2719	0.88203	30	0.85843	0.095201
Polyfit5	0.27681	0.87989	31	0.86052	0.094496
Polyfit4	0.30502	0.86765	32	0.85111	0.097632
Polyfit3	0.33355	0.85528	33	0.84212	0.10054
Cosinusfit	0.33475	0.85475	33	0.84155	0.10072

Line2

	sse	rsquare	dfe	adjrsquare	rmse
Polyfit7	0.24498	0.96434	29	0.95573	0.09191
Polyfit6	0.3472	0.94946	30	0.93935	0.10758
Polyfit5	0.54028	0.92135	31	0.90867	0.13202
Polyfit4	0.54037	0.92134	32	0.91151	0.12995
Polyfit3	1.4881	0.78338	33	0.76368	0.21236
Cosinusfit	6.8885	-0.0027322	33	-0.09389	0.45688

Line3

	sse	rsquare	dfe	adjrsquare	rmse
Polyfit7	0.21523	0.98786	29	0.98493	0.08615
Polyfit6	0.35117	0.98019	30	0.97623	0.10819
Polyfit5	1.1036	0.93775	31	0.92771	0.18868
Polyfit4	1.1818	0.93334	32	0.92501	0.19218
Polyfit3	3.8294	0.784	33	0.76437	0.34065
Cosinusfit	0.90457	0.94898	33	0.94434	0.16556

Line4

	sse	rsquare	dfe	adjrsquare	rmse
Polyfit7	0.19178	0.998	29	0.99752	0.081321
Polyfit6	0.93377	0.99027	30	0.98832	0.17642
Polyfit5	2.0012	0.97914	31	0.97578	0.25408
Polyfit4	3.0141	0.96859	32	0.96466	0.30691
Polyfit3	16.261	0.83053	33	0.81513	0.70197
Cosinusfit	90.756	0.054163	33	-0.031823	1.6584

Line5

	sse	rsquare	dfe	adjrsquare	rmse
Polyfit7	0.24737	0.99873	29	0.99842	0.092359
Polyfit6	0.97635	0.99497	30	0.99397	0.1804
Polyfit5	4.0012	0.9794	31	0.97608	0.35926
Polyfit4	5.9028	0.96961	32	0.96581	0.42949
Polyfit3	37.811	0.80536	33	0.78766	1.0704
Cosinusfit	187.78	0.033326	33	-0.054553	2.3855

Line6

	sse	rsquare	dfe	adjrsquare	rmse
Polyfit7	2.1667	0.99358	29	0.99202	0.27334
Polyfit6	2.6288	0.9922	30	0.99065	0.29602
Polyfit5	6.9961	0.97925	31	0.97591	0.47506
Polyfit4	11.106	0.96707	32	0.96295	0.58913
Polyfit3	72.645	0.78459	33	0.765	1.4837
Cosinusfit	6.358	0.98115	33	0.97943	0.43894

Line7

	sse	rsquare	dfe	adjrsquare	rmse
Polyfit7	4.5856	0.98964	29	0.98714	0.39765
Polyfit6	4.8298	0.98909	30	0.98691	0.40124
Polyfit5	10.348	0.97663	31	0.97286	0.57775
Polyfit4	13.587	0.96931	32	0.96547	0.65161
Polyfit3	83.946	0.81038	33	0.79314	1.5949
Cosinusfit	7.2344	0.98366	33	0.98217	0.46821

Run39

Line1

	sse	rsquare	dfe	adjrsquare	rmse
Polyfit7	0.094104	0.92436	21	0.89914	0.066941
Polyfit6	0.11191	0.91004	22	0.88551	0.071323
Polyfit5	0.12996	0.89553	23	0.87282	0.07517
Polyfit4	0.14297	0.88508	24	0.86593	0.077182
Polyfit3	0.14305	0.88501	25	0.87121	0.075645
Cosinusfit	0.18402	0.85208	25	0.83433	0.085795

Line2

	sse	rsquare	dfe	adjrsquare	rmse
Polyfit7	0.032396	0.99034	21	0.98712	0.039277
Polyfit6	0.037683	0.98876	22	0.9857	0.041387
Polyfit5	0.090337	0.97307	23	0.96721	0.062671
Polyfit4	0.18348	0.94529	24	0.93618	0.087437
Polyfit3	0.27678	0.91748	25	0.90757	0.10522
Cosinusfit	0.3019	0.90999	25	0.89919	0.10989

Line3

	sse	rsquare	dfe	adjrsquare	rmse
Polyfit7	0.11783	0.98257	21	0.97676	0.074906
Polyfit6	0.11825	0.98251	22	0.97773	0.073316
Polyfit5	0.19163	0.97165	23	0.96549	0.091278
Polyfit4	0.23427	0.96534	24	0.95957	0.098798
Polyfit3	0.96912	0.85663	25	0.83942	0.19689
Cosinusfit	7.8279	-0.15807	25	-0.29704	0.55957

Line4

	sse	rsquare	dfe	adjrsquare	rmse
Polyfit7	0.12146	0.99215	21	0.98953	0.076053
Polyfit6	0.15306	0.9901	22	0.9874	0.083411
Polyfit5	0.22061	0.98574	23	0.98263	0.097938
Polyfit4	0.29618	0.98085	24	0.97766	0.11109
Polyfit3	1.3646	0.91177	25	0.90118	0.23363
Cosinusfit	0.76064	0.95082	25	0.94492	0.17443

Line5

	sse	rsquare	dfe	adjrsquare	rmse
Polyfit7	0.20263	0.99295	21	0.9906	0.098229
Polyfit6	0.345	0.98799	22	0.98472	0.12523
Polyfit5	1.094	0.96193	23	0.95365	0.21809
Polyfit4	1.17	0.95928	24	0.95249	0.22079
Polyfit3	5.4036	0.81194	25	0.78937	0.46491
Cosinusfit	28.734	-4.08E-05	25	-0.12005	1.0721

Line6

	sse	rsquare	dfe	adjrsquare	rmse
Polyfit7	1.3235	0.98255	21	0.97673	0.25105
Polyfit6	1.6758	0.9779	22	0.97188	0.276
Polyfit5	6.4566	0.91487	23	0.89637	0.52983
Polyfit4	7.6705	0.89887	24	0.88201	0.56534
Polyfit3	22.514	0.70316	25	0.66754	0.94899
Cosinusfit	5.1141	0.93257	25	0.92448	0.45229

Run42

Line1

	sse	rsquare	dfe	adjrsquare	rmse
Polyfit7	0.01593	0.96671	21	0.95561	0.027542
Polyfit6	0.0226	0.95277	22	0.93988	0.032051
Polyfit5	0.02361	0.95065	23	0.93993	0.032039
Polyfit4	0.027672	0.94216	24	0.93253	0.033956
Polyfit3	0.027956	0.94157	25	0.93456	0.03344
Cosinusfit	0.025995	0.94567	25	0.93915	0.032246

Line2

	sse	rsquare	dfe	adjrsquare	rmse
Polyfit7	0.01295	0.69207	21	0.58943	0.024833
Polyfit6	0.013028	0.69021	22	0.60572	0.024335
Polyfit5	0.015876	0.6225	23	0.54044	0.026273
Polyfit4	0.017086	0.59372	24	0.52601	0.026682
Polyfit3	0.017684	0.57951	25	0.52905	0.026596
Cosinusfit	0.051045	-0.21377	25	-0.35943	0.045186

Line3

	sse	rsquare	dfe	adjrsquare	rmse
Polyfit7	0.019485	0.9947	21	0.99294	0.030461
Polyfit6	0.089023	0.9758	22	0.9692	0.063612
Polyfit5	0.14425	0.96079	23	0.95227	0.079194
Polyfit4	0.37464	0.89817	24	0.8812	0.12494
Polyfit3	0.59609	0.83798	25	0.81854	0.15441
Cosinusfit	0.29181	0.92068	25	0.91117	0.10804

Line4

	sse	rsquare	dfe	adjrsquare	rmse
Polyfit7	0.51331	0.97054	21	0.96072	0.15634
Polyfit6	0.56508	0.96757	22	0.95873	0.16027
Polyfit5	2.5854	0.85163	23	0.81938	0.33527
Polyfit4	2.5856	0.85162	24	0.82689	0.32823
Polyfit3	6.8865	0.60481	25	0.55739	0.52484
Cosinusfit	15.027	0.13767	25	0.034193	0.77529

Line5

	sse	rsquare	dfe	adjrsquare	rmse
Polyfit7	0.53099	0.98662	21	0.98216	0.15901
Polyfit6	0.5487	0.98618	22	0.9824	0.15793
Polyfit5	3.1152	0.92151	23	0.90445	0.36802
Polyfit4	3.3243	0.91624	24	0.90228	0.37217
Polyfit3	11.741	0.70418	25	0.66868	0.68531
Cosinusfit	5.0102	0.87376	25	0.85862	0.44767

Line6

	sse	rsquare	dfe	adjrsquare	rmse
Polyfit7	1.0344	0.98563	21	0.98083	0.22194
Polyfit6	1.6246	0.97742	22	0.97127	0.27175
Polyfit5	6.8864	0.9043	23	0.8835	0.54718
Polyfit4	7.9576	0.88942	24	0.87098	0.57582
Polyfit3	25.249	0.64912	25	0.60702	1.005
Cosinusfit	5.735	0.9203	25	0.91074	0.47896

Run63

Line1

	sse	rsquare	dfe	adjrsquare	rmse
Polyfit7	0.017642	0.96528	21	0.95371	0.028984
Polyfit6	0.017642	0.96528	22	0.95581	0.028318
Polyfit5	0.019142	0.96233	23	0.95414	0.028849
Polyfit4	0.025398	0.95002	24	0.94169	0.032531
Polyfit3	0.038814	0.92362	25	0.91445	0.039403
Cosinusfit	0.027736	0.94542	25	0.93887	0.033308

Line2

	sse	rsquare	dfe	adjrsquare	rmse
Polyfit7	0.025548	0.91283	21	0.88377	0.034879
Polyfit6	0.029238	0.90024	22	0.87304	0.036455
Polyfit5	0.041528	0.85831	23	0.82751	0.042492
Polyfit4	0.042737	0.85418	24	0.82988	0.042199
Polyfit3	0.056016	0.80888	25	0.78594	0.047335
Cosinusfit	0.040957	0.86026	25	0.84349	0.040476

Line3

	sse	rsquare	dfe	adjrsquare	rmse
Polyfit7	0.1619	0.94054	21	0.92072	0.087804
Polyfit6	0.1863	0.93158	22	0.91292	0.092023
Polyfit5	0.54493	0.79986	23	0.75635	0.15392
Polyfit4	0.6305	0.76843	24	0.72984	0.16208
Polyfit3	1.0782	0.60401	25	0.55649	0.20767
Cosinusfit	0.68187	7.50E-01	25	0.71951	0.16515

Line4

	sse	rsquare	dfe	adjrsquare	rmse
Polyfit7	2.725	0.89956	21	0.86608	0.36023
Polyfit6	2.794	0.89702	22	0.86893	0.35637
Polyfit5	7.5623	0.72127	23	0.66067	0.57341
Polyfit4	7.6268	0.71889	24	0.67203	0.56372
Polyfit3	11.173	0.58819	25	0.53878	0.66851
Cosinusfit	9.4956	6.50E-01	25	0.60801	0.6163

Line5

	sse	rsquare	dfe	adjrsquare	rmse
Polyfit7	2.5993	0.94491	21	0.92655	0.35182
Polyfit6	2.6949	0.94289	22	0.92731	0.34999
Polyfit5	8.9564	0.81019	23	0.76893	0.62403
Polyfit4	9.1014	0.80712	24	0.77497	0.61581
Polyfit3	25.826	0.45267	25	0.38699	1.0164
Cosinusfit	6.0629	0.87151	25	0.85609	0.49246

Run76

Line1

	sse	rsquare	dfe	adjrsquare	rmse
Polyfit7	0.010393	0.97436	15	0.9624	0.026323
Polyfit6	0.010823	0.97331	16	0.96329	0.026008
Polyfit5	0.012421	0.96936	17	0.96035	0.027031
Polyfit4	0.013805	0.96595	18	0.95838	0.027694
Polyfit3	0.031643	0.92195	19	0.90963	0.04081
Cosinusfit	0.025953	0.93599	19	0.92588	0.036959

Line2

	sse	rsquare	dfe	adjrsquare	rmse
Polyfit7	0.010324	0.90553	15	0.86145	0.026235
Polyfit6	0.010623	0.90279	16	0.86634	0.025767
Polyfit5	0.011659	0.89331	17	0.86193	0.026189
Polyfit4	0.01235	0.887	18	0.86189	0.026193
Polyfit3	0.035066	0.67913	19	0.62847	0.04296
Cosinusfit	0.034736	0.68215	19	0.63197	0.042758

Line3

	sse	rsquare	dfe	adjrsquare	rmse
Polyfit7	0.052578	0.9705	15	0.95674	0.059205
Polyfit6	0.072795	0.95916	16	0.94385	0.067451
Polyfit5	0.074417	0.95825	17	0.94597	0.066162
Polyfit4	0.17265	0.90314	18	0.88162	0.097938
Polyfit3	0.34589	0.80596	19	0.77532	0.13492
Cosinusfit	0.14887	0.91648	19	0.9033	0.088517

Line4

	sse	rsquare	dfe	adjrsquare	rmse
Polyfit7	0.10124	0.99272	15	0.98932	0.082156
Polyfit6	0.3474	0.97502	16	0.96565	0.14735
Polyfit5	0.3492	0.97489	17	0.96751	0.14332
Polyfit4	1.3458	0.90323	18	0.88173	0.27344
Polyfit3	1.8168	0.86937	19	0.84874	0.30922
Cosinusfit	1.0313	0.92585	19	0.91414	0.23298

Line5

	sse	rsquare	dfe	adjrsquare	rmse
Polyfit7	0.12375	0.99671	15	0.99517	0.090829
Polyfit6	0.88588	0.97644	16	0.9676	0.2353
Polyfit5	0.89188	0.97628	17	0.9693	0.22905
Polyfit4	4.2243	0.88765	18	0.86268	0.48444
Polyfit3	4.9946	0.86716	19	0.84619	0.51271
Cosinusfit	37.185	0.011021	19	-0.14513	1.399

Line6

	sse	rsquare	dfe	adjrsquare	rmse
Polyfit7	0.34773	0.99419	15	0.99148	0.15226
Polyfit6	1.1343	0.98105	16	0.97395	0.26626
Polyfit5	1.1704	0.98045	17	0.9747	0.26239
Polyfit4	6.9121	0.88455	18	0.85889	0.61968
Polyfit3	8.6574	0.8554	19	0.83257	0.67502
Cosinusfit	4.7217	0.92113	19	0.90868	0.49851

- **Bound of coefficients**

Run3

- Line1

```
Linear model Poly7:
ans(x) = p1*x^7 + p2*x^6 + p3*x^5 + p4*x^4 + p5*x^3 +
             p6*x^2 + p7*x + p8
  where x is normalized by mean -1.034 and std 10.84
Coefficients (with 95% confidence bounds):
  p1 =    -0.02111  (-0.1041, 0.06188)
  p2 =    -0.02438  (-0.09429, 0.04552)
  p3 =      0.1492  (-0.2429, 0.5414)
  p4 =      0.1388  (-0.1427, 0.4203)
  p5 =     -0.3325  (-0.8773, 0.2122)
  p6 =     -0.4494  (-0.7474, -0.1515)
  p7 =      0.2824  (0.0648, 0.5001)
  p8 =        12.8  (12.73, 12.87)
```

```
Linear model Poly6:
ans(x) = p1*x^6 + p2*x^5 + p3*x^4 + p4*x^3 + p5*x^2 +
             p6*x + p7
  where x is normalized by mean -1.034 and std 10.84
Coefficients (with 95% confidence bounds):
  p1 =    -0.02486  (-0.09378, 0.04407)
  p2 =     0.05063  (-0.007396, 0.1087)
  p3 =      0.1403  (-0.1373, 0.4179)
  p4 =     -0.2032  (-0.3959, -0.01045)
  p5 =     -0.4506  (-0.7445, -0.1567)
  p6 =      0.2411  (0.09834, 0.3838)
  p7 =        12.8  (12.73, 12.87)
```

```
Linear model Poly5:
ans(x) = p1*x^5 + p2*x^4 + p3*x^3 + p4*x^2 + p5*x + p6
  where x is normalized by mean -1.034 and std 10.84
Coefficients (with 95% confidence bounds):
  p1 =     0.05011  (-0.007389, 0.1076)
  p2 =     0.04177  (-0.007158, 0.0907)
  p3 =     -0.2019  (-0.3929, -0.01094)
  p4 =     -0.3553  (-0.4829, -0.2277)
  p5 =      0.2406  (0.09913, 0.3821)
  p6 =       12.79  (12.73, 12.85)
```

```
Linear model Poly4:
ans(x) = p1*x^4 + p2*x^3 + p3*x^2 + p4*x + p5
  where x is normalized by mean -1.034 and std 10.84
Coefficients (with 95% confidence bounds):
  p1 =     0.04286  (-0.007608, 0.09333)
  p2 =    -0.03957  (-0.083, 0.003848)
  p3 =     -0.3575  (-0.4891, -0.2258)
  p4 =      0.1392  (0.05615, 0.2223)
  p5 =       12.79  (12.73, 12.85)
```

```
Linear model Poly3:
ans(x) = p1*x^3 + p2*x^2 + p3*x + p4
  where x is normalized by mean -1.034 and std 10.84
Coefficients (with 95% confidence bounds):
  p1 =    -0.03897  (-0.08363, 0.005682)
  p2 =     -0.2503  (-0.2889, -0.2117)
  p3 =      0.1386  (0.05317, 0.224)
  p4 =       12.76  (12.71, 12.81)
```

```
General model:
ans(x) = a*cos(x*b+c)+d
Coefficients (with 95% confidence bounds):
  a =      0.3799  (0.2509, 0.5089)
  b =     -0.1359  (-0.1784, -0.09336)
  c =      0.1053  (-0.02192, 0.2325)
  d =       12.43  (12.27, 12.58)
```

- Line2

```
Linear model Poly7:
ans(x) = p1*x^7 + p2*x^6 + p3*x^5 + p4*x^4 + p5*x^3 +
             p6*x^2 + p7*x + p8
  where x is normalized by mean -0.9879 and std 10.81
Coefficients (with 95% confidence bounds):
  p1 =     -0.1333  (-0.2116, -0.05492)
  p2 =     -0.1533  (-0.2193, -0.08722)
  p3 =      0.6195  (0.2481, 0.9908)
  p4 =      0.8535  (0.5872, 1.12)
  p5 =     -0.7776  (-1.296, -0.2597)
  p6 =      -1.593  (-1.875, -1.31)
  p7 =     0.02916  (-0.1785, 0.2368)
  p8 =       10.97  (10.9, 11.04)
```

```
Linear model Poly6:
ans(x) = p1*x^6 + p2*x^5 + p3*x^4 + p4*x^3 + p5*x^2 +
             p6*x + p7
  where x is normalized by mean -0.9879 and std 10.81
Coefficients (with 95% confidence bounds):
  p1 =     -0.1544  (-0.2315, -0.07718)
  p2 =   -0.005005  (-0.07042, 0.06041)
  p3 =      0.8591  (0.5479, 1.17)
  p4 =     0.04449  (-0.1729, 0.2619)
  p5 =      -1.599  (-1.929, -1.269)
  p6 =      -0.235  (-0.3961, -0.07391)
  p7 =       10.97  (10.89, 11.05)
```

```
Linear model Poly5:
ans(x) = p1*x^5 + p2*x^4 + p3*x^3 + p4*x^2 + p5*x + p6
  where x is normalized by mean -0.9879 and std 10.81
Coefficients (with 95% confidence bounds):
  p1 =   -0.002899  (-0.08306, 0.07726)
  p2 =      0.2468  (0.1785, 0.3151)
  p3 =     0.03967  (-0.2267, 0.3061)
  p4 =      -1.006  (-1.184, -0.8277)
  p5 =     -0.2338  (-0.4312, -0.03644)
  p6 =       10.89  (10.8, 10.97)
```

```
Linear model Poly4:
ans(x) = p1*x^4 + p2*x^3 + p3*x^2 + p4*x + p5
  where x is normalized by mean -0.9879 and std 10.81
Coefficients (with 95% confidence bounds):
  p1 =      0.2469  (0.1797, 0.314)
  p2 =     0.03027  (-0.02744, 0.08799)
  p3 =      -1.006  (-1.181, -0.8309)
  p4 =      -0.228  (-0.3384, -0.1175)
  p5 =       10.89  (10.81, 10.97)
```

- Line3

```
Linear model Poly7:
ans(x) = p1*x^7 + p2*x^6 + p3*x^5 + p4*x^4 + p5*x^3 +
              p6*x^2 + p7*x + p8
  where x is normalized by mean -0.9709 and std 10.84
Coefficients (with 95% confidence bounds):
  p1 =     -0.1568  (-0.2317, -0.08184)
  p2 =     -0.3184  (-0.3819, -0.2549)
  p3 =      0.8066  (0.4542, 1.159)
  p4 =       1.671  (1.417, 1.925)
  p5 =      -1.279  (-1.767, -0.7904)
  p6 =      -2.948  (-3.215, -2.681)
  p7 =      0.6058  (0.4107, 0.8009)
  p8 =       9.859  (9.796, 9.923)
```

```
Linear model Poly6:
ans(x) = p1*x^6 + p2*x^5 + p3*x^4 + p4*x^3 + p5*x^2 +
              p6*x + p7
  where x is normalized by mean -0.9709 and std 10.84
Coefficients (with 95% confidence bounds):
  p1 =     -0.3123  (-0.3918, -0.2327)
  p2 =     0.07792  (0.01068, 0.1452)
  p3 =       1.649  (1.331, 1.968)
  p4 =     -0.3261  (-0.5478, -0.1045)
  p5 =       -2.93  (-3.265, -2.595)
  p6 =      0.3015  (0.1384, 0.4646)
  p7 =       9.857  (9.778, 9.937)
```

```
General model:
ans(x) = a*cos(x*b+c)+d
Coefficients (with 95% confidence bounds):
  a =      0.9146  (0.8387, 0.9906)
  b =      0.2065  (0.1946, 0.2184)
  c =     0.07813  (-0.01463, 0.1709)
  d =       8.874  (8.808, 8.94)
```

- Line4

```
Linear model Poly7:
ans(x) = p1*x^7 + p2*x^6 + p3*x^5 + p4*x^4 + p5*x^3 +
              p6*x^2 + p7*x + p8
  where x is normalized by mean -0.968 and std 10.83
Coefficients (with 95% confidence bounds):
  p1 =     -0.3553  (-0.4239, -0.2867)
  p2 =     -0.3617  (-0.4192, -0.3042)
  p3 =       1.972  (1.645, 2.299)
  p4 =       2.366  (2.134, 2.598)
  p5 =      -3.187  (-3.645, -2.729)
  p6 =      -5.391  (-5.639, -5.143)
  p7 =       1.143  (0.9587, 1.327)
  p8 =       9.289  (9.229, 9.349)
```

```
Linear model Poly6:
ans(x) = p1*x^6 + p2*x^5 + p3*x^4 + p4*x^3 + p5*x^2 +
              p6*x + p7
  where x is normalized by mean -0.968 and std 10.83
Coefficients (with 95% confidence bounds):
  p1 =     -0.3572  (-0.4817, -0.2326)
  p2 =      0.2993  (0.1924, 0.4062)
  p3 =       2.348  (1.844, 2.851)
  p4 =     -0.9698  (-1.324, -0.6155)
  p5 =      -5.373  (-5.91, -4.836)
  p6 =       0.425  (0.1623, 0.6878)
  p7 =       9.286  (9.156, 9.416)
```

- Line5

```
Linear model Poly7:
ans(x) = p1*x^7 + p2*x^6 + p3*x^5 + p4*x^4 + p5*x^3 +
         p6*x^2 + p7*x + p8
  where x is normalized by mean -0.9337 and std 10.9
Coefficients (with 95% confidence bounds):
  p1 =     -0.3569  (-0.4358, -0.2779)
  p2 =      -0.606  (-0.6727, -0.5393)
  p3 =       2.097  (1.723, 2.471)
  p4 =       3.828  (3.56, 4.096)
  p5 =      -3.846  (-4.367, -3.325)
  p6 =      -8.229  (-8.512, -7.946)
  p7 =       1.985  (1.776, 2.195)
  p8 =       9.195  (9.127, 9.262)
```

```
Linear model Poly6:
ans(x) = p1*x^6 + p2*x^5 + p3*x^4 + p4*x^3 + p5*x^2 +
         p6*x + p7
  where x is normalized by mean -0.9337 and std 10.9
Coefficients (with 95% confidence bounds):
  p1 =     -0.6142  (-0.7443, -0.4841)
  p2 =      0.4279  (0.3169, 0.5389)
  p3 =       3.854  (3.332, 4.377)
  p4 =       -1.65  (-2.017, -1.282)
  p5 =      -8.251  (-8.803, -7.699)
  p6 =       1.277  (1.006, 1.549)
  p7 =       9.199  (9.067, 9.33)
```

- Line6

```
Linear model Poly7:
ans(x) = p1*x^7 + p2*x^6 + p3*x^5 + p4*x^4 + p5*x^3 +
         p6*x^2 + p7*x + p8
  where x is normalized by mean -1.028 and std 10.89
Coefficients (with 95% confidence bounds):
  p1 =     -0.2926  (-0.5332, -0.05197)
  p2 =     -0.7631  (-0.9645, -0.5617)
  p3 =       1.942  (0.8106, 3.074)
  p4 =       5.022  (4.216, 5.827)
  p5 =      -4.072  (-5.638, -2.506)
  p6 =      -10.96  (-11.81, -10.12)
  p7 =       2.544  (1.922, 3.166)
  p8 =       9.458  (9.256, 9.659)
```

```
Linear model Poly6:
ans(x) = p1*x^6 + p2*x^5 + p3*x^4 + p4*x^3 + p5*x^2 +
         p6*x + p7
  where x is normalized by mean -1.028 and std 10.89
Coefficients (with 95% confidence bounds):
  p1 =     -0.7519  (-0.9695, -0.5344)
  p2 =      0.5818  (0.3981, 0.7654)
  p3 =       4.987  (4.116, 5.858)
  p4 =      -2.294  (-2.901, -1.688)
  p5 =      -10.94  (-11.86, -10.02)
  p6 =       1.977  (1.531, 2.422)
  p7 =       9.457  (9.239, 9.675)
```

- Line7

```
Linear model Poly7:
ans(x) = p1*x^7 + p2*x^6 + p3*x^5 + p4*x^4 + p5*x^3 +
         p6*x^2 + p7*x + p8
  where x is normalized by mean -0.9641 and std 10.84
Coefficients (with 95% confidence bounds):
  p1 =     -0.2068  (-0.547, 0.1335)
  p2 =     -0.8149  (-1.1, -0.5302)
  p3 =       1.526  (-0.08791, 3.141)
  p4 =       5.383  (4.235, 6.53)
  p5 =      -3.573  (-5.827, -1.32)
  p6 =      -12.04  (-13.26, -10.82)
  p7 =       2.552  (1.653, 3.451)
  p8 =       9.529  (9.236, 9.822)
```

```
Linear model Poly6:
ans(x) = p1*x^6 + p2*x^5 + p3*x^4 + p4*x^3 + p5*x^2 +
         p6*x + p7
  where x is normalized by mean -0.9641 and std 10.84
Coefficients (with 95% confidence bounds):
  p1 =     -0.8217  (-1.108, -0.535)
  p2 =      0.5565  (0.3119, 0.8012)
  p3 =       5.405  (4.25, 6.561)
  p4 =      -2.293  (-3.101, -1.486)
  p5 =      -12.06  (-13.29, -10.83)
  p6 =       2.141  (1.544, 2.739)
  p7 =       9.532  (9.237, 9.827)
```

Run39

- Line1

```
Linear model Poly7:
ans(x) = p1*x^7 + p2*x^6 + p3*x^5 + p4*x^4 + p5*x^3 +
             p6*x^2 + p7*x + p8
  where x is normalized by mean 0.9815 and std 8.525
Coefficients (with 95% confidence bounds):
  p1 =    -0.06587  (-0.1346, 0.00284)
  p2 =    -0.05732  (-0.1148, 0.0001379)
  p3 =      0.3431  (0.02153, 0.6646)
  p4 =      0.2219  (-0.007182, 0.451)
  p5 =     -0.5938  (-1.036, -0.1516)
  p6 =     -0.3949  (-0.6356, -0.1542)
  p7 =      0.4274  (0.2534, 0.6015)
  p8 =       6.676  (6.619, 6.733)
```

```
Linear model Poly6:
ans(x) = p1*x^6 + p2*x^5 + p3*x^4 + p4*x^3 + p5*x^2 +
             p6*x + p7
  where x is normalized by mean 0.9815 and std 8.525
Coefficients (with 95% confidence bounds):
  p1 =    -0.05541  (-0.1164, 0.005599)
  p2 =     0.03831  (-0.0129, 0.08951)
  p3 =      0.2154  (-0.02789, 0.4587)
  p4 =     -0.1978  (-0.3656, -0.02998)
  p5 =     -0.3897  (-0.6454, -0.134)
  p6 =      0.3024  (0.1799, 0.4249)
  p7 =       6.675  (6.615, 6.735)
```

```
Linear model Poly5:
ans(x) = p1*x^5 + p2*x^4 + p3*x^3 + p4*x^2 + p5*x + p6
  where x is normalized by mean 0.9815 and std 8.525
Coefficients (with 95% confidence bounds):
  p1 =     0.03947  (-0.01434, 0.09328)
  p2 =    -0.00198  (-0.04783, 0.04387)
  p3 =     -0.2008  (-0.3772, -0.02445)
  p4 =     -0.1813  (-0.2998, -0.06276)
  p5 =      0.3031  (0.1744, 0.4319)
  p6 =       6.646  (6.592, 6.701)
```

```
Linear model Poly4:
ans(x) = p1*x^4 + p2*x^3 + p3*x^2 + p4*x + p5
  where x is normalized by mean 0.9815 and std 8.525
Coefficients (with 95% confidence bounds):
  p1 =   -0.002683  (-0.04964, 0.04428)
  p2 =    -0.07463  (-0.1144, -0.03488)
  p3 =     -0.1793  (-0.3007, -0.05786)
  p4 =      0.2257  (0.1502, 0.3012)
  p5 =       6.646  (6.59, 6.701)
```

```
Linear model Poly3:
ans(x) = p1*x^3 + p2*x^2 + p3*x + p4
  where x is normalized by mean 0.9815 and std 8.525
Coefficients (with 95% confidence bounds):
  p1 =    -0.07466  (-0.1135, -0.03578)
  p2 =     -0.1859  (-0.2193, -0.1525)
  p3 =      0.2257  (0.1519, 0.2996)
  p4 =       6.648  (6.604, 6.691)
```

```
General model:
ans(x) = a*cos(x*b+c)+d
Coefficients (with 95% confidence bounds):
  a =      0.2954  (0.2284, 0.3624)
  b =      0.1816  (0.1395, 0.2238)
  c =     -0.6966  (-0.9239, -0.4692)
  d =        6.42  (6.339, 6.501)
```

- Line2

```
Linear model Poly7:
ans(x) = p1*x^7 + p2*x^6 + p3*x^5 + p4*x^4 + p5*x^3 +
             p6*x^2 + p7*x + p8
  where x is normalized by mean 0.973 and std 8.547
Coefficients (with 95% confidence bounds):
  p1 =     0.03785  (-0.004669, 0.08038)
  p2 =    -0.09657  (-0.131, -0.06216)
  p3 =     -0.2812  (-0.4788, -0.08364)
  p4 =      0.4669  (0.3307, 0.603)
  p5 =      0.5406  (0.2711, 0.8101)
  p6 =     -0.8397  (-0.9813, -0.6981)
  p7 =    0.006108  (-0.09891, 0.1111)
  p8 =        6.11  (6.077, 6.144)
```

```
Linear model Poly6:
ans(x) = p1*x^6 + p2*x^5 + p3*x^4 + p4*x^3 + p5*x^2 +
             p6*x + p7
  where x is normalized by mean 0.973 and std 8.547
Coefficients (with 95% confidence bounds):
  p1 =    -0.09665  (-0.1328, -0.0605)
  p2 =     -0.1072  (-0.1375, -0.07694)
  p3 =      0.4673  (0.3242, 0.6104)
  p4 =      0.3159  (0.2168, 0.4149)
  p5 =     -0.8402  (-0.989, -0.6913)
  p6 =     0.07705  (0.005174, 0.1489)
  p7 =       6.111  (6.075, 6.146)
```

```
Linear model Poly5:
ans(x) = p1*x^5 + p2*x^4 + p3*x^3 + p4*x^2 + p5*x + p6
  where x is normalized by mean 0.973 and std 8.547
Coefficients (with 95% confidence bounds):
  p1 =     -0.1076  (-0.1534, -0.06192)
  p2 =     0.09078  (0.05251, 0.1291)
  p3 =      0.3168  (0.1672, 0.4665)
  p4 =     -0.4829  (-0.5819, -0.384)
  p5 =     0.07616  (-0.03241, 0.1847)
  p6 =       6.062  (6.017, 6.107)
```

```
Linear model Poly4:
ans(x) = p1*x^4 + p2*x^3 + p3*x^2 + p4*x + p5
  where x is normalized by mean 0.973 and std 8.547
Coefficients (with 95% confidence bounds):
  p1 =     0.09016  (0.0369, 0.1434)
  p2 =    -0.02713  (-0.07215, 0.01789)
  p3 =     -0.4824  (-0.6201, -0.3446)
  p4 =      0.2869  (0.2015, 0.3724)
  p5 =       6.062  (5.999, 6.125)
```

- Line3

```
Linear model Poly7:
ans(x) = p1*x^7 + p2*x^6 + p3*x^5 + p4*x^4 + p5*x^3 +
             p6*x^2 + p7*x + p8
  where x is normalized by mean 0.9617 and std 8.553
Coefficients (with 95% confidence bounds):
  p1 =     0.01065  (-0.07001, 0.09132)
  p2 =     -0.1172  (-0.1845, -0.04988)
  p3 =     -0.1206  (-0.4926, 0.2514)
  p4 =      0.7112  (0.4455, 0.977)
  p5 =      0.3222  (-0.1814, 0.8258)
  p6 =      -1.546  (-1.821, -1.271)
  p7 =    -0.05268  (-0.2488, 0.1434)
  p8 =       5.292  (5.228, 5.355)
```

```
Linear model Poly6:
ans(x) = p1*x^6 + p2*x^5 + p3*x^4 + p4*x^3 + p5*x^2 +
           p6*x + p7
  where x is normalized by mean 0.9617 and std 8.553
Coefficients (with 95% confidence bounds):
  p1 =      -0.117  (-0.1827, -0.05132)
  p2 =    -0.07199  (-0.1259, -0.01813)
  p3 =      0.7106  (0.4513, 0.97)
  p4 =      0.2601  (0.08437, 0.4358)
  p5 =      -1.545  (-1.814, -1.277)
  p6 =    -0.03341  (-0.1613, 0.09444)
  p7 =       5.291  (5.229, 5.354)
```

```
Linear model Poly5:
ans(x) = p1*x^5 + p2*x^4 + p3*x^3 + p4*x^2 + p5*x + p6
  where x is normalized by mean 0.9617 and std 8.553
Coefficients (with 95% confidence bounds):
  p1 =    -0.07314  (-0.14, -0.006259)
  p2 =      0.2557  (0.1995, 0.3118)
  p3 =      0.2629  (0.04468, 0.4811)
  p4 =      -1.114  (-1.258, -0.9696)
  p5 =    -0.03432  (-0.1931, 0.1244)
  p6 =       5.234  (5.168, 5.299)
```

```
Linear model Poly4:
ans(x) = p1*x^4 + p2*x^3 + p3*x^2 + p4*x + p5
  where x is normalized by mean 0.9617 and std 8.553
Coefficients (with 95% confidence bounds):
  p1 =      0.2551  (0.1944, 0.3157)
  p2 =     0.03005  (-0.0215, 0.0816)
  p3 =      -1.112  (-1.268, -0.9568)
  p4 =      0.1086  (0.01123, 0.206)
  p5 =       5.233  (5.162, 5.304)
```

- Line4

```
Linear model Poly7:
ans(x) = p1*x^7 + p2*x^6 + p3*x^5 + p4*x^4 + p5*x^3 +
             p6*x^2 + p7*x + p8
  where x is normalized by mean 0.9714 and std 8.57
Coefficients (with 95% confidence bounds):
  p1 =     0.08981  (0.009902, 0.1697)
  p2 =     -0.1087  (-0.1746, -0.04272)
  p3 =     -0.5097  (-0.8823, -0.1371)
  p4 =      0.7281  (0.4665, 0.9898)
  p5 =       0.954  (0.443, 1.465)
  p6 =      -1.955  (-2.228, -1.681)
  p7 =     -0.4641  (-0.6653, -0.263)
  p8 =       4.693  (4.628, 4.758)
```

```
Linear model Poly6:
ans(x) = p1*x^6 + p2*x^5 + p3*x^4 + p4*x^3 + p5*x^2 +
           p6*x + p7
  where x is normalized by mean 0.9714 and std 8.57
Coefficients (with 95% confidence bounds):
  p1 =     -0.1084  (-0.1805, -0.03624)
  p2 =    -0.09561  (-0.1562, -0.03501)
  p3 =      0.7273  (0.4412, 1.014)
  p4 =      0.4172  (0.2186, 0.6158)
  p5 =      -1.954  (-2.253, -1.656)
  p6 =     -0.2938  (-0.4384, -0.1492)
  p7 =       4.693  (4.622, 4.764)
```

```
Linear model Poly5:
ans(x) = p1*x^5 + p2*x^4 + p3*x^3 + p4*x^2 + p5*x + p6
  where x is normalized by mean 0.9714 and std 8.57
Coefficients (with 95% confidence bounds):
  p1 =    -0.09631  (-0.1673, -0.02533)
  p2 =      0.3042  (0.2446, 0.3639)
  p3 =      0.4196  (0.187, 0.6522)
  p4 =      -1.551  (-1.706, -1.397)
  p5 =     -0.2956  (-0.465, -0.1263)
  p6 =       4.638  (4.567, 4.709)
```

```
Linear model Poly4:
ans(x) = p1*x^4 + p2*x^3 + p3*x^2 + p4*x + p5
  where x is normalized by mean 0.9714 and std 8.57
Coefficients (with 95% confidence bounds):
  p1 =      0.3044  (0.2369, 0.3719)
  p2 =      0.1116  (0.05424, 0.1689)
  p3 =      -1.552  (-1.726, -1.377)
  p4 =     -0.1061  (-0.2145, 0.002285)
  p5 =       4.638  (4.558, 4.718)
```

- Line5

```
Linear model Poly7:
ans(x) = p1*x^7 + p2*x^6 + p3*x^5 + p4*x^4 + p5*x^3 +
             p6*x^2 + p7*x + p8
  where x is normalized by mean 0.9841 and std 8.577
Coefficients (with 95% confidence bounds):
  p1 =      0.1894  (0.08687, 0.292)
  p2 =     -0.3697  (-0.4555, -0.284)
  p3 =     -0.9507  (-1.428, -0.4733)
  p4 =        2.05  (1.709, 2.39)
  p5 =       1.607  (0.9539, 2.259)
  p6 =        -3.9  (-4.257, -3.544)
  p7 =     -0.8677  (-1.124, -0.6116)
  p8 =       4.461  (4.377, 4.545)
```

```
Linear model Poly6:
ans(x) = p1*x^6 + p2*x^5 + p3*x^4 + p4*x^3 + p5*x^2 +
             p6*x + p7
  where x is normalized by mean 0.9841 and std 8.577
Coefficients (with 95% confidence bounds):
  p1 =     -0.3629  (-0.4718, -0.254)
  p2 =    -0.07872  (-0.1691, 0.01168)
  p3 =       2.029  (1.596, 2.463)
  p4 =      0.4804  (0.1843, 0.7766)
  p5 =      -3.888  (-4.341, -3.434)
  p6 =     -0.5141  (-0.7305, -0.2978)
  p7 =       4.461  (4.354, 4.567)
```

- Line6

```
Linear model Poly7:
ans(x) = p1*x^7 + p2*x^6 + p3*x^5 + p4*x^4 + p5*x^3 +
             p6*x^2 + p7*x + p8
  where x is normalized by mean 1.082 and std 8.582
Coefficients (with 95% confidence bounds):
  p1 =      0.3084  (0.03713, 0.5796)
  p2 =     -0.9273  (-1.15, -0.7049)
  p3 =      -1.819  (-3.075, -0.5634)
  p4 =       4.761  (3.882, 5.641)
  p5 =       3.486  (1.78, 5.193)
  p6 =      -7.797  (-8.712, -6.882)
  p7 =      -2.209  (-2.873, -1.544)
  p8 =        4.35  (4.136, 4.565)
```

```
Linear model Poly6:
ans(x) = p1*x^6 + p2*x^5 + p3*x^4 + p4*x^3 + p5*x^2 +
             p6*x + p7
  where x is normalized by mean 1.082 and std 8.582
Coefficients (with 95% confidence bounds):
  p1 =     -0.9314  (-1.175, -0.6875)
  p2 =      -0.407  (-0.6093, -0.2047)
  p3 =       4.774  (3.809, 5.738)
  p4 =        1.67  (1.011, 2.329)
  p5 =      -7.804  (-8.807, -6.8)
  p6 =       -1.64  (-2.119, -1.16)
  p7 =       4.351  (4.116, 4.586)
```

Run42

- Line1

```
Linear model Poly7:
ans(x) = p1*x^7 + p2*x^6 + p3*x^5 + p4*x^4 + p5*x^3 +
             p6*x^2 + p7*x + p8
  where x is normalized by mean 1.014 and std 8.544
Coefficients (with 95% confidence bounds):
  p1 =     0.04035  (0.01205, 0.06864)
  p2 =      0.0132  (-0.01026, 0.03666)
  p3 =     -0.2089  (-0.3415, -0.0762)
  p4 =    -0.05667  (-0.1504, 0.03708)
  p5 =      0.3501  (0.1674, 0.5329)
  p6 =     0.02403  (-0.07461, 0.1227)
  p7 =     -0.3033  (-0.3754, -0.2311)
  p8 =       8.509  (8.485, 8.532)
```

```
Linear model Poly6:
ans(x) = p1*x^6 + p2*x^5 + p3*x^4 + p4*x^3 + p5*x^2 +
             p6*x + p7
  where x is normalized by mean 1.014 and std 8.544
Coefficients (with 95% confidence bounds):
  p1 =     0.01302  (-0.01421, 0.04025)
  p2 =     -0.0218  (-0.04466, 0.001062)
  p3 =    -0.05622  (-0.165, 0.05257)
  p4 =      0.1065  (0.03131, 0.1817)
  p5 =     0.02388  (-0.09059, 0.1384)
  p6 =     -0.2259  (-0.2811, -0.1707)
  p7 =       8.509  (8.481, 8.536)
```

```
Linear model Poly5:
ans(x) = p1*x^5 + p2*x^4 + p3*x^3 + p4*x^2 + p5*x + p6
  where x is normalized by mean 1.014 and std 8.544
Coefficients (with 95% confidence bounds):
  p1 =    -0.02192  (-0.04471, 0.0008758)
  p2 =   -0.005033  (-0.02442, 0.01436)
  p3 =      0.1068  (0.03186, 0.1818)
  p4 =    -0.02529  (-0.07543, 0.02485)
  p5 =     -0.2261  (-0.2811, -0.1711)
  p6 =       8.515  (8.492, 8.539)
```

```
Linear model Poly4:
ans(x) = p1*x^4 + p2*x^3 + p3*x^2 + p4*x + p5
  where x is normalized by mean 1.014 and std 8.544
Coefficients (with 95% confidence bounds):
  p1 =   -0.004929  (-0.02543, 0.01557)
  p2 =     0.03652  (0.01901, 0.05403)
  p3 =    -0.02549  (-0.0785, 0.02753)
  p4 =     -0.1826  (-0.2158, -0.1495)
  p5 =       8.515  (8.491, 8.54)
```

```
Linear model Poly3:
ans(x) = p1*x^3 + p2*x^2 + p3*x + p4
  where x is normalized by mean 1.014 and std 8.544
Coefficients (with 95% confidence bounds):
  p1 =     0.03654  (0.01933, 0.05374)
  p2 =    -0.03771  (-0.05255, -0.02287)
  p3 =     -0.1827  (-0.2152, -0.1501)
  p4 =       8.519  (8.5, 8.538)
```

```
General model:
ans(x) = a*cos(x*b+c)+d
Coefficients (with 95% confidence bounds):
  a =      0.1735  (0.1476, 0.1995)
  b =      0.1368  (0.108, 0.1656)
  c =      0.9407  (0.7733, 1.108)
  d =       8.448  (8.416, 8.479)
```

- Line2

```
Linear model Poly7:
ans(x) = p1*x^7 + p2*x^6 + p3*x^5 + p4*x^4 + p5*x^3 +
             p6*x^2 + p7*x + p8
  where x is normalized by mean 1.229 and std 8.792
Coefficients (with 95% confidence bounds):
  p1 =   -0.004446  (-0.03038, 0.02149)
  p2 =    -0.02062  (-0.04261, 0.001362)
  p3 =     0.01322  (-0.1081, 0.1346)
  p4 =     0.09024  (0.004158, 0.1763)
  p5 =     0.03242  (-0.1348, 0.1997)
  p6 =     -0.1158  (-0.2051, -0.0265)
  p7 =    -0.05855  (-0.1238, 0.006681)
  p8 =        6.41  (6.39, 6.431)
```

```
Linear model Poly6:
ans(x) = p1*x^6 + p2*x^5 + p3*x^4 + p4*x^3 + p5*x^2 +
             p6*x + p7
  where x is normalized by mean 1.229 and std 8.792
Coefficients (with 95% confidence bounds):
  p1 =    -0.02172  (-0.04227, -0.001178)
  p2 =   -0.007348  (-0.02539, 0.01069)
  p3 =     0.09374  (0.01203, 0.1755)
  p4 =     0.05922  (0.0009494, 0.1175)
  p5 =     -0.1183  (-0.2044, -0.03212)
  p6 =    -0.06698  (-0.1089, -0.02511)
  p7 =       6.411  (6.39, 6.431)
```

```
Linear model Poly5:
ans(x) = p1*x^5 + p2*x^4 + p3*x^3 + p4*x^2 + p5*x + p6
  where x is normalized by mean 1.229 and std 8.792
Coefficients (with 95% confidence bounds):
  p1 =    -0.01205  (-0.03088, 0.006776)
  p2 =    0.008851  (-0.007483, 0.02519)
  p3 =     0.07162  (0.01016, 0.1331)
  p4 =    -0.03703  (-0.07901, 0.004939)
  p5 =     -0.0729  (-0.1176, -0.02822)
  p6 =         6.4  (6.381, 6.418)
```

```
Linear model Poly4:
ans(x) = p1*x^4 + p2*x^3 + p3*x^2 + p4*x + p5
  where x is normalized by mean 1.229 and std 8.792
Coefficients (with 95% confidence bounds):
  p1 =    0.007263  (-0.009095, 0.02362)
  p2 =     0.03326  (0.01945, 0.04707)
  p3 =    -0.03433  (-0.07665, 0.00798)
  p4 =    -0.04964  (-0.07598, -0.0233)
  p5 =       6.399  (6.38, 6.418)
```

```
Linear model Poly3:
ans(x) = p1*x^3 + p2*x^2 + p3*x + p4
  where x is normalized by mean 1.229 and std 8.792
Coefficients (with 95% confidence bounds):
  p1 =     0.03402  (0.0204, 0.04765)
  p2 =    -0.01628  (-0.02796, -0.004609)
  p3 =    -0.05019  (-0.07636, -0.02402)
  p4 =       6.394  (6.379, 6.409)
```

- Line3

```
Linear model Poly7:
ans(x) = p1*x^7 + p2*x^6 + p3*x^5 + p4*x^4 + p5*x^3 +
             p6*x^2 + p7*x + p8
  where x is normalized by mean 1.019 and std 8.538
Coefficients (with 95% confidence bounds):
  p1 =      0.1296  (0.09849, 0.1608)
  p2 =    -0.08549  (-0.1115, -0.05944)
  p3 =     -0.7725  (-0.9185, -0.6265)
  p4 =      0.4701  (0.3663, 0.574)
  p5 =        1.54  (1.338, 1.741)
  p6 =     -0.9014  (-1.01, -0.7926)
  p7 =      -1.145  (-1.225, -1.065)
  p8 =       4.912  (4.886, 4.938)
```

```
Linear model Poly6:
ans(x) = p1*x^6 + p2*x^5 + p3*x^4 + p4*x^3 + p5*x^2 +
             p6*x + p7
  where x is normalized by mean 1.019 and std 8.538
Coefficients (with 95% confidence bounds):
  p1 =    -0.09617  (-0.1502, -0.04218)
  p2 =     -0.1716  (-0.2171, -0.1261)
  p3 =      0.5053  (0.2897, 0.7209)
  p4 =      0.7573  (0.6072, 0.9074)
  p5 =      -0.929  (-1.155, -0.7029)
  p6 =     -0.8958  (-1.006, -0.7858)
  p7 =       4.915  (4.861, 4.969)
```

```
Linear model Poly5:
ans(x) = p1*x^5 + p2*x^4 + p3*x^3 + p4*x^2 + p5*x + p6
  where x is normalized by mean 1.019 and std 8.538
Coefficients (with 95% confidence bounds):
  p1 =     -0.1652  (-0.2215, -0.1088)
  p2 =      0.1274  (0.07981, 0.175)
  p3 =      0.7408  (0.5548, 0.9268)
  p4 =     -0.5673  (-0.6908, -0.4438)
  p5 =     -0.8881  (-1.025, -0.7516)
  p6 =       4.866  (4.809, 4.923)
```

- Line4

```
Linear model Poly7:
ans(x) = p1*x^7 + p2*x^6 + p3*x^5 + p4*x^4 + p5*x^3 +
         p6*x^2 + p7*x + p8
  where x is normalized by mean 1.041 and std 8.548
Coefficients (with 95% confidence bounds):
  p1 =      0.1142  (-0.04899, 0.2773)
  p2 =       -0.59  (-0.7256, -0.4544)
  p3 =     -0.5373  (-1.298, 0.2237)
  p4 =       2.916  (2.377, 3.454)
  p5 =      0.8778  (-0.1657, 1.921)
  p6 =      -4.215  (-4.777, -3.653)
  p7 =      -0.922  (-1.333, -0.5109)
  p8 =        4.37  (4.237, 4.503)
```

```
Linear model Poly6:
ans(x) = p1*x^6 + p2*x^5 + p3*x^4 + p4*x^3 + p5*x^2 +
         p6*x + p7
  where x is normalized by mean 1.041 and std 8.548
Coefficients (with 95% confidence bounds):
  p1 =     -0.5926  (-0.7312, -0.454)
  p2 =    -0.01074  (-0.1268, 0.1053)
  p3 =       2.925  (2.374, 3.475)
  p4 =      0.1958  (-0.1854, 0.577)
  p5 =      -4.223  (-4.798, -3.649)
  p6 =      -0.706  (-0.9834, -0.4285)
  p7 =       4.371  (4.235, 4.507)
```

- Line5

```
Linear model Poly7:
ans(x) = p1*x^7 + p2*x^6 + p3*x^5 + p4*x^4 + p5*x^3 +
         p6*x^2 + p7*x + p8
  where x is normalized by mean 1.028 and std 8.538
Coefficients (with 95% confidence bounds):
  p1 =     0.06794  (-0.1009, 0.2368)
  p2 =     -0.6787  (-0.8195, -0.5379)
  p3 =     -0.4984  (-1.281, 0.2841)
  p4 =       3.496  (2.938, 4.053)
  p5 =       1.315  (0.2496, 2.38)
  p6 =      -5.611  (-6.19, -5.033)
  p7 =      -1.471  (-1.889, -1.053)
  p8 =       4.268  (4.132, 4.403)
```

```
Linear model Poly6:
ans(x) = p1*x^6 + p2*x^5 + p3*x^4 + p4*x^3 + p5*x^2 +
         p6*x + p7
  where x is normalized by mean 1.028 and std 8.538
Coefficients (with 95% confidence bounds):
  p1 =     -0.6815  (-0.8208, -0.5421)
  p2 =     -0.1871  (-0.3024, -0.07175)
  p3 =       3.504  (2.953, 4.056)
  p4 =      0.9146  (0.5366, 1.293)
  p5 =      -5.618  (-6.19, -5.045)
  p6 =      -1.345  (-1.62, -1.071)
  p7 =       4.268  (4.134, 4.403)
```

- Line6

```
Linear model Poly7:
ans(x) = p1*x^7 + p2*x^6 + p3*x^5 + p4*x^4 + p5*x^3 +
         p6*x^2 + p7*x + p8
  where x is normalized by mean 1.046 and std 8.54
Coefficients (with 95% confidence bounds):
  p1 =      0.3866  (0.1544, 0.6189)
  p2 =     -0.9521  (-1.142, -0.7619)
  p3 =      -2.127  (-3.214, -1.04)
  p4 =       4.939  (4.183, 5.695)
  p5 =       3.735  (2.238, 5.232)
  p6 =      -7.954  (-8.743, -7.165)
  p7 =      -2.314  (-2.906, -1.721)
  p8 =       4.217  (4.03, 4.405)
```

```
Linear model Poly6:
ans(x) = p1*x^6 + p2*x^5 + p3*x^4 + p4*x^3 + p5*x^2 +
         p6*x + p7
  where x is normalized by mean 1.046 and std 8.54
Coefficients (with 95% confidence bounds):
  p1 =     -0.9447  (-1.177, -0.7126)
  p2 =      -0.338  (-0.5347, -0.1414)
  p3 =       4.917  (3.995, 5.84)
  p4 =       1.404  (0.7575, 2.051)
  p5 =      -7.939  (-8.903, -6.975)
  p6 =      -1.567  (-2.041, -1.094)
  p7 =       4.216  (3.987, 4.444)
```

Run63

- Line1

```
Linear model Poly7:
ans(x) = p1*x^7 + p2*x^6 + p3*x^5 + p4*x^4 + p5*x^3 +
             p6*x^2 + p7*x + p8
  where x is normalized by mean 0.9434 and std 8.556
Coefficients (with 95% confidence bounds):
  p1 =   0.0002592  (-0.02983, 0.03035)
  p2 =     0.01586  (-0.008826, 0.04054)
  p3 =    -0.02804  (-0.1691, 0.113)
  p4 =    -0.02912  (-0.1277, 0.06943)
  p5 =      0.1166  (-0.07761, 0.3108)
  p6 =     -0.1493  (-0.2528, -0.04575)
  p7 =     -0.1663  (-0.2428, -0.08972)
  p8 =       8.541  (8.517, 8.566)
```

```
Linear model Poly6:
ans(x) = p1*x^6 + p2*x^5 + p3*x^4 + p4*x^3 + p5*x^2 +
             p6*x + p7
  where x is normalized by mean 0.9434 and std 8.556
Coefficients (with 95% confidence bounds):
  p1 =     0.01585  (-0.008189, 0.03989)
  p2 =    -0.02684  (-0.04709, -0.006596)
  p3 =     -0.0291  (-0.1251, 0.0669)
  p4 =      0.1151  (0.04844, 0.1817)
  p5 =     -0.1493  (-0.2502, -0.04844)
  p6 =     -0.1658  (-0.2147, -0.1169)
  p7 =       8.541  (8.517, 8.565)
```

```
Linear model Poly5:
ans(x) = p1*x^5 + p2*x^4 + p3*x^3 + p4*x^2 + p5*x + p6
  where x is normalized by mean 0.9434 and std 8.556
Coefficients (with 95% confidence bounds):
  p1 =    -0.02725  (-0.04782, -0.00669)
  p2 =     0.03318  (0.01573, 0.05062)
  p3 =      0.1161  (0.04842, 0.1838)
  p4 =      -0.209  (-0.2541, -0.164)
  p5 =     -0.1663  (-0.2159, -0.1166)
  p6 =       8.549  (8.529, 8.57)
```

```
Linear model Poly4:
ans(x) = p1*x^4 + p2*x^3 + p3*x^2 + p4*x + p5
  where x is normalized by mean 0.9434 and std 8.556
Coefficients (with 95% confidence bounds):
  p1 =     0.03385  (0.01423, 0.05346)
  p2 =     0.02862  (0.01183, 0.04541)
  p3 =     -0.2104  (-0.2611, -0.1597)
  p4 =     -0.1121  (-0.1439, -0.08032)
  p5 =        8.55  (8.526, 8.573)
```

```
Linear model Poly3:
ans(x) = p1*x^3 + p2*x^2 + p3*x + p4
  where x is normalized by mean 0.9434 and std 8.556
Coefficients (with 95% confidence bounds):
  p1 =     0.02808  (0.007788, 0.04837)
  p2 =     -0.1265  (-0.144, -0.1091)
  p3 =     -0.1113  (-0.1497, -0.07284)
  p4 =       8.525  (8.503, 8.548)
```

```
General model:
ans(x) = a*cos(x*b+c)+d
Coefficients (with 95% confidence bounds):
  a =       0.2038  (0.1697, 0.238)
  b =       0.1745  (0.1458, 0.2032)
  c =       0.2621  (0.1622, 0.362)
  d =        8.362  (8.32, 8.403)
```

- Line2

```
Linear model Poly7:
ans(x) = p1*x^7 + p2*x^6 + p3*x^5 + p4*x^4 + p5*x^3 +
             p6*x^2 + p7*x + p8
  where x is normalized by mean -0.04697 and std 8.556
Coefficients (with 95% confidence bounds):
  p1 =     0.03079  (-0.005979, 0.06756)
  p2 =      -0.047  (-0.07758, -0.01642)
  p3 =     -0.1287  (-0.2996, 0.04215)
  p4 =      0.2173  (0.09594, 0.3386)
  p5 =      0.1334  (-0.09983, 0.3667)
  p6 =     -0.3172  (-0.4437, -0.1907)
  p7 =    -0.09353  (-0.1849, -0.002152)
  p8 =       6.075  (6.045, 6.105)
```

```
Linear model Poly6:
ans(x) = p1*x^6 + p2*x^5 + p3*x^4 + p4*x^3 + p5*x^2 +
             p6*x + p7
  where x is normalized by mean -0.04697 and std 8.556
Coefficients (with 95% confidence bounds):
  p1 =    -0.04674  (-0.07861, -0.01486)
  p2 =     0.01277  (-0.01373, 0.03927)
  p3 =      0.2165  (0.09008, 0.3429)
  p4 =    -0.04907  (-0.1357, 0.03759)
  p5 =     -0.3168  (-0.4487, -0.185)
  p6 =    -0.03624  (-0.09937, 0.02689)
  p7 =       6.075  (6.044, 6.106)
```

```
Linear model Poly5:
ans(x) = p1*x^5 + p2*x^4 + p3*x^3 + p4*x^2 + p5*x + p6
  where x is normalized by mean -0.04697 and std 8.556
Coefficients (with 95% confidence bounds):
  p1 =     0.01219  (-0.01861, 0.04299)
  p2 =     0.03404  (0.008028, 0.06005)
  p3 =    -0.04739  (-0.1481, 0.05335)
  p4 =     -0.1429  (-0.2099, -0.07588)
  p5 =     -0.0373  (-0.1107, 0.0361)
  p6 =       6.052  (6.021, 6.082)
```

```
Linear model Poly4:
ans(x) = p1*x^4 + p2*x^3 + p3*x^2 + p4*x + p5
  where x is normalized by mean -0.04697 and std 8.556
Coefficients (with 95% confidence bounds):
  p1 =      0.0341  (0.008327, 0.05987)
  p2 =   -0.008498  (-0.03036, 0.01337)
  p3 =     -0.1429  (-0.2093, -0.07655)
  p4 =    -0.06118  (-0.1026, -0.01981)
  p5 =       6.052  (6.021, 6.082)
```

```
General model:
ans(x) = a*cos(x*b+c)+d
Coefficients (with 95% confidence bounds):
  a =      0.2291  (-0.0159, 0.4741)
  b =      0.1029  (0.0245, 0.1812)
  c =      0.5449  (0.134, 0.9557)
  d =       5.849  (5.59, 6.107)
```

- Line3

```
Linear model Poly7:
ans(x) = p1*x^7 + p2*x^6 + p3*x^5 + p4*x^4 + p5*x^3 +
             p6*x^2 + p7*x + p8
  where x is normalized by mean -0.01541 and std 8.547
Coefficients (with 95% confidence bounds):
  p1 =     0.07842  (-0.01325, 0.1701)
  p2 =     -0.2528  (-0.3294, -0.1762)
  p3 =     -0.4592  (-0.886, -0.03251)
  p4 =       1.186  (0.8818, 1.49)
  p5 =      0.8774  (0.2934, 1.461)
  p6 =       -1.67  (-1.987, -1.352)
  p7 =     -0.6076  (-0.8374, -0.3777)
  p8 =       4.745  (4.67, 4.82)
```

```
Linear model Poly6:
ans(x) = p1*x^6 + p2*x^5 + p3*x^4 + p4*x^3 + p5*x^2 +
             p6*x + p7
  where x is normalized by mean -0.01541 and std 8.547
Coefficients (with 95% confidence bounds):
  p1 =     -0.2511  (-0.3311, -0.1711)
  p2 =    -0.09831  (-0.165, -0.03162)
  p3 =        1.18  (0.8625, 1.498)
  p4 =       0.411  (0.1925, 0.6295)
  p5 =      -1.665  (-1.997, -1.333)
  p6 =     -0.4606  (-0.6202, -0.301)
  p7 =       4.745  (4.667, 4.822)
```

- Line4

```
Linear model Poly7:
ans(x) = p1*x^7 + p2*x^6 + p3*x^5 + p4*x^4 + p5*x^3 +
             p6*x^2 + p7*x + p8
  where x is normalized by mean -0.003 and std 8.558
Coefficients (with 95% confidence bounds):
  p1 =      0.1337  (-0.2478, 0.5153)
  p2 =     -0.9288  (-1.246, -0.6112)
  p3 =     -0.6902  (-2.461, 1.08)
  p4 =       4.172  (2.916, 5.428)
  p5 =      0.8128  (-1.603, 3.229)
  p6 =      -5.561  (-6.865, -4.257)
  p7 =     -0.3275  (-1.277, 0.6217)
  p8 =       4.173  (3.867, 4.479)
```

```
Linear model Poly6:
ans(x) = p1*x^6 + p2*x^5 + p3*x^4 + p4*x^3 + p5*x^2 +
             p6*x + p7
  where x is normalized by mean -0.003 and std 8.558
Coefficients (with 95% confidence bounds):
  p1 =     -0.9253  (-1.238, -0.6121)
  p2 =    -0.07669  (-0.338, 0.1846)
  p3 =        4.16  (2.921, 5.398)
  p4 =     0.02216  (-0.8319, 0.8762)
  p5 =      -5.551  (-6.837, -4.265)
  p6 =    -0.07837  (-0.699, 0.5422)
  p7 =       4.172  (3.87, 4.474)
```

- Line5

```
Linear model Poly7:
ans(x) = p1*x^7 + p2*x^6 + p3*x^5 + p4*x^4 + p5*x^3 +
             p6*x^2 + p7*x + p8
  where x is normalized by mean -0.04 and std 8.545
Coefficients (with 95% confidence bounds):
  p1 =     -0.1548  (-0.5212, 0.2115)
  p2 =       -1.03  (-1.334, -0.7271)
  p3 =      0.8862  (-0.8254, 2.598)
  p4 =        5.24  (4.032, 6.449)
  p5 =      -1.368  (-3.717, 0.98)
  p6 =      -7.821  (-9.087, -6.556)
  p7 =      0.3638  (-0.56, 1.288)
  p8 =       4.218  (3.921, 4.516)
```

```
Linear model Poly6:
ans(x) = p1*x^6 + p2*x^5 + p3*x^4 + p4*x^3 + p5*x^2 +
             p6*x + p7
  where x is normalized by mean -0.04 and std 8.545
Coefficients (with 95% confidence bounds):
  p1 =      -1.036  (-1.337, -0.7358)
  p2 =      0.1709  (-0.08067, 0.4224)
  p3 =       5.259  (4.061, 6.457)
  p4 =     -0.4405  (-1.267, 0.3858)
  p5 =      -7.834  (-9.089, -6.579)
  p6 =     0.07067  (-0.5347, 0.6761)
  p7 =       4.218  (3.923, 4.514)
```

Run76

- Line1

```
Linear model Poly7:
ans(x) = p1*x^7 + p2*x^6 + p3*x^5 + p4*x^4 + p5*x^3 +
              p6*x^2 + p7*x + p8
  where x is normalized by mean -2.964 and std 6.831
Coefficients (with 95% confidence bounds):
  p1 =    -0.01293  (-0.04794, 0.02207)
  p2 =    -0.02026  (-0.0487, 0.008173)
  p3 =     0.04275  (-0.1163, 0.2018)
  p4 =      0.1235  (0.01287, 0.234)
  p5 =     0.03675  (-0.1753, 0.2488)
  p6 =     -0.2289  (-0.3418, -0.1159)
  p7 =     -0.2285  (-0.3095, -0.1476)
  p8 =       7.908  (7.882, 7.934)
```

```
Linear model Poly6:
ans(x) = p1*x^6 + p2*x^5 + p3*x^4 + p4*x^3 + p5*x^2 +
              p6*x + p7
  where x is normalized by mean -2.964 and std 6.831
Coefficients (with 95% confidence bounds):
  p1 =    -0.02026  (-0.04821, 0.00768)
  p2 =     -0.0154  (-0.03822, 0.007419)
  p3 =      0.1235  (0.01479, 0.2321)
  p4 =      0.1101  (0.03673, 0.1834)
  p5 =     -0.2288  (-0.3398, -0.1179)
  p6 =      -0.251  (-0.3035, -0.1986)
  p7 =       7.908  (7.883, 7.934)
```

```
Linear model Poly5:
ans(x) = p1*x^5 + p2*x^4 + p3*x^3 + p4*x^2 + p5*x + p6
  where x is normalized by mean -2.964 and std 6.831
Coefficients (with 95% confidence bounds):
  p1 =     -0.0154  (-0.039, 0.008207)
  p2 =     0.04587  (0.02624, 0.0655)
  p3 =      0.1102  (0.03429, 0.186)
  p4 =     -0.1563  (-0.2061, -0.1065)
  p5 =     -0.2512  (-0.3055, -0.197)
  p6 =       7.899  (7.876, 7.921)
```

```
Linear model Poly4:
ans(x) = p1*x^4 + p2*x^3 + p3*x^2 + p4*x + p5
  where x is normalized by mean -2.964 and std 6.831
Coefficients (with 95% confidence bounds):
  p1 =     0.04597  (0.02594, 0.066)
  p2 =     0.06185  (0.04506, 0.07864)
  p3 =     -0.1566  (-0.2074, -0.1058)
  p4 =     -0.2221  (-0.2534, -0.1907)
  p5 =       7.899  (7.876, 7.922)
```

```
Linear model Poly3:
ans(x) = p1*x^3 + p2*x^2 + p3*x + p4
  where x is normalized by mean -2.964 and std 6.831
Coefficients (with 95% confidence bounds):
  p1 =     0.06194  (0.03729, 0.08659)
  p2 =    -0.04469  (-0.06561, -0.02377)
  p3 =      -0.222  (-0.268, -0.176)
  p4 =       7.867  (7.84, 7.894)
```

```
General model:
ans(x) = a*cos(x*b+c)+d
Coefficients (with 95% confidence bounds):
  a =      0.1741  (0.152, 0.1962)
  b =      0.2279  (0.2009, 0.2548)
  c =        1.84  (1.643, 2.037)
  d =       7.811  (7.791, 7.831)
```

- Line2

```
Linear model Poly7:
ans(x) = p1*x^7 + p2*x^6 + p3*x^5 + p4*x^4 + p5*x^3 +
              p6*x^2 + p7*x + p8
  where x is normalized by mean -2.942 and std 6.801
Coefficients (with 95% confidence bounds):
  p1 =    -0.01095  (-0.04636, 0.02445)
  p2 =    -0.01719  (-0.04601, 0.01163)
  p3 =     0.03715  (-0.123, 0.1973)
  p4 =      0.1169  (0.005435, 0.2284)
  p5 =      0.0272  (-0.1854, 0.2398)
  p6 =     -0.1834  (-0.2966, -0.07008)
  p7 =     -0.1363  (-0.2172, -0.05549)
  p8 =       5.921  (5.895, 5.947)
```

```
Linear model Poly6:
ans(x) = p1*x^6 + p2*x^5 + p3*x^4 + p4*x^3 + p5*x^2 +
              p6*x + p7
  where x is normalized by mean -2.942 and std 6.801
Coefficients (with 95% confidence bounds):
  p1 =    -0.01655  (-0.04462, 0.01153)
  p2 =    -0.01187  (-0.03478, 0.01105)
  p3 =      0.1149  (0.006171, 0.2236)
  p4 =     0.08875  (0.01547, 0.162)
  p5 =     -0.1818  (-0.2923, -0.07125)
  p6 =     -0.1551  (-0.2072, -0.103)
  p7 =       5.921  (5.896, 5.946)
```

```
Linear model Poly5:
ans(x) = p1*x^5 + p2*x^4 + p3*x^3 + p4*x^2 + p5*x + p6
  where x is normalized by mean -2.942 and std 6.801
Coefficients (with 95% confidence bounds):
  p1 =      -0.011  (-0.03413, 0.01213)
  p2 =      0.0518  (0.03259, 0.071)
  p3 =      0.0866  (0.01256, 0.1606)
  p4 =     -0.1231  (-0.1717, -0.07455)
  p5 =     -0.1542  (-0.2069, -0.1015)
  p6 =       5.913  (5.891, 5.935)
```

```
Linear model Poly4:
ans(x) = p1*x^4 + p2*x^3 + p3*x^2 + p4*x + p5
  where x is normalized by mean -2.942 and std 6.801
Coefficients (with 95% confidence bounds):
  p1 =     0.05231  (0.03321, 0.07141)
  p2 =     0.05223  (0.03628, 0.06817)
  p3 =     -0.1241  (-0.1724, -0.07581)
  p4 =     -0.1335  (-0.1632, -0.1038)
  p5 =       5.913  (5.892, 5.935)
```

- Line3

```
Linear model Poly7:
ans(x) = p1*x^7 + p2*x^6 + p3*x^5 + p4*x^4 + p5*x^3 +
              p6*x^2 + p7*x + p8
  where x is normalized by mean -2.947 and std 6.827
Coefficients (with 95% confidence bounds):
  p1 =    -0.08684  (-0.1639, -0.009767)
  p2 =    -0.02023  (-0.08282, 0.04236)
  p3 =      0.5201  (0.1674, 0.8727)
  p4 =      0.2195  (-0.02568, 0.4647)
  p5 =      -1.064  (-1.536, -0.5909)
  p6 =     -0.6249  (-0.8766, -0.3732)
  p7 =      0.8145  (0.6328, 0.9963)
  p8 =        4.49  (4.432, 4.548)
```

```
Linear model Poly6:
ans(x) = p1*x^6 + p2*x^5 + p3*x^4 + p4*x^3 + p5*x^2 +
              p6*x + p7
  where x is normalized by mean -2.947 and std 6.827
Coefficients (with 95% confidence bounds):
  p1 =    -0.01998  (-0.0909, 0.05095)
  p2 =       0.127  (0.06896, 0.185)
  p3 =      0.2191  (-0.05872, 0.497)
  p4 =     -0.5649  (-0.753, -0.3768)
  p5 =     -0.6247  (-0.9099, -0.3395)
  p6 =      0.6604  (0.5248, 0.796)
  p7 =        4.49  (4.424, 4.556)
```

```
Linear model Poly5:
ans(x) = p1*x^5 + p2*x^4 + p3*x^3 + p4*x^2 + p5*x + p6
  where x is normalized by mean -2.947 and std 6.827
Coefficients (with 95% confidence bounds):
  p1 =      0.1271  (0.07052, 0.1838)
  p2 =      0.1421  (0.09492, 0.1892)
  p3 =     -0.5653  (-0.7489, -0.3817)
  p4 =     -0.5523  (-0.6726, -0.4319)
  p5 =      0.6606  (0.5282, 0.793)
  p6 =        4.48  (4.426, 4.535)
```

```
General model:
ans(x) = a*cos(x*b+c)+d
Coefficients (with 95% confidence bounds):
  a =     -0.3805  (-0.4356, -0.3255)
  b =      0.2975  (0.2733, 0.3218)
  c =       3.227  (3.075, 3.378)
  d =       4.208  (4.165, 4.251)
```

- Line4

```
Linear model Poly7:
ans(x) = p1*x^7 + p2*x^6 + p3*x^5 + p4*x^4 + p5*x^3 +
              p6*x^2 + p7*x + p8
  where x is normalized by mean -2.962 and std 6.832
Coefficients (with 95% confidence bounds):
  p1 =      -0.303  (-0.4099, -0.196)
  p2 =    -0.03101  (-0.1174, 0.05535)
  p3 =        1.78  (1.29, 2.27)
  p4 =      0.3554  (0.01769, 0.6932)
  p5 =      -3.491  (-4.15, -2.832)
  p6 =      -1.324  (-1.671, -0.9767)
  p7 =       2.468  (2.214, 2.722)
  p8 =       3.925  (3.844, 4.005)
```

```
Linear model Poly6:
ans(x) = p1*x^6 + p2*x^5 + p3*x^4 + p4*x^3 + p5*x^2 +
              p6*x + p7
  where x is normalized by mean -2.962 and std 6.832
Coefficients (with 95% confidence bounds):
  p1 =    -0.02087  (-0.1748, 0.133)
  p2 =      0.4063  (0.2789, 0.5337)
  p3 =      0.3226  (-0.2796, 0.9247)
  p4 =      -1.741  (-2.153, -1.33)
  p5 =      -1.298  (-1.917, -0.6787)
  p6 =       1.924  (1.628, 2.22)
  p7 =       3.922  (3.779, 4.066)
```

```
Linear model Poly5:
ans(x) = p1*x^5 + p2*x^4 + p3*x^3 + p4*x^2 + p5*x + p6
  where x is normalized by mean -2.962 and std 6.832
Coefficients (with 95% confidence bounds):
  p1 =      0.4069  (0.2836, 0.5301)
  p2 =      0.2422  (0.1393, 0.3451)
  p3 =      -1.743  (-2.141, -1.344)
  p4 =      -1.222  (-1.484, -0.9602)
  p5 =       1.925  (1.639, 2.212)
  p6 =       3.912  (3.794, 4.031)
```

```
General model:
ans(x) = a*cos(x*b+c)+d
Coefficients (with 95% confidence bounds):
  a =       1.058  (0.9134, 1.203)
  b =      -0.293  (-0.3166, -0.2695)
  c =    -0.09626  (-0.2391, 0.04656)
  d =       3.198  (3.082, 3.313)
```

- Line5

```
Linear model Poly7:
ans(x) = p1*x^7 + p2*x^6 + p3*x^5 + p4*x^4 + p5*x^3 +
             p6*x^2 + p7*x + p8
  where x is normalized by mean -2.976 and std 6.812
Coefficients (with 95% confidence bounds):
  p1 =     -0.5257  (-0.6422, -0.4091)
  p2 =      0.0428  (-0.05207, 0.1377)
  p3 =       3.123  (2.587, 3.658)
  p4 =      0.1218  (-0.2513, 0.4948)
  p5 =      -6.308  (-7.028, -5.587)
  p6 =       -1.53  (-1.914, -1.146)
  p7 =       4.472  (4.195, 4.75)
  p8 =       3.354  (3.266, 3.443)
```

```
Linear model Poly6:
ans(x) = p1*x^6 + p2*x^5 + p3*x^4 + p4*x^3 + p5*x^2 +
             p6*x + p7
  where x is normalized by mean -2.976 and std 6.812
Coefficients (with 95% confidence bounds):
  p1 =     0.03797  (-0.2065, 0.2824)
  p2 =      0.7335  (0.5331, 0.934)
  p3 =      0.1388  (-0.8223, 1.1)
  p4 =      -3.266  (-3.918, -2.613)
  p5 =      -1.546  (-2.536, -0.5568)
  p6 =       3.532  (3.059, 4.004)
  p7 =       3.359  (3.132, 3.587)
```

```
Linear model Poly5:
ans(x) = p1*x^5 + p2*x^4 + p3*x^3 + p4*x^2 + p5*x + p6
  where x is normalized by mean -2.976 and std 6.812
Coefficients (with 95% confidence bounds):
  p1 =      0.7335  (0.5394, 0.9277)
  p2 =      0.2859  (0.1239, 0.4478)
  p3 =      -3.265  (-3.898, -2.633)
  p4 =      -1.685  (-2.099, -1.27)
  p5 =       3.531  (3.073, 3.988)
  p6 =       3.378  (3.19, 3.566)
```

- Line6

```
Linear model Poly7:
ans(x) = p1*x^7 + p2*x^6 + p3*x^5 + p4*x^4 + p5*x^3 +
             p6*x^2 + p7*x + p8
  where x is normalized by mean -3.025 and std 6.806
Coefficients (with 95% confidence bounds):
  p1 =     -0.5391  (-0.7364, -0.3419)
  p2 =       0.128  (-0.0321, 0.288)
  p3 =       3.412  (2.507, 4.317)
  p4 =    -0.08146  (-0.7085, 0.5456)
  p5 =      -7.337  (-8.554, -6.12)
  p6 =      -1.716  (-2.361, -1.072)
  p7 =       5.546  (5.079, 6.013)
  p8 =       3.087  (2.941, 3.234)
```

```
Linear model Poly6:
ans(x) = p1*x^6 + p2*x^5 + p3*x^4 + p4*x^3 + p5*x^2 +
             p6*x + p7
  where x is normalized by mean -3.025 and std 6.806
Coefficients (with 95% confidence bounds):
  p1 =     0.09338  (-0.1841, 0.3709)
  p2 =      0.9649  (0.7359, 1.194)
  p3 =     0.02618  (-1.062, 1.115)
  p4 =      -4.223  (-4.964, -3.481)
  p5 =      -1.797  (-2.916, -0.6777)
  p6 =       4.587  (4.051, 5.123)
  p7 =         3.1  (2.845, 3.355)
```

```
Linear model Poly5:
ans(x) = p1*x^5 + p2*x^4 + p3*x^3 + p4*x^2 + p5*x + p6
  where x is normalized by mean -3.025 and std 6.806
Coefficients (with 95% confidence bounds):
  p1 =      0.9701  (0.746, 1.194)
  p2 =      0.3867  (0.1991, 0.5744)
  p3 =      -4.234  (-4.961, -3.508)
  p4 =      -2.136  (-2.614, -1.659)
  p5 =        4.59  (4.064, 5.116)
  p6 =       3.144  (2.93, 3.358)
```

- **Residuals plots**

Run3

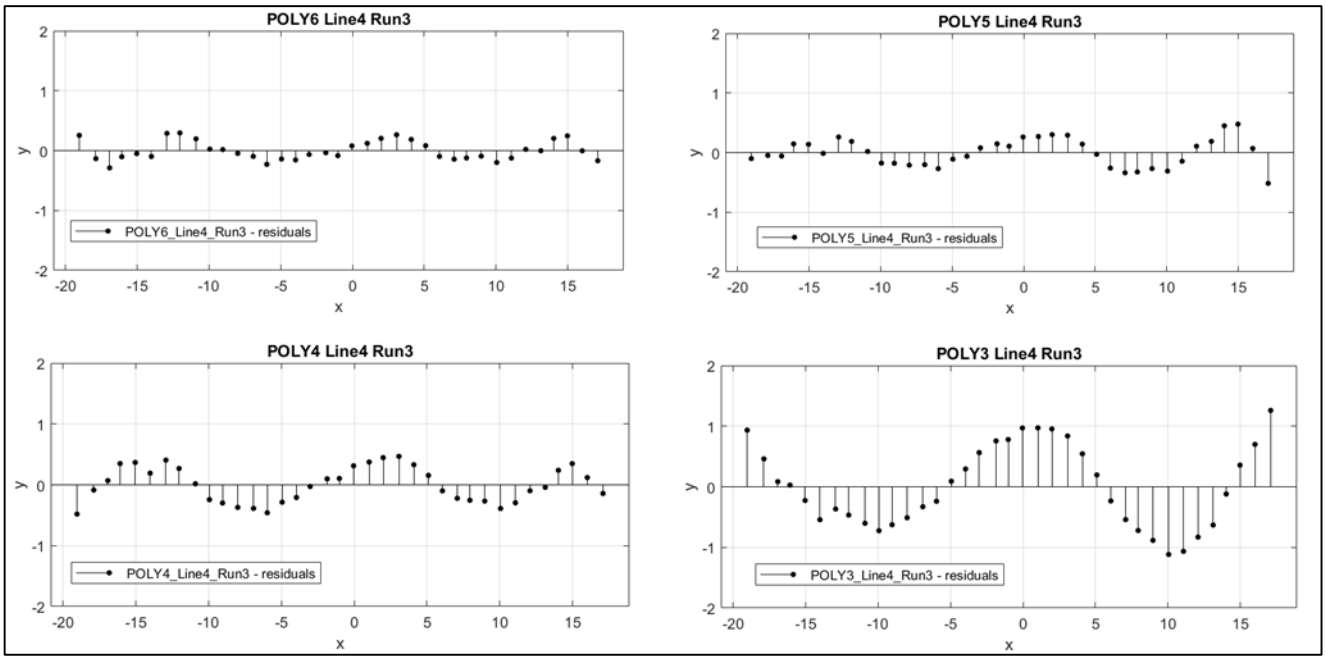

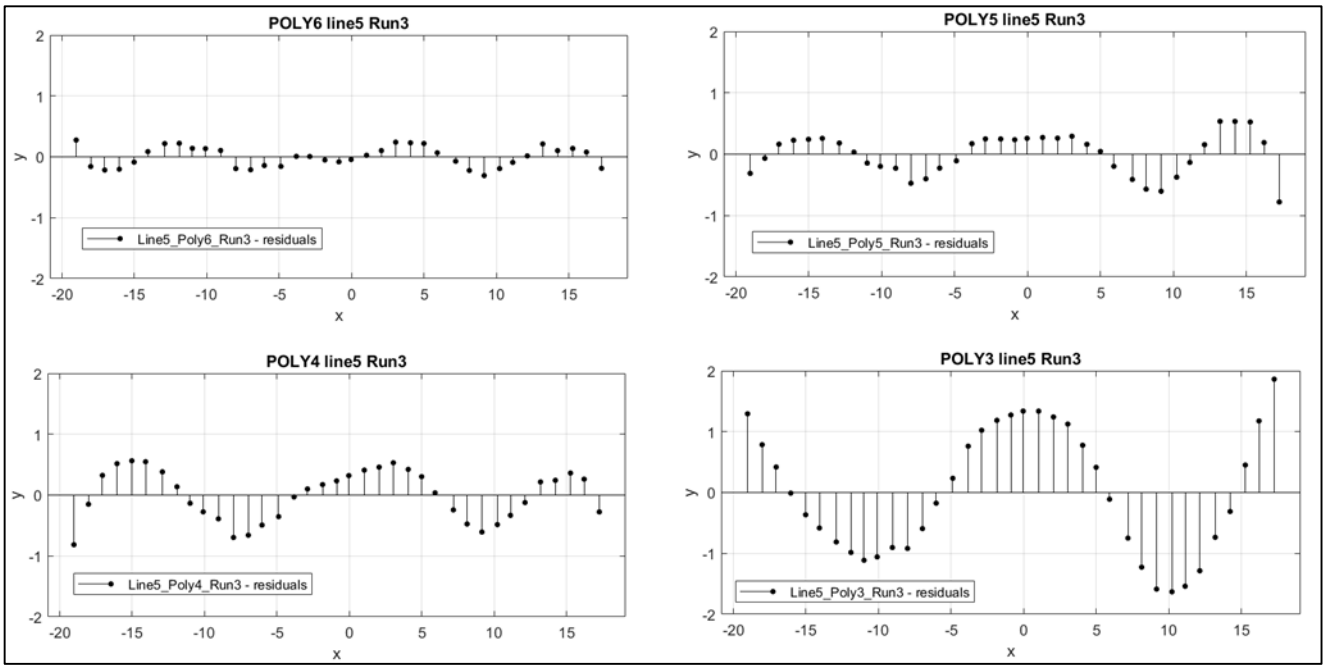

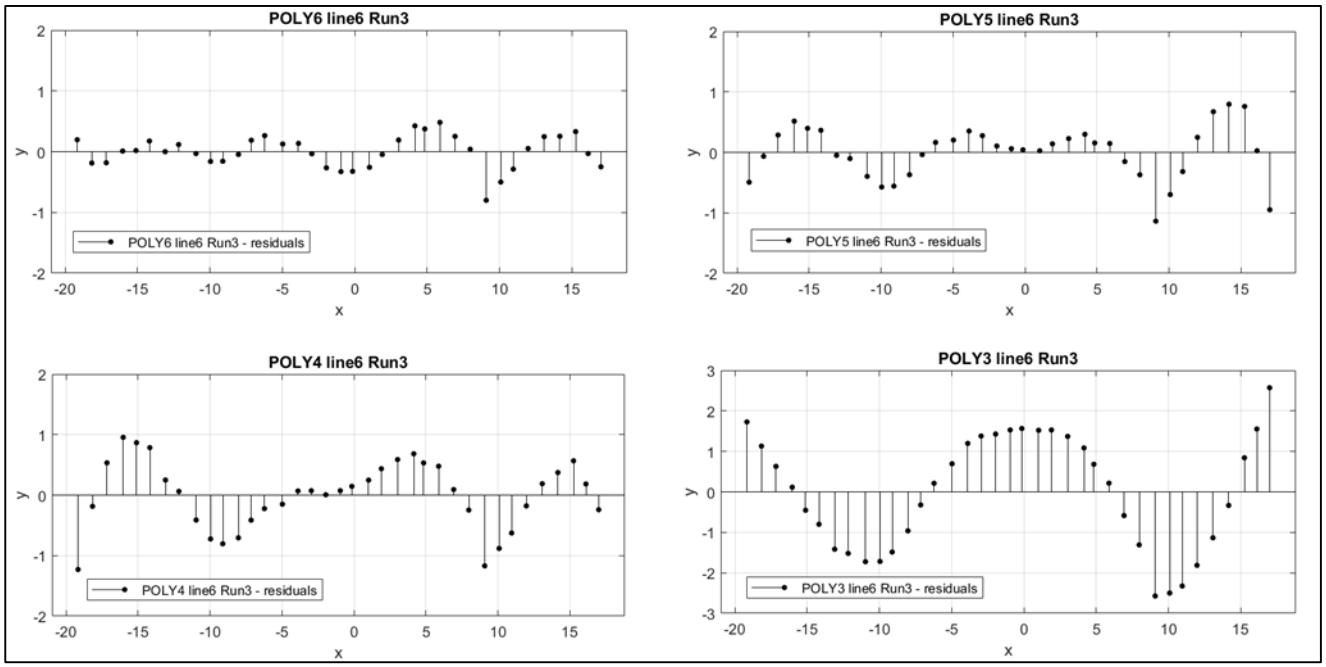
POLY6 line6 Run3
POLY6 line6 Run3 - residuals
POLY5 line6 Run3
POLY5 line6 Run3 - residuals
POLY4 line6 Run3
POLY4 line6 Run3 - residuals
POLY3 line6 Run3
POLY3 line6 Run3 - residuals
x
y

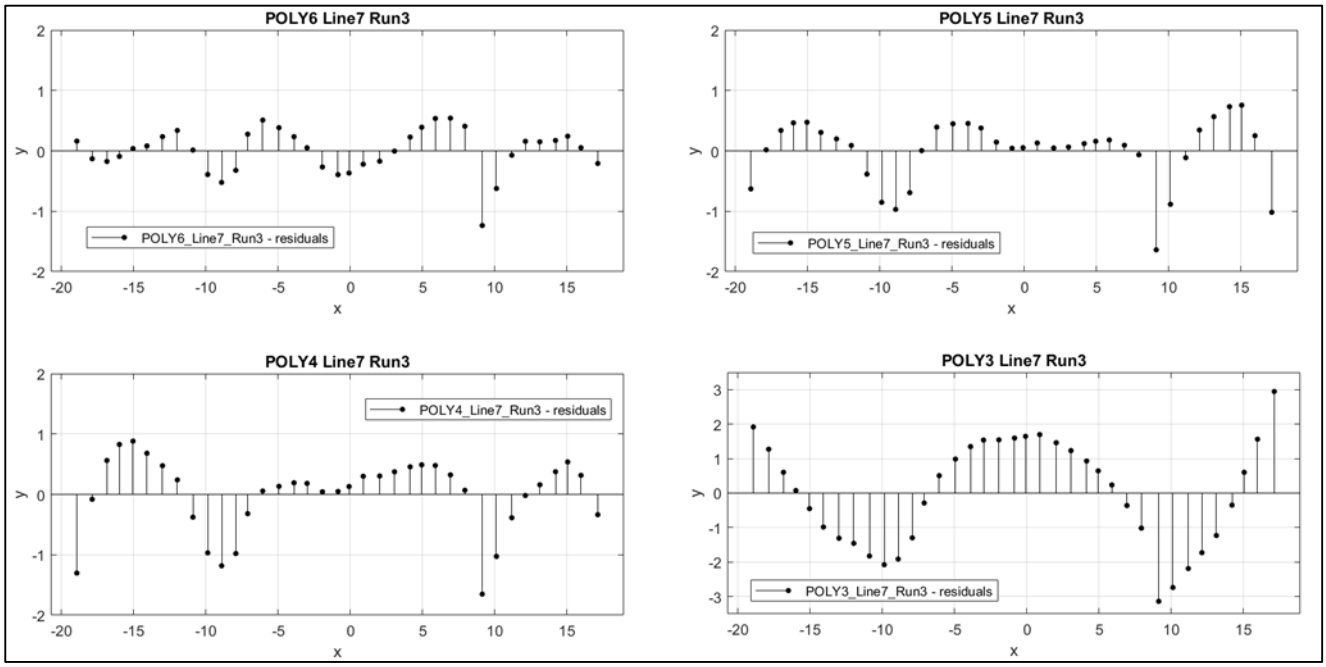
POLY6 Line7 Run3
POLY6_Line7_Run3 - residuals
POLY5 Line7 Run3
POLY5_Line7_Run3 - residuals
POLY4 Line7 Run3
POLY4_Line7_Run3 - residuals
POLY3 Line7 Run3
POLY3_Line7_Run3 - residuals
x
y

Run39

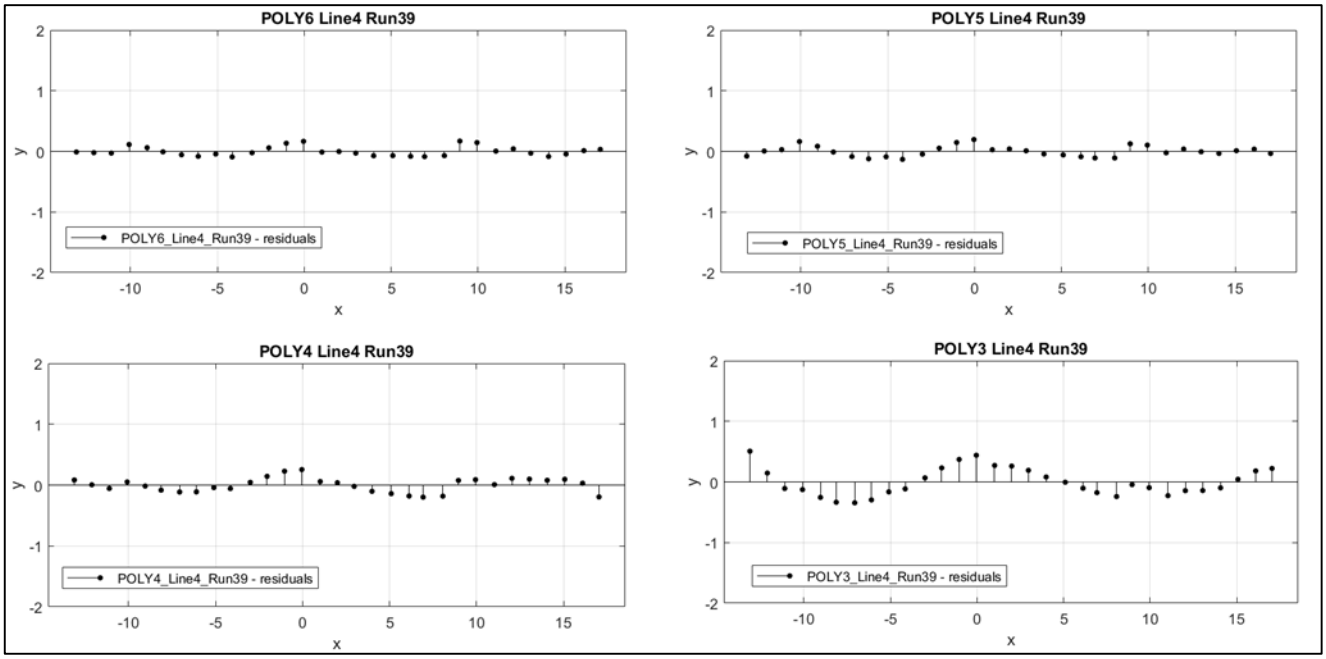
POLY6 Line4 Run39
POLY6_Line4_Run39 - residuals
POLY5 Line4 Run39
POLY5_Line4_Run39 - residuals
POLY4 Line4 Run39
POLY4_Line4_Run39 - residuals
POLY3 Line4 Run39
POLY3_Line4_Run39 - residuals
x
y

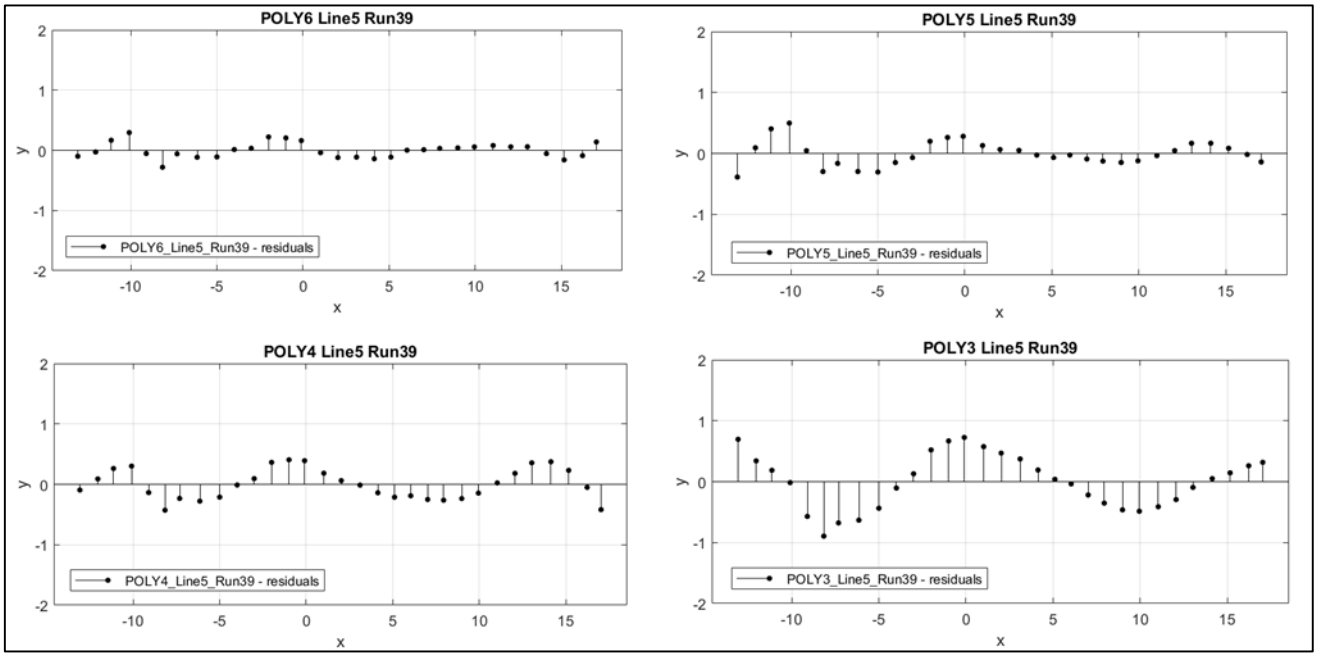
POLY6 Line5 Run39
POLY6_Line5_Run39 - residuals
POLY5 Line5 Run39
POLY5_Line5_Run39 - residuals
POLY4 Line5 Run39
POLY4_Line5_Run39 - residuals
POLY3 Line5 Run39
POLY3_Line5_Run39 - residuals
x
y

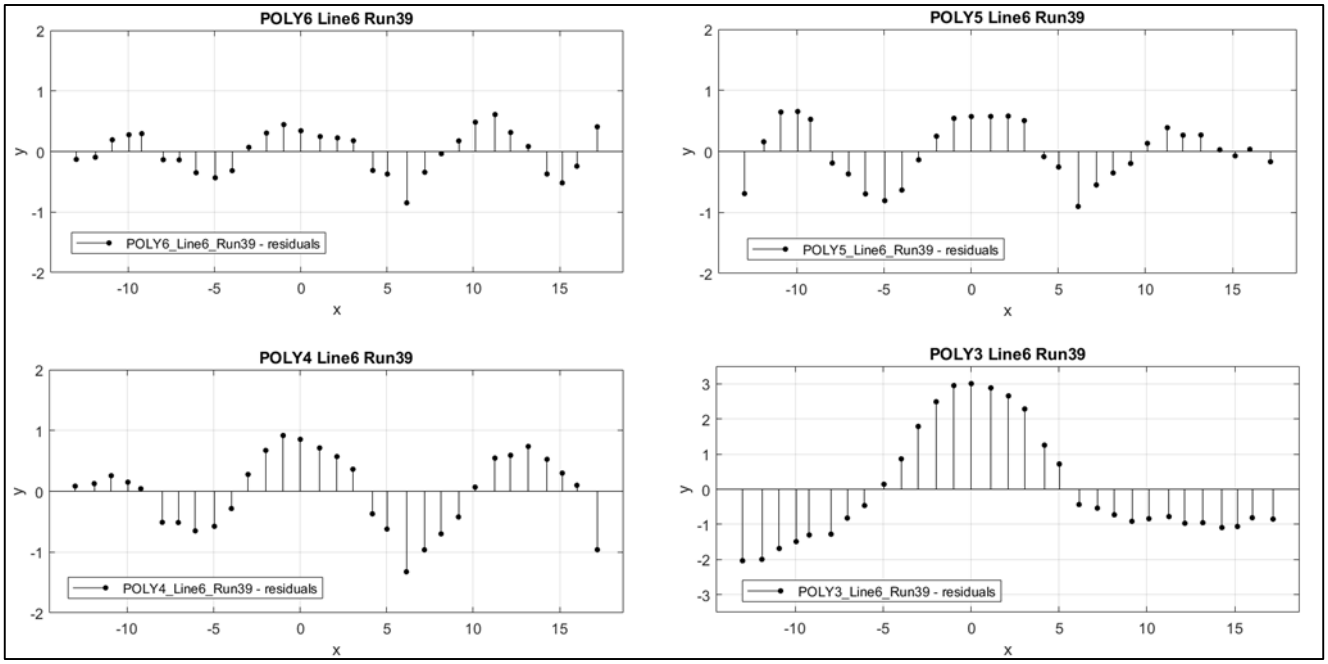
POLY6 Line6 Run39
POLY6_Line6_Run39 - residuals
POLY5 Line6 Run39
POLY5_Line6_Run39 - residuals
POLY4 Line6 Run39
POLY4_Line6_Run39 - residuals
POLY3 Line6 Run39
POLY3_Line6_Run39 - residuals
x
y

Run42

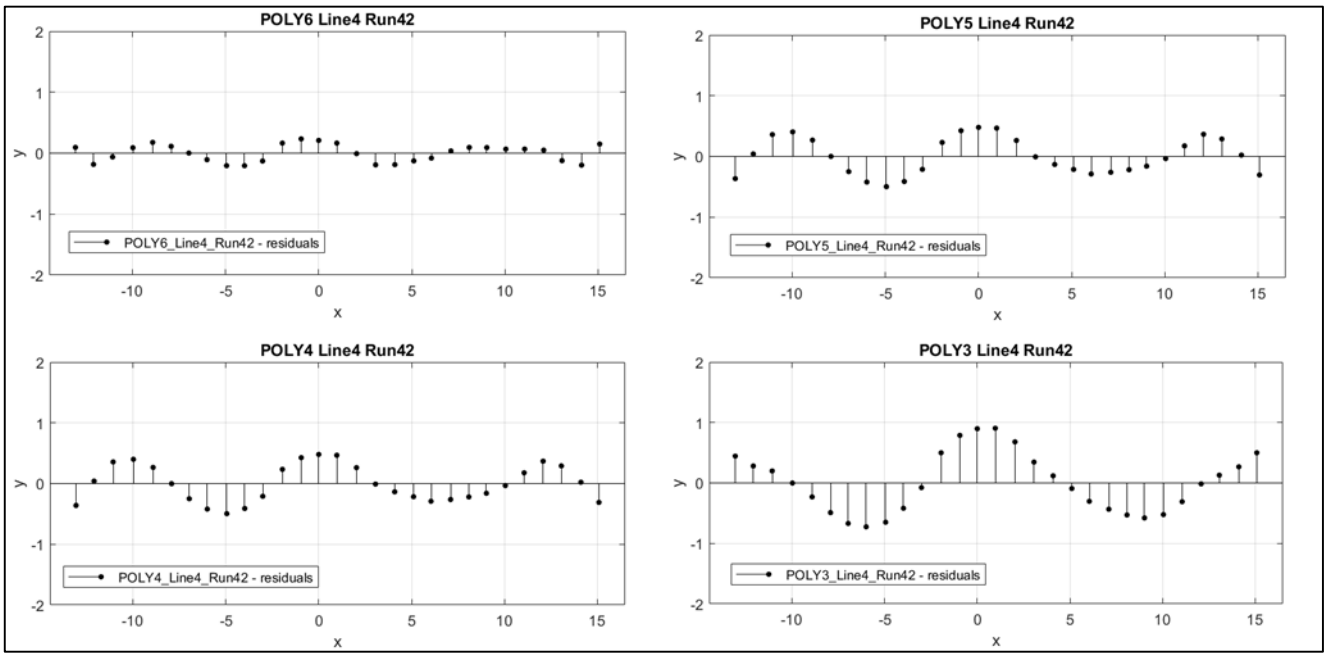
POLY6 Line4 Run42
POLY6_Line4_Run42 - residuals
POLY5 Line4 Run42
POLY5_Line4_Run42 - residuals
POLY4 Line4 Run42
POLY4_Line4_Run42 - residuals
POLY3 Line4 Run42
POLY3_Line4_Run42 - residuals
x
y

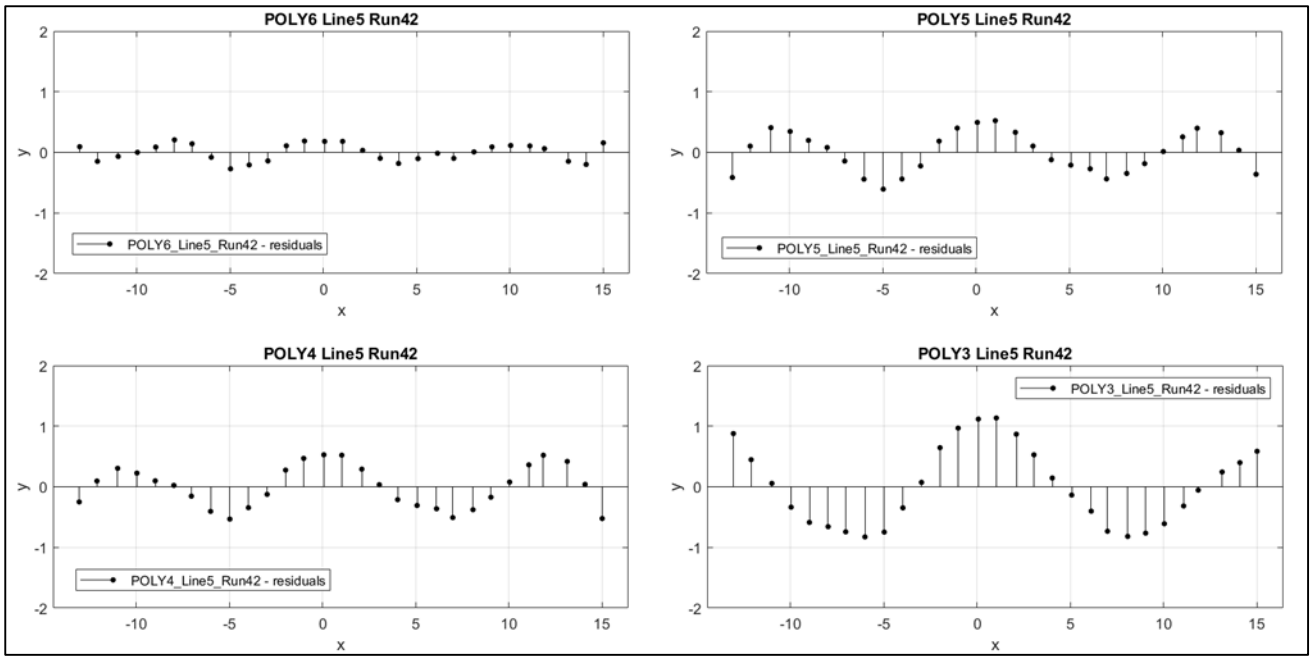
POLY6 Line5 Run42
POLY6_Line5_Run42 - residuals
POLY5 Line5 Run42
POLY5_Line5_Run42 - residuals
POLY4 Line5 Run42
POLY4_Line5_Run42 - residuals
POLY3 Line5 Run42
POLY3_Line5_Run42 - residuals
x
y

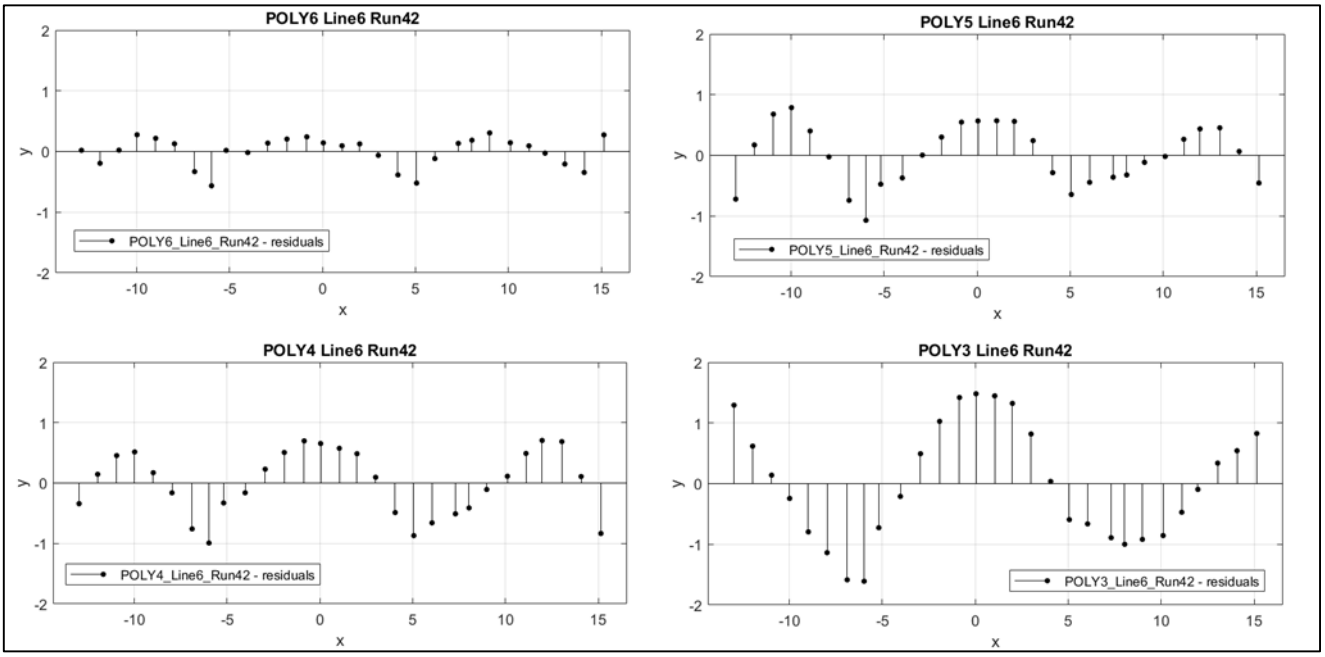
POLY6 Line6 Run42
POLY6_Line6_Run42 - residuals
POLY5 Line6 Run42
POLY5_Line6_Run42 - residuals
POLY4 Line6 Run42
POLY4_Line6_Run42 - residuals
POLY3 Line6 Run42
POLY3_Line6_Run42 - residuals
x
y

Run63

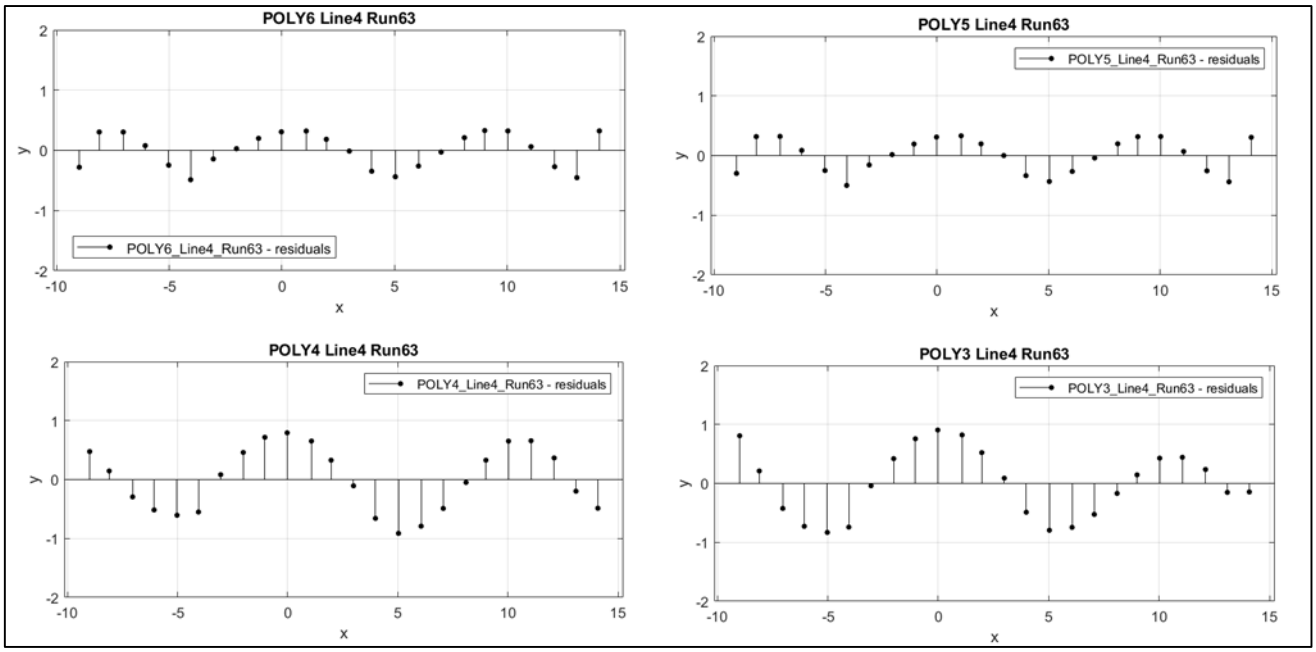
POLY6 Line4 Run63
POLY6_Line4_Run63 - residuals
POLY5 Line4 Run63
POLY5_Line4_Run63 - residuals
POLY4 Line4 Run63
POLY4_Line4_Run63 - residuals
POLY3 Line4 Run63
POLY3_Line4_Run63 - residuals
x
y

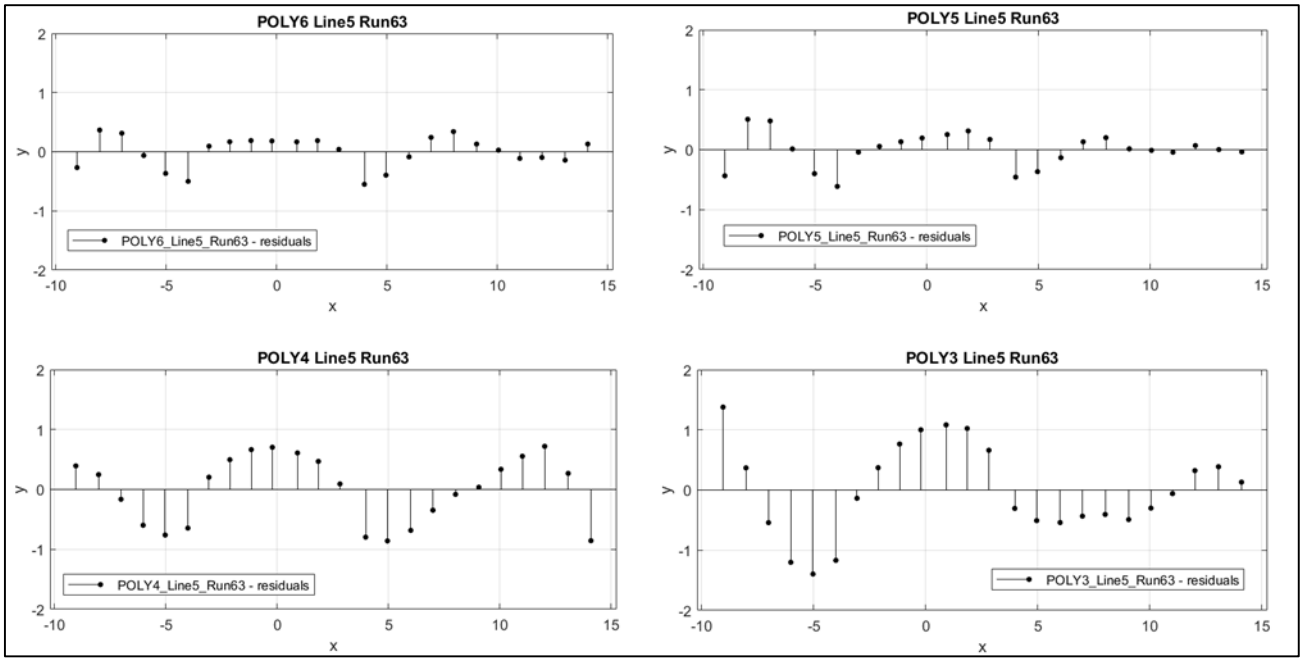
POLY6 Line5 Run63
POLY6_Line5_Run63 - residuals
POLY5 Line5 Run63
POLY5_Line5_Run63 - residuals
POLY4 Line5 Run63
POLY4_Line5_Run63 - residuals
POLY3 Line5 Run63
POLY3_Line5_Run63 - residuals
x
y

Run76

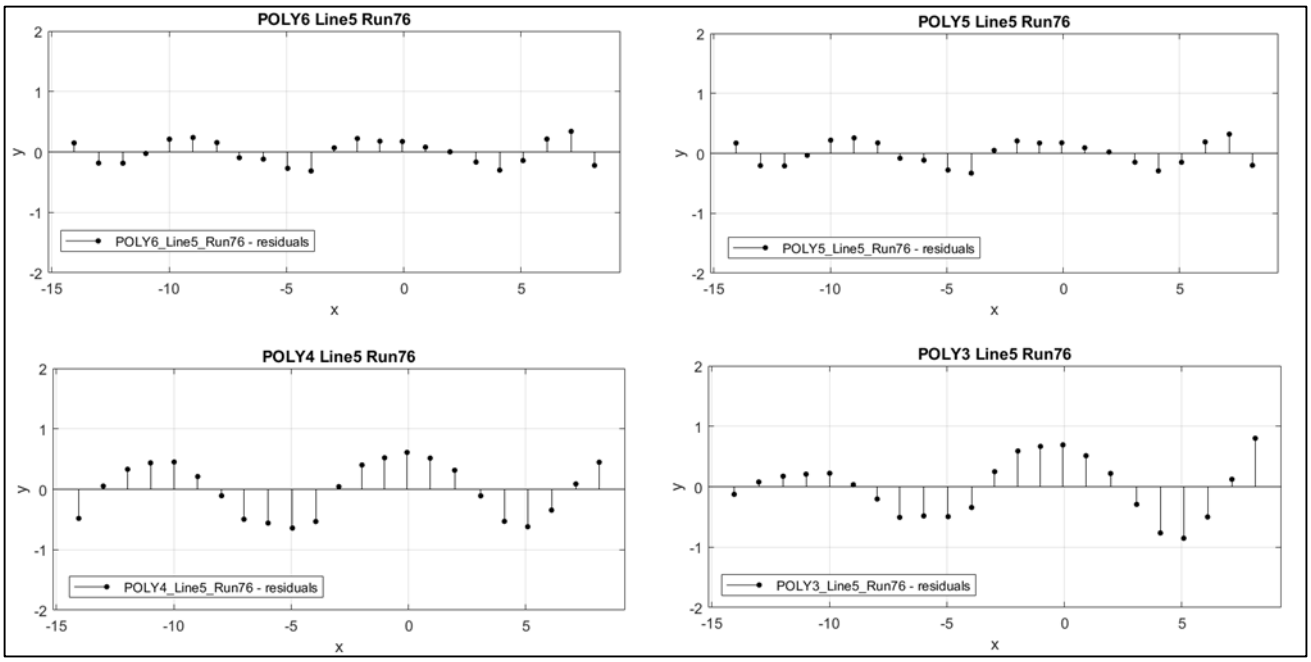
POLY6 Line5 Run76
POLY6_Line5_Run76 - residuals
POLY5 Line5 Run76
POLY5_Line5_Run76 - residuals
POLY4 Line5 Run76
POLY4_Line5_Run76 - residuals
POLY3 Line5 Run76
POLY3_Line5_Run76 - residuals
x
y

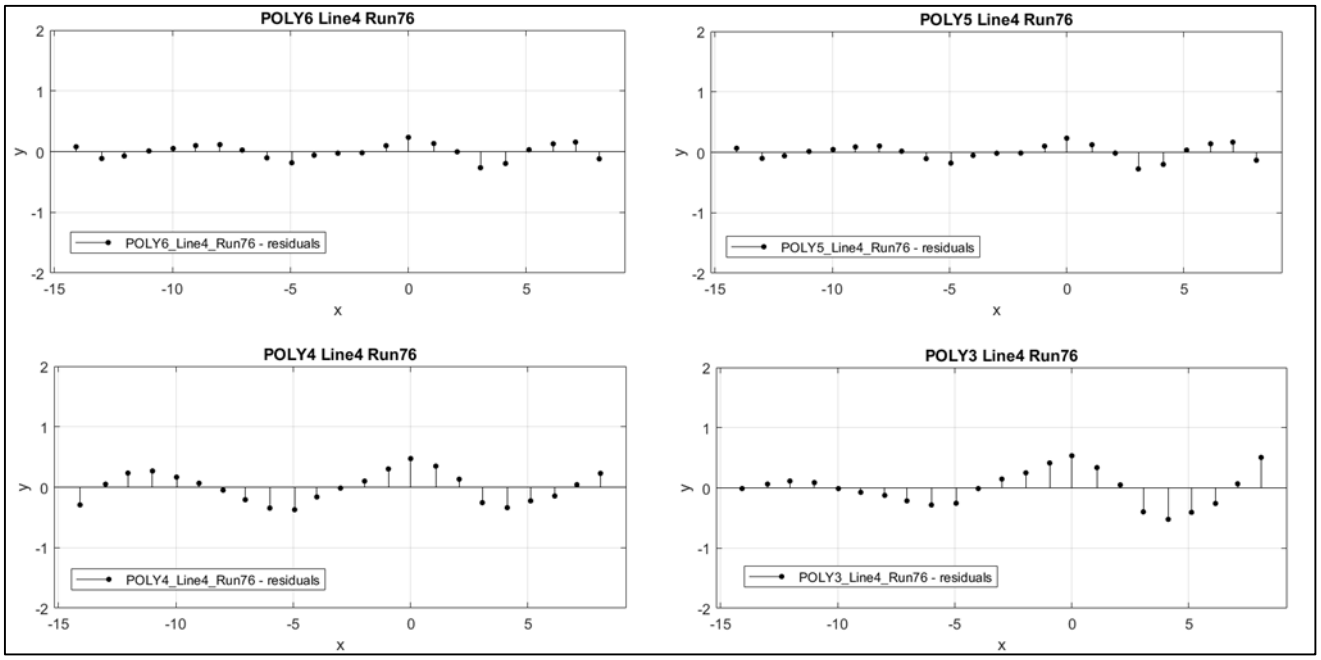
POLY6 Line4 Run76
POLY6_Line4_Run76 - residuals
POLY5 Line4 Run76
POLY5_Line4_Run76 - residuals
POLY4 Line4 Run76
POLY4_Line4_Run76 - residuals
POLY3 Line4 Run76
POLY3_Line4_Run76 - residuals
x
y

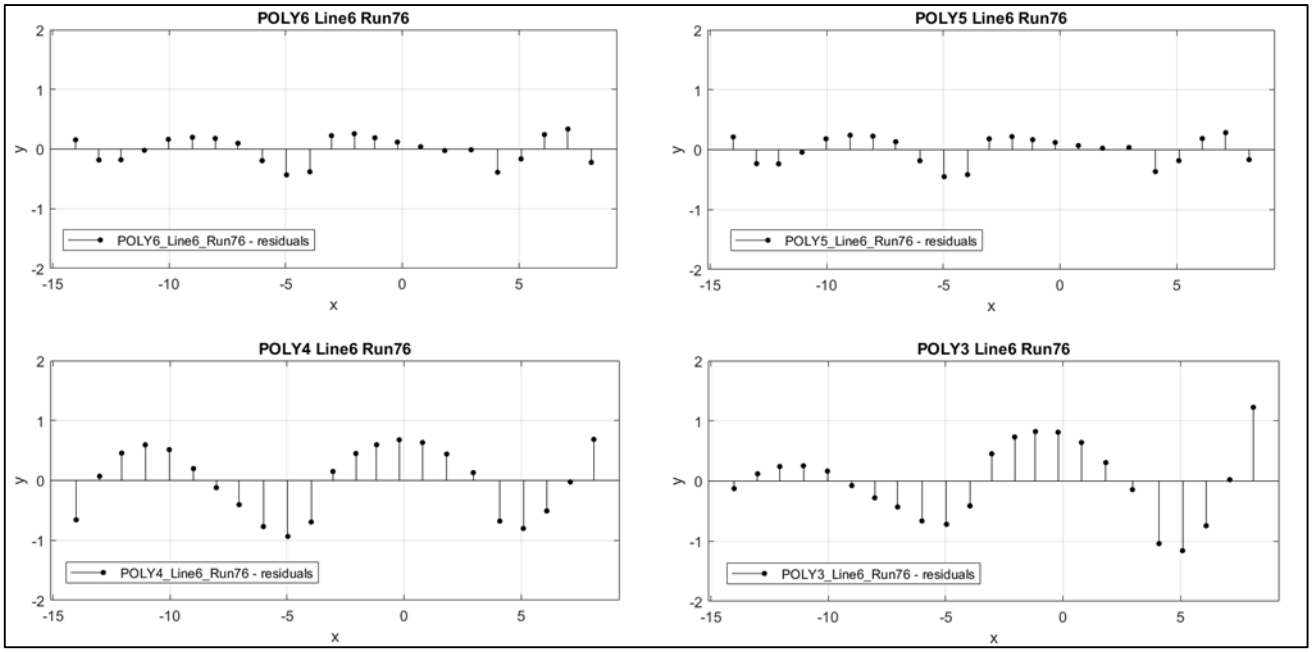

- **Residual values classified by polynomial**

	Residuals POLY6				Residuals POLY5				Residuals POLY4				Residuals POLY3			
x	Line4	Line5	Line6	Line7	Line4	Line5	Line6	Line7	Line4	Line5	Line6	Line7	Line4	Line5	Line6	Line7
-20	0.255	0.275	0.197	0.162	0.102	0.313	0.494	0.630	0.482	0.815	1.230	1.302	0.935	1.293	1.727	1.917
-19	0.000	0.000	0.000	0.000	0.000	0.000	0.000	0.000	0.000	0.000	0.000	0.000	0.000	0.000	0.000	0.000
-18	0.134	0.159	0.187	0.131	0.049	0.067	0.065	0.017	0.086	0.150	0.186	0.082	0.460	0.786	1.130	1.273
-17	0.306	0.297	0.182	0.198	0.157	0.280	0.590	0.574	0.355	0.610	1.094	0.999	0.090	0.419	0.641	0.607
-16	0.049	0.087	0.019	0.037	0.138	0.242	0.398	0.473	0.368	0.564	0.868	0.882	0.226	0.367	0.453	0.450
-15	0.128	0.172	0.235	0.081	0.014	0.258	0.364	0.305	0.191	0.548	0.785	0.681	0.544	0.583	0.800	0.985
-14	0.095	0.136	0.132	0.000	0.374	0.568	0.999	0.000	0.370	0.268	0.352	0.000	0.674	1.120	2.410	0.000
-13	0.471	0.434	0.355	0.411	0.345	0.353	0.408	0.218	0.571	0.646	0.736	0.532	0.676	1.402	2.950	1.958
-12	0.062	0.181	0.194	0.000	0.361	0.573	0.937	0.000	0.361	0.401	0.522	0.000	0.226	0.195	1.691	0.000
-11	0.196	0.327	0.279	0.013	0.174	0.559	0.801	0.385	0.239	0.467	0.632	0.377	0.626	1.126	2.291	1.824
-10	0.146	0.365	0.529	0.653	0.487	0.512	1.253	1.291	0.639	0.831	1.434	1.529	0.995	1.570	2.646	2.822
-9	0.451	0.541	0.256	0.000	0.402	0.564	0.445	0.000	0.551	0.590	0.538	0.000	0.906	1.745	1.505	0.000
-8	0.348	0.464	0.281	0.322	0.586	0.782	0.619	0.693	0.423	0.811	0.918	0.979	0.828	1.384	1.726	1.296
-7	0.125	0.287	0.519	0.276	0.472	0.707	1.018	0.005	0.559	0.750	1.082	0.319	0.908	1.264	1.684	0.288
-6	0.368	0.432	0.785	0.509	0.517	0.590	1.357	0.394	0.836	1.028	1.237	0.056	1.089	1.615	1.685	0.506
-5	0.578	0.650	0.551	0.384	0.593	0.759	0.839	0.449	0.904	1.141	0.897	0.134	1.103	1.676	1.482	0.985
-4	0.334	0.415	0.434	0.240	0.715	0.890	0.749	0.591	0.837	0.991	1.019	0.265	1.097	1.839	2.707	2.044
-3	0.038	0.287	0.379	0.000	0.174	0.388	0.486	0.000	0.232	0.677	0.966	0.000	0.235	0.639	2.522	0.000
-2	0.276	0.386	0.696	0.477	0.330	0.475	0.657	0.151	0.582	0.757	1.061	0.064	1.328	2.023	3.785	2.219
-1	0.407	0.358	0.563	0.368	0.569	0.605	0.823	0.052	0.931	1.038	1.200	0.131	1.546	2.046	3.744	1.646
1	0.355	0.309	0.208	0.000	0.676	0.740	0.822	0.000	0.734	0.907	1.055	0.000	1.340	1.726	2.228	0.000
2	0.460	0.287	0.362	0.280	0.651	0.540	0.603	0.139	1.274	1.285	1.105	0.427	1.926	2.513	3.689	2.238
3	0.015	0.174	0.314	0.000	0.354	0.472	0.953	0.000	0.548	0.757	1.046	0.000	0.976	1.556	3.797	0.000
4	0.545	0.646	0.373	0.004	0.294	0.356	0.345	0.063	0.508	0.641	0.828	0.374	0.916	1.437	2.052	1.232
5	0.329	0.421	0.692	0.228	0.337	0.251	0.415	0.120	0.439	0.485	0.850	0.456	0.685	0.842	1.096	0.930
6	0.464	0.499	0.759	0.391	0.451	0.588	0.800	0.159	0.800	1.072	1.374	0.490	0.747	0.933	1.554	0.644
7	0.317	0.240	1.069	0.537	0.601	0.528	1.170	0.180	1.025	1.164	1.997	0.478	0.993	1.100	1.518	0.237
8	0.250	0.487	0.443	0.678	0.617	0.859	0.571	0.114	0.911	1.128	0.767	0.329	1.275	1.857	1.845	1.077
9	0.429	0.530	0.870	1.237	0.465	0.828	1.282	1.638	0.635	0.878	1.486	1.652	1.197	1.973	2.997	3.135
10	0.092	0.106	0.573	0.000	0.190	0.223	0.175	0.000	0.183	0.225	0.127	0.000	0.586	0.907	1.244	0.000
11	0.385	0.225	0.521	0.623	0.445	0.375	0.697	0.884	0.510	0.493	0.889	1.027	1.242	1.809	2.641	2.735
12	0.155	0.197	0.681	0.072	0.392	0.292	0.567	0.113	0.738	0.595	0.965	0.387	1.211	1.653	2.497	2.186
13	0.278	0.130	0.320	0.158	0.388	0.432	0.568	0.345	0.769	0.791	0.938	0.019	0.952	1.322	2.058	1.727
14	0.470	0.302	0.333	0.150	0.428	0.651	0.855	0.566	0.480	0.931	1.025	0.159	0.700	0.845	1.518	1.228
15	0.495	0.298	0.657	0.298	0.791	0.768	1.102	1.053	0.473	0.635	0.867	0.655	0.497	0.782	1.518	0.696
16	0.150	0.224	0.587	0.000	0.306	0.371	0.462	0.000	0.325	0.573	0.887	0.000	0.501	0.604	1.343	0.000
17	0.004	0.118	0.244	0.052	0.078	0.191	0.044	0.251	0.123	0.267	0.210	0.316	0.723	1.205	1.752	1.561
18	0.169	0.234	0.478	0.209	0.517	0.791	0.964	1.017	0.241	0.501	0.991	0.337	1.279	1.888	2.709	2.944
19	0.000	0.000	0.000	0.000	0.000	0.000	0.000	0.000	0.000	0.000	0.000	0.000	0.000	0.000	0.000	0.000
20	0.000	0.000	0.000	0.000	0.000	0.000	0.000	0.000	0.000	0.000	0.000	0.000	0.000	0.000	0.000	0.000

C. Assessment tables

- **Constant term a_0, y max values third repeat trial**

			0		1		2		3		4		5	
			ymin	ymax	ymin	ymax	ymin	ymax	ymin	ymax	ymin	ymax	ymin	ymax
ply0/90	Ø18mm	4					1.657	9.203	3.203	9.099			4.778	9.199
		8					2.040	9.130			4.050	9.180		
		12	-0.219	9.283			2.200	9.344			3.627	9.240	5.081	9.240
		16					1.878	9.223	3.654	9.266	4.414	9.263		
			-0.219	**9.283**			**1.944**	**9.225**	**3.429**	**9.183**	**4.030**	**9.228**	**4.930**	**9.220**
	Ø9mm	3			0.980	4.530	2.010	4.660			3.950	4.860		
		7	-0.169	4.617	1.053	4.660	2.290	4.620			3.917	4.746	5.328	4.635
		11					1.656	4.580	3.044	4.672	4.129	5.034		
		15	-0.040	4.530			1.850	4.550			3.970	4.800		
			-0.105	**4.574**	**1.017**	**4.595**	**1.952**	**4.603**	**3.044**	**4.672**	**3.992**	**4.860**	**5.328**	**4.635**
ply 45/45	Ø18mm	2					1.980	8.980	2.960	9.180	4.000	9.090		
		6	-0.377	9.076			2.160	9.162	3.226	9.263			4.928	9.160
		10					1.820	9.020	3.150	9.070	4.480	9.220		
		14							3.340	9.010			5.210	9.080
			-0.377	**9.076**			**1.987**	**9.054**	**3.169**	**9.131**	**4.240**	**9.155**	**5.069**	**9.120**
	Ø9mm	1			0.940	4.520	1.970	4.760			3.980	5.320		
		5	0.030	4.650	0.960	5.360	1.970	5.510					5.000	5.860
		9			0.735	4.568			3.453	4.801			4.640	5.264
		13			0.618	4.662	2.105	4.863			4.297	5.386		
			0.030	**4.650**	**0.813**	**4.778**	**2.015**	**5.044**	**3.453**	**4.801**	**4.139**	**5.353**	**4.820**	**5.562**

			6		7		8		9		10	
			ymin	ymax	ymin	ymax	ymin	ymax	ymin	ymax	ymin	ymax
ply0/90	Ø18mm	4	6.070	9.285	7.211	9.102	8.418	9.887			9.726	11.034
		8	6.020	9.090			8.050	9.480			10.080	10.450
		12	6.380	9.684			8.089	10.492			9.604	11.300
		16	6.285	9.341			8.029	9.866	9.422	10.532		
			6.189	**9.350**	**7.211**	**9.102**	**8.147**	**9.931**	**9.422**	**10.532**	**9.803**	**10.928**
	Ø9mm	3			6.830	6.830						
		7					7.622	7.392				
		11	6.029	5.979			8.010	7.769				
		15	6.020	6.020			8.030	8.050				
			6.025	**6.000**	**6.830**	**6.830**	**7.887**	**7.737**				
ply 45/45	Ø18mm	2	5.990	9.370	6.970	9.530	7.990	9.700	9.030	9.880	10.040	10.390
		6	6.132	9.202	7.219	9.504					9.775	10.772
		10	6.090	9.370	7.430	9.680			8.970	10.170		
		14	6.500	9.360	7.360	9.730			9.340	10.290		
			6.178	**9.326**	**7.245**	**9.611**	**7.990**	**9.700**	**9.113**	**10.113**	**9.908**	**10.581**
	Ø9mm	1	5.950	6.630			7.980	8.230			10.060	10.160
		5			7.010	7.850			9.010	9.640		
		9	5.787	6.392			7.618	8.161	8.966	9.369	9.892	10.375
		13	6.107	6.713			7.990	8.000				
			5.948	**6.578**	**7.010**	**7.850**	**7.863**	**8.130**	**8.988**	**9.505**	**9.976**	**10.268**

- **Constant term a_0, gap tables**

Ø18mm ply0/90

t	ymax	gap	incr.ymax	abs(incr)
0	9.277	0.277		
1	9.250	0.250	-0.027	0.027
2	9.223	0.223	-0.027	0.027
3	9.195	0.195	-0.028	0.028
4	9.226	0.226	0.031	0.031
5	9.227	0.227	0.001	0.001
6	9.330	0.330	0.103	0.103
7	9.153	0.153	-0.177	0.177
8	9.801	0.801	0.648	0.648
9	10.333	1.333	0.532	0.532
10	11.133	2.133	0.800	0.800

Ø9mm ply0/90

t	ymax	gap	incr.ymax	abs(incr)
0	4.576	0.076		
1	4.595	0.095	0.019	0.019
2	4.606	0.106	0.011	0.011
3	4.669	0.169	0.063	0.063
4	4.859	0.359	0.189	0.189
5	4.690	0.190	-0.168	0.168
6	5.951	1.451	1.261	1.261
7	6.976	2.476	1.025	1.025
8	7.834	3.334	0.858	0.858
9				
10				

Ø18mm ply 45/45

t	ymax	gap	incr.ymax	abs(incr)
0	9.072	0.072		
1	9.063	0.063	-0.009	0.009
2	9.055	0.055	-0.008	0.008
3	9.120	0.120	0.065	0.065
4	9.150	0.150	0.030	0.030
5	9.123	0.123	-0.027	0.027
6	9.293	0.293	0.170	0.170
7	9.546	0.546	0.253	0.253
8	9.704	0.704	0.158	0.158
9	10.071	1.071	0.368	0.368
10	10.635	1.635	0.564	0.564

Ø9mm ply45/45

t	ymax	gap	incr.ymax	abs(incr)
0	4.645	0.145		
1	4.819	0.319	0.174	0.174
2	5.041	0.541	0.221	0.221
3	4.878	0.378	-0.163	0.163
4	5.241	0.741	0.364	0.364
5	5.724	1.224	0.483	0.483
6	6.640	2.140	0.916	0.916
7	7.838	3.338	1.198	1.198
8	8.297	3.797	0.459	0.459
9	9.514	5.014	1.217	1.217
10	10.287	5.787	0.772	0.772

D. Matlab code

- **Regression type selection**

```
%%
% **DATA ANALYSIS AND REGRESSION TYPE SELECTION**
%  INTRODUCTION
%This code allows import data from an excel file,from where the x,y coordinates
%are read. Only is used the upper half information of each image..it usually means
%7 path lines (14 rows). The regression selection is done by the comparison of
plots and
%parameters that show the goddnes of fit.

%ATENTION: if more than 7 paths need to be analised. The code needs samall changes
%(made the tables, cells, variable c.. bigger.)

%OUTPUTS and GET INFO
% In the command window:
%#Plots of each line with the different fits
%#Table with the data imported from the excel files (x and y data)
%#Tables with statistics info, each row one fittype (as tables as paths)

%In the workspace
%#Table with the data imported
%# cell f. It contains the constant values of each fit of the last path. If we
want this informations of the other paths we need to change the value of c (ex:
c=1:2 to know info of path 2)
%To read the cell info type for example: "f{1,7}{1,1}" in the comand window

%% modify if change the name of the woorksheet, sheet or range!!!!
woorksheetimage='fibrecoordinates_Run 42.xlsx';
sheet='Sheet1';
range='B11:M36';
%%%%%%%%%%%%%%%%%%%%%%%%%%%%%%%%%%%%%%%%%%%%%%%%%%%%%%%%%%%%%%%%%%%%%%%%%%%%

tabledata=importfile(woorksheetimage)
data=xlsread(woorksheetimage,sheet,range);


for c=1:6 % c indicates the numer of paths
    x=data(:,2*c-1);
    y=data(:,2*c);
    %%%%%%%%%%%%%%%%%%
    f=cell(1,6);
    f{c}=createFits(x,y);
    title(['Line' num2str(c)])
    %%%%%%%%%%%%%%%%%%%%%%%%%
end


function tableout = importdata(workbookFile,sheetName,startRow,endRow)
%IMPORTFILE Import data from a spreadsheet
%   DATA = IMPORTFILE(FILE) reads data from the first worksheet in the
%   Microsoft Excel spreadsheet file named FILE and returns the data as a
%   table.
%
```

```
%   DATA = IMPORTFILE(FILE,SHEET) reads from the specified worksheet.
%
%   DATA = IMPORTFILE(FILE,SHEET,STARTROW,ENDROW) reads from the specified
%   worksheet for the specified row interval(s). Specify STARTROW and
%   ENDROW as a pair of scalars or vectors of matching size for
%   dis-contiguous row intervals. To read to the end of the file specify an
%   ENDROW of inf.%
% Example:
%   sampledotsdata = importfile('180614_sample_dots_data.xlsx','S1',5,23);
%   See also XLSREAD.

%% Input handling

% If no sheet is specified, read first sheet
if nargin == 1 || isempty(sheetName)
    sheetName = 1;
end

% If row start and end points are not specified, define defaults
if nargin <= 3
    startRow = 5;
    endRow = 42;
end

%% Import the data
data = xlsread(workbookFile, sheetName, sprintf('B%d:M%d',startRow(1),endRow(1)));



%% Create table
tableout = table

%% Allocate imported array to column variable names
tableout.Line1_X = data(:,1);
tableout.Line1_Y = data(:,2);
tableout.Line2_X = data(:,3);
tableout.Line2_Y = data(:,4);
tableout.Line3_X= data(:,5);
tableout.Line3_Y= data(:,6);
tableout.Line4_X= data(:,7);
tableout.Line4_Y = data(:,8);
tableout.Line5_X= data(:,9);
tableout.Line5_Y= data(:,10);
tableout.Line6_X= data(:,11);
tableout.Line6_Y= data(:,12);
%tableout.Line7_X= data(:,13);
%tableout.Line7_Y= data(:,14);
end


function [fitresult, gof] = createFits(x1, y1)
%CREATEFITS(X1,Y1)
%  Create fits. Polynomial from 3rd order to 7th and cosinus
%  function.
%
%  Output:
%      fitresult : a cell-array of fit objects representing the fits.
```

```
%      gof : structure array with goodness-of fit info.
%
%  See also FIT, CFIT, SFIT.

%% Initialization.

% Initialize arrays to store fits and goodness-of-fit.
fitresult = cell( 5, 1 );
gof  = struct( 'sse', cell( 5, 1 ),'rsquare', [], 'dfe', [], 'adjrsquare', [],
'rmse', [] );

%% Fit: 'poly7'.
[xData, yData] = prepareCurveData( x1, y1 );

% Set up fittype and options.
ft = fittype( 'poly7' );

% Fit model to data.
[fitresult{1}, gof(1)] = fit( xData, yData, ft, 'Normalize', 'on' );

% Plot fit.
figure( 'Name', 'CreateFits');
plot( fitresult{1},xData,yData,'o');

grid on

%% Fit: 'fit poly6'.

% Set up fittype and options.
ft = fittype( 'poly6' );

% Fit model to data.
[fitresult{2}, gof(2)] = fit( xData, yData, ft );

% Plot fit with data.
hold on
plot( fitresult{2},'g--');

grid on
%% Fit: 'poly5'.

% Set up fittype and options.
ft = fittype( 'poly5' );

% Fit model to data.
[fitresult{3}, gof(3)] = fit( xData, yData, ft, 'Normalize', 'on' );

% Plot fit.
hold on
plot( fitresult{3},'m');

grid on
%% Fit: 'poly4'.

% Set up fittype and options.
ft = fittype( 'poly4' );
```

```
% Fit model to data.
[fitresult{4}, gof(4)] = fit( xData, yData, ft, 'Normalize', 'on' );

% Plot fit.
hold on
plot( fitresult{4},'b');

grid on
%% Fit: 'poly3'.


% Set up fittype and options.
ft = fittype( 'poly3' );

% Fit model to data.
[fitresult{5}, gof(5)] = fit( xData, yData, ft, 'Normalize', 'on' );

% Plot fit.
hold on
plot( fitresult{5},'b--');


%% Fit: 'fitcosinus'.


% Set up fittype and options.
ft = fittype( 'a*cos(x*b+c)+d', 'independent', 'x', 'dependent', 'y' );
opts = fitoptions( 'Method', 'NonlinearLeastSquares' );
opts.Display = 'Off';
opts.Robust = 'Bisquare';
opts.StartPoint = [1.0 0.100 0.1 0.1];% Using the curve fitting tool we can loof
for the best initial values.

% Fit model to data.
[fitresult{6}, gof(6)] = fit( xData, yData, ft, opts );

% Plot fit with data
plot( fitresult{6},'m--');


%axis
axis([-16 16 -20 20]);

%Labels
legend('real points','fitpoly7', 'fit
poly6','fitpoly5','fitpoly4','fitpoly3','fitcosinus','Location','SouthEast');
xlabel x1
ylabel y1
hold off
grid on


tablegof = struct2table(gof);
tablegof.Properties.RowNames =
{'Polyfit7','Polyfit6','Polyfit5','Polyfit4','Polyfit3','Cosinusfit'}

end
```

- **Model plot**

```
%%
% *PLOT OF THE MODEL*
% The purpose of this simple code is made the plot using the selfdeveloped
% model expression.
%Some inputs are needed:

%info of the file from where the coefficient need to be imported
%'coef=xlsread('Filename.xlsx','sheet name','data range')
coef=xlsread('Deformed area.xlsx','coef model','I20:K26');
r=4.5; % radius in mm
xdef=11; % xdef and ydef, constraints values of the deformed region.
ydef=6.849;
xmax=20; % desired size of the plot
ymax=12;
t=6 % number of studied t
%%%%%%%%%%%%%%%%%%%%%%%%%%%%%%%%%%%%%%%%%%%%%%%%%%%%
for i=1:t
    s=i-1;
    a=coef(i);
    b=coef(i,2);
    c=coef(i,3);
    f1= @(x) a+b*x^2+c*x^4;
    f2= @(x) -a-b*x^2-c*x^4;
    f3=@(x) s;
    f4=@(x) -s;
    fplot(f1, [-xdef xdef],'k','LineWidth',1)
    fplot(f2, [-xdef xdef],'k','LineWidth',1)
    fplot(f3, [xdef xmax], 'k','LineWidth',0.75)
    fplot(f3, [-xmax -xdef], 'k','LineWidth',0.75)
    fplot(f4, [xdef xmax], 'k','LineWidth',0.75)
    fplot(f4, [-xmax -xdef], 'k','LineWidth',0.75)
    hold on

end
t=(ydef+1):1:ymax;
f5=@(x) t;
f6=@(x)-t;
fplot(f5, [-xmax xmax],'k','LineWidth',0.75);
fplot(f6, [-xmax xmax],'k','LineWidth',0.75);
hold on
theta=linspace(0,2*pi);
v=r*cos(theta);
w=r*sin(theta);
plot(v,w,'k','LineStyle','--','LineWidth', 0.75)
axis equal
line(xlim,[0 0],'Color','k')
line([0 0], ylim,'Color','k')
```

8 References

A. C. Long (2005), 'Design and manufacture of textile composites' [15.05.2018].

Advani, S. G. & Tucker, C. L. (1987), 'The Use of Tensors to Describe and Predict Fiber Orientation in Short Fiber Composites', *Journal of Rheology*, vol. 31, no. 8, pp. 751–784 [14.03.2018].

Brebbia & A, C. (2006), 'Design and Nature III. Comparing Design in Nature with Science and Engineering' [16.03.2018].

Callister, W. D. (2007), *Materials science and engineering*. *An introduction,* John Wiley & Sons, New York [14.05.2018].

D. Reuschel, C. M. (1999), 'Optimization of fiber arrangement with CAIO (computer aided internal optimization) and application to tensile samples', *Transactions on the Built Environment*, vol. 37 [16.03.2018].

David Abram Jack (2006), 'Advanced analysis of short-fiber polymer composite material behavior'.

Dr.Abdul & Mirzana, I. M. (2016), 'Stress Concentration of Rectangular Plate with a Hole Made With Composite Material Using Finite Element Analysis', *IOSR Journal of Mechanical and Civil Engineering*, vol. 13, no. 04, pp. 1–5 [03.04.2018].

Fransisco Folgar and Charles L. Tucker & III (1983), 'Orientation Behavior of Fibers in Concentrated Suspensions' [16.03.2018].

Gebhardt, J. (2018), *Strukturoptimierung von in FVK eingebetteten metallischen Lasteinleitungselementen*.

Gebhardt, J. & Fleischer, J. (2014), 'Experimental Investigation and Performance Enhancement of Inserts in Composite Parts', *Procedia CIRP*, vol. 23, pp. 7–12 [21.05.2018].

Ghiasi, H.; Fayazbakhsh, K.; Pasini, D. & Lessard, L. (2010), 'Optimum stacking sequence design of composite materials Part II: Variable stiffness design', *Composite Structures*, vol. 93, no. 1, pp. 1–13 [16.03.2018].

H. J. Lin & C. S. Tang (1994), 'Fatigue strength of woven fabric composites with drilled and moulded-in holes' [16.03.2018].

Hubert Temmen, Richard Degenhardt, Tilmann Raible (2006), 'Tailored Fibre Placement optimization tool' [16.03.2018].

Jahn, J.; Weeber, M.; Boehner, J. & Steinhilper, R. (2016), 'Assessment Strategies for Composite-metal Joining Technologies – A Review', *Procedia CIRP*, vol. 50, pp. 689–694 [21.05.2018].

Jeffery & G (1922), 'The Motion of Ellipsoidal Particles Immersed in a Viscous Fluid' [16.03.2018].

Jordy Luberizky Permadi (2018), *Characterization of carbon fibre flow in an innovative joining technique in Multi-Material-Design*. Bachelor Thesis, KIT, Karlsruher Institüt für Technologie, Karlsruhe, Institüt für Produktiontechnik.

Kar, K. K. (2017), *Composite Materials,* Springer Berlin Heidelberg, Berlin, Heidelberg [13.05.2018].

Lee, C.-J.; Lee, J.-M.; Ryu, H.-Y.; Lee, K.-H.; Kim, B.-M. & Ko, D.-C. (2014), 'Design of hole-clinching process for joining of dissimilar materials – Al6061-T4 alloy with DP780 steel, hot-pressed 22MnB5 steel, and carbon fiber reinforced plastic', *Journal of Materials Processing Technology*, vol. 214, no. 10, pp. 2169–2178 [21.05.2018].

Minitab Inc (2017), 'Introducción a Minitab 18' [23.04.2018].

Parkes, P. N.; Butler, R.; Meyer, J. & Oliveira, A. de (2014), 'Static strength of metal-composite joints with penetrative reinforcement', *Composite Structures*, vol. 118, pp. 250–256 [21.05.2018].

Phelps, J. H. & Tucker, C. L. (2009), 'An anisotropic rotary diffusion model for fiber orientation in short- and long-fiber thermoplastics', *Journal of Non-Newtonian Fluid Mechanics*, vol. 156, no. 3, pp. 165–176 [16.03.2018].

Prat Bartés, A.; Tort-Martorell Llabrés, X.; Grima Cintas, P. & Pozueta Fernández, L. (2000), 'Métodos estadísticos. Control y mejora de la calidad' [23.04.2018].

Seidlitz, H.; Ulke-Winter, L. & Kroll, L. (2014), 'New Joining Technology for Optimized Metal/Composite Assemblies', *Journal of Engineering*, vol. 2014, no. 9, pp. 1–11.

W R Broughton, L E Crocker and M R L Gower (2002), 'Design Requirements for Bonded and Bolted Composite Structures' [30.05.2018].

Wang, J.; O'Gara, J. F. & Tucker, C. L. (2008), 'An objective model for slow orientation kinetics in concentrated fiber suspensions: Theory and rheological evidence', *Journal of Rheology*, vol. 52, no. 5, pp. 1179–1200 [16.03.2018].

Xavier Oliver Olivella i Carlos Agelet de Saracíbar Bosch (2003), 'Mecànica de medis continus per a enginyers' [05.04.2018].

Zhu, Y.; Liu, J.; Liu, D.; Xu, H.; Yan, C.; Huang, B. & Hui, D. (2016), 'Fiber path optimization based on a family of curves in composite laminate with a center hole', *Composites Part B: Engineering*, vol. 111, pp. 91–102 [02.04.2018].